Studies in South African Marine Molluscan Chemistry

A thesis submitted in fulfilment of the

requirements for the degree of

Master of Science

of

Rhodes University

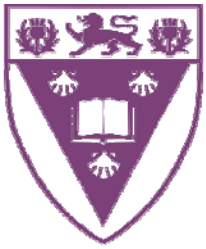

by

Candice Leigh Bromley

February 2011

Abstract

This thesis investigates the variability occurring in the secondary metabolites produced by three South African marine molluscs. Chapter Two discusses the isolation and spectroscopic structure elucidation of the metabolites isolated from two *Siphonaria* species. The re-investigation of *Siphonaria capensis* yielded siphonarienfuranone (**2.2**) as the only common polypropionate isolated from both the 1998 and 2009 collections of *S. capensis* from the same areas suggesting possible seasonal or genetic variation in polypropionate production. The sterol cholest-7-en-3,5,7-triol (**2.33**) was also isolated form the 2009 collection of *S. capensis* and this is the first time this compound has been isolated from a *Siphonaria* species. The second species, *Siphonaria oculus* is closely related to *S. capensis* and the investigation into the former's secondary metabolite production revealed **2.2** as a major metabolite suggesting an inter-species overlap in polypropionate production. Three new polypropionate metabolites, **2.35**, **2.36** and **2.37** were also isolated from *S. oculus*. An unsuccessful attempt was made to establish the absolute configuration of **2.37** using the modified Mosher's method and the limited amount of **2.37** available prevented any further attempts at resolving the absolute configuration of this compound. The ^{1}H NMR analysis of the defensive mucus collected directly from *S. oculus* revealed the presence of the acyclic polypropionate **2.37** as a minor metabolite. The absence of characteristic signals for the furanone containing compounds **2.2**, **2.35** and **2.36**, might suggest that these compounds cyclise from a hypothetical acyclic precursor (**2.38**) during standard work up of bulk acetone extracts of *Siphonaria* species.

Chapter Three discusses the re-isolation and spectroscopic structure elucidation of the metabolites isolated from the nudibranch, *Leminda millecra*. Three known natural products, millecrone A (**3.1**), 8-hydroxycalamenene (**3.6**) and cubebenone (**3.8**) were re-isolated from our 2010 collection of *L. millecra*, as well as the new minor metabolite 8-acetoxycalamenene (**3.16**). The cytotoxic prenylated toluquinones and toluhydroquinones (**3.9**-**3.15**) initially isolated from the 1998 collection of *L. millecra* were not found in the 2010 collection supporting the hypothesis that these compounds may be of fungal origin. *L. millecra* clearly shows variability in the compounds sequestered by this species with millecrone A (**3.1**) being the only common metabolite in the three investigations of *L. millecra* to date. An unsuccessful attempt was made to establish the absolute configuration of **3.1**, **3.6** and **3.8** through initial LAH reduction of the ketone moiety contained in **3.1** and **3.8** and esterification of the resultant diastereomeric alcohol mixtures and the phenol functionality in **3.6** with (1*S*)-camphanic chloride. Crystallisation of the (*S*)-camphanate esters of **3.6** and **3.8** for X-ray analysis were unsuccessful, while the unexpected conjugate addition of a hydride in **3.1** resulted in complex diastereomeric mixtures which could not be separated by HPLC.

Table of Contents

		Page
Abstract		ii
Table of Contents		iii
List of Figures		vi
List of Schemes		viii
List of Tables		ix
List of Abbreviations		x
Acknowledgements		xii
Chapter One: General Introduction		
1.1	What are marine natural products?	2
1.2	The challenge of supply	3
1.3	The challenge of variability	7
1.4	Aims of this thesis	9
Chapter Two: Polypropionates from Two Species of South African *Siphonaria*		
2.1	Introduction	11
2.1.1	General biology of *Siphonaria*	11
2.1.2	Biosynthesis of polypropionate secondary metabolites	12
2.1.3	Polypropionate metabolites isolated from *Siphonaria* species (1998-2010)	15
2.2	Chromatographic material	22

2.2.1	Poly(styrene-divinylbenzene) (PSDVB)	22
2.2.2	DIOL	25
2.3	*Siphonaria capensis*	26
2.3.1	Recollection and re-isolation of *Siphonaria capensis* metabolites	26
2.4	*Siphonaria oculus*	35
2.4.1	Collection and isolation of *Siphonaria oculus* metabolites	35
2.4.2	Investigation into the cellular structure of the lateral pedal glands of *S. oculus*	52
2.4.3	Analysis of the mucus secretions from *S. oculus*	54
2.5	Concluding remarks	57

Chapter Three: Sesquiterpenes from the South African Nudibranch *Leminda millecra*

3.1	Introduction	59
3.1.1	Opisthobranch nudibranchs	59
3.1.2	*Leminda millecra*	59
3.2	Re-isolation of known sesquiterpenes from *Leminda millecra*	64
3.3	Isolation and structure elucidation of a new sesquiterpenes from *L. millecra*	69
3.4	An attempt to establish the absolute configuration of millecrone A (**3.1**), 8-hydroxycalamenene (**3.6**) and cubebenone (**3.8**)	73
3.5	Concluding remarks	80

Chapter Four: Experimental Details

4.1	**General Experimental Procedures**	83
4.1.1	*Analytical*	83
4.1.2	*Chromatography*	83

4.1.3 Synthesis 83

4.1.4 Computer modelling 84

4.2 Chapter Two Experimental 84

4.2.1 Extraction and isolation of *Siphonaria capensis* metabolites 84

4.2.2 Extraction and isolation of *Siphonaria oculus* metabolites 85

4.2.2.1 Mosher's esterification of hexanol 87

*4.2.2.2 Attempted Mosher's esterification of **2.37*** 88

4.2.2.3 Collection of mucus from Siphonaria oculus 88

4.3 Chapter Three Experimental 88

4.3.1 Extraction and isolation of *Leminda millecra* metabolites 88

*4.3.1.1 Acetylation of 8-hyxdroxycalamenene (**3.6**)* 91

4.3.2 Attempts to establish the absolute configuration of **3.1**, **3.6** and **3.8** 91

4.3.2.1 Lithium aluminium hydride reduction of hispanolone 91

4.3.2.2 Sodium borohydride reduction of hispanolone 92

4.3.2.3 Esterification of meta-*cresol* 93

4.3.2.4 Reduction of millercrone A using lithium aluminium hydride 93

*4.3.2.5 Further lithium aluminium hydride reduction of **3.21*** 94

4.3.2.6 Attempted reduction of millecrone A using sodium borohydride 95

*4.3.2.7 Preparation of the camphanate ester **3.23** from **3.6*** 95

4.3.2.8 Lithium aluminium hydride reduction of cubebenone 96

*4.3.2.9 Preparation of the camphanate ester of **3.24*** 96

References 99

List of Figures

		Page
Figure 2.1	Distribution of acetate and propionate subunits in placidene A (**2.9**), C (**2.10**) and E (**2.11**)	14
Figure 2.2	Proposed distribution of acetate and propionate units in **2.12**	22
Figure 2.3	The chemical structure of the stationary phase poly(styrene-divinylbezene) (PSDVB)	23
Figure 2.4	Photograph illustrating the process of cyclic loading using PSDVB stationary phase	24
Figure 2.5	Collection of *Siphonaria capensis*, made by Dr W. Popplewell and myself, from the rocky intertidal zone along the Kenton coast line	26
Figure 2.6	^{1}H NMR ($CDCl_3$, 600 MHz) spectra of crude fractions eluted from HP-20 resin	27
Figure 2.7	^{1}H ($CDCl_3$ 600 MHz) and ^{13}C (150 MHz) NMR spectra of siphonarienfuranone (**2.2**)	29
Figure 2.8	A region (F1 = δ 1.4-2.2 ppm; F2 = δ 90-205 ppm) of the gHMBC spectrum ($CDCl_3$, 600 MHz) of **2.2**.	31
Figure 2.9	^{1}H ($CDCl_3$, 600 MHz) and ^{13}C ($CDCl_3$, 150 MHz) NMR spectra of **2.33**	33
Figure 2.10	Colony of *Siphonaria oculus* found on the banks of the Kariega River	35
Figure 2.11	^{1}H ($CDCl_3$, 600 MHz) and ^{13}C ($CDCl_3$, 150 MHz) NMR spectra obtained for **2.35**	38
Figure 2.12	A region (F1 = δ 1.4-2.2 ppm; F2 = δ 10-50 ppm) of the gHMBC spectrum ($CDCl_3$, 600 MHz) of **2.35** illustrating the five bond gHMBC correlations	39
Figure 2.13	^{1}H ($CDCl_3$, 600 MHz) and ^{13}C ($CDCl_3$, 150 MHz) NMR spectra obtained for **2.36**	41
Figure 2.14	A region of the NOESY spectra (F = 0.6-3.0 ppm) obtained for **2.36**	43
Figure 2.15	^{1}H ($CDCl_3$, 600 MHz) and ^{13}C ($CDCl_3$, 150 MHz) NMR spectra obtained for **2.37**	45
Figure 2.16	A region (F1 = δ 1.0-2.0 ppm; F2 = δ 60-220 ppm) of the gHMBC spectrum ($CDCl_3$, 600 MHz) of **2.37**	46
Figure 2.17	Conformation of (*R*)- and (*S*)-MTPA esters derived from a secondary alcohol	48
Figure 2.18	The model used to determine the absolute configurations of secondary alcohols using the modified Mosher's method	49
Figure 2.19	^{1}H ($CDCl_3$, 600 MHz) and ^{13}C ($CDCl_3$, 150 MHz) NMR spectra obtained for **2.38**	50

Figure 2.20	The gHMBC spectrum obtained for **2.38**	51
Figure 2.21	Up field section (0.50-4.00 ppm) of the ^{1}H NMR spectra of **2.37** (top) and the product of the attempted esterification of **2.37**	52
Figure 2.22	Light microscope image (x 40) of the cross-section through the pedal gland of *S. oculus,* stained with Toluidine Blue and showing the presence of different cell types	53
Figure 2.23	Light microscope image (x 20) of the cross section through glands of *S. oculus*, stained with Alcian Blue (right) and Aldehyde Fuchsin (left)	54
Figure 2.24	Photographs of the agitation of the underside of a *S.oculus* false limpet (left) and the capillary collection of the defensive mucus produced after agitation (right)	55
Figure 2.25	^{1}H NMR ($CDCl_3$, 600 MHz) of the isolated metabolites **2.2**, **2.34**, **2.35**, **2.36** and the crude mucus extract (top to bottom respectively)	56
Figure 3.1	Two *Leminda millecra* specimens photographed in Algoa Bay, 2010	60
Figure 3.2	*Leminda millecra* photographed feeding on a species of gorgonian (sea fan)	62
Figure 3.3	^{1}H ($CDCl_3$, 600 MHz) NMR spectra of the known metabolites, **3.1**, **3.6** and **3.8** isolated from *L. millecra*	67
Figure 3.4	^{13}C ($CDCl_3$, 150 MHz) NMR spectra of the known metabolites, **3.1**, **3.6** and **3.8** isolated from *L. millecra*	68
Figure 3.5	^{1}H ($CDCl_3$, 600 MHz) and ^{13}C ($CDCl_3$, 150 MHz) NMR spectra obtained for **3.16**	70
Figure 3.6	A region (F1 = δ 2.1-2.5 ppm; F2 = δ 115-175 ppm) of the gHMBC spectrum ($CDCl_3$, 600 MHz) of **3.16**	71
Figure 3.7	^{1}H ($CDCl_3$, 600 MHz) NMR spectra obtained for **3.16** isolated from *L. millecra* (top) and **3.16** synthesised from acetylation of **3.6** (bottom)	73
Figure 3.8	^{13}C NMR ($CDCl_3$, 150 MHz) spectra of **3.1** (top), **3.21** (middle) and **3.22** (bottom)	76
Figure 3.9	Stick representation of the computer-modelled global energy minimum conformation of millecrone A (**3.1**)	77
Figure 3.10	Downfield region (F1 = δ 6.3-7.5 ppm; F2 = δ 115-180 ppm) of the gHMBC spectrum ($CDCl_3$, 600 MHz) of **3.23**	78
Figure 3.11	Downfield region (F1 = δ 5.0-6.0 ppm; F2 = δ 165-170 ppm) of the gHMBC spectrum ($CDCl_3$, 600 MHz) of **3.25**	79

List of Schemes

		Page
Scheme 2.1	Biosynthesis of denticulatins A (**2.5**) and B (**2.6**)	13
Scheme 2.2	Proposed biosynthesis of siphonarin A (**2.7**) *via* a putative precyclisation intermediate	14
Scheme 2.3	Proposed mechanism for the formation of siserrone A (**2.21**) from dihydrosiphonarin A (**2.19**)	17
Scheme 2.4	The formation of baconipyrones A (**2.13**) and C (**2.14**) and siphonarin B (**2.8**) from a common precursor **2.27**	20
Scheme 2.5	Chromatography protocol used to isolate *Siphonaria capensis* metabolites	28
Scheme 2.6	Chromatography protocol used to isolate *Siphonaria oculus* metabolites	36
Scheme 2.7	Proposed possible formation of **2.2**, **2.35** and **2.36** from the theoretical precursor **2.39**	57
Scheme 3.1	Chromatography protocol used to isolate metabolites from *Leminda millecra*	65
Scheme 3.2	Proposed mechanism for the conjugate addition of hydride in the reduction of **3.1** to yield **3.21**	75

List of Tables

		Page
Table 2.1	^{1}H (600 MHz) and ^{13}C NMR (150 MHz) data obtained in $CDCl_3$ for **2.2** alongside those obtained previously by Beukes and Davies-Coleman	30
Table 2.2	^{1}H (600 MHz) and ^{13}C (150 MHz) NMR data obtained in $CDCl_3$ for **2.33** isolated from *S. capensis* and *T. costatus*	34
Table 2.3	^{1}H ($CDCl_3$, 600 MHz), ^{13}C ($CDCl_3$, 150 MHz) and 2D NMR data obtained for **2.35**	40
Table 2.4	^{1}H ($CDCl_3$, 600 MHz), ^{13}C ($CDCl_3$, 150 MHz) and 2D NMR data obtained for **2.36**	42
Table 2.5	^{1}H ($CDCl_3$, 600 MHz), ^{13}C ($CDCl_3$, 150 MHz) and 2D NMR data obtained for **2.37**	47
Table 3.1	IC_{50} values of compounds **3.9**-**3.15** tested against oesophageal cancer cells (WHCO1 cell line)	63
Table 3.2	^{13}C (150 MHz, $CDCl_3$) NMR data obtained for compounds **3.1**, **3.6** and **3.8** alongside those obtained by McPhail *et al.*	66
Table 3.3	Optical rotation data obtained for compounds **3.1**, **3.6** and **3.8** compared with those obtained by McPhail *et al*.	69
Table 3.4	^{1}H ($CDCl_3$, 600 MHz), ^{13}C ($CDCl_3$, 150 MHz) and 2D NMR data obtained for **3.16**	72

List of Abbreviations

1D	one dimensional
2D	two dimensional
$[\alpha]_D$	specific rotation
Ac	acetyl
aq	aqueous
br	broad
c	concentration (quoted in g/100 mL)
calcd	calculated
conc.	concentrated
d	doublet
DCC	1,3-dicyclohexylcarbodiimide
ddd	doublet of double doublets
DEPT	distortionless enhancement of polarisation transfer
DMAP	4-dimethylaminopyridine
EIMS	electron impact mass spectrometry
eq	molar equivalent
Et_3N	triethylamine
EtOAc	ethyl acetate
EtOH	ethanol
GC	gas chromatography
gCOSY	gradient ^1H-^1H homonuclear correlation spectroscopy
gHMBC	gradient heteronuclear multiple bond correlation
gHSQC	gradient heteronuclear single quantum coherence
h	hour(s)
HPLC	high performance liquid chromatography
HREIMS	high resolution electron impact mass spectrometry
IC_{50}	median inhibitory concentration
int.	integration
IR	infrared
LAH	lithium aluminium hydride
lit.	literature
m	multiplet
MeOH	methanol
mmol	millimoles
mol	moles
mp	melting point
MS	mass spectrometry
MTPA	α-methoxy-α-trifluoromethylphenylacetic acid
MTT	3-(4,5-dimethylthiazol-2-yl)-2,5-diphenyltetrazolium bromide
mult.	multiplicity
NCI	National Cancer Institute
NMR	nuclear magnetic resonance

NOE	nuclear Overhauser enhancement
NOESY	nuclear Overhauser enhancement spectroscopy
ocet	octet
ppm	parts per million
q	quartet
qn	quintet
R	alkyl group
rel. int	relative intensity
ROS	reactive oxygen species
RT	room temperature
s	singlet
SAM	*S*-adenosyl methionine
sat.	saturated
SCUBA	self-contained underwater breathing apparatus
sext	sextuplet
sp.	species
t	triplet
THF	tetrahydrofuran
TLC	thin layer chromatography

Acknowledgements

I am extremely grateful to the following people for their assistance:

Professor Davies-Coleman, my supervisor, for his support and guidance, for always having a plan and being excited about my work. I am very grateful to have him as a supervisor.

Dr. Sunny Sunassee and Dr. Wendy Popplewell for all their guidance and friendship throughout the course of this degree.

I am grateful to Shirley Pinchuck for the microscopy work included in this thesis and Shirley Parker-Nance for the SCUBA collections and photographs. I am also indebted to Mr Aubrey Sonemann for his amazing ability to repair virtually anything and to Ms. Benita Tarr for all her help over the years.

Many thanks to the past and present students of the Marine Biodiscovery Research Group, and members of the Chemistry Department. To all my friends who kept me going and especially Michael and Annalene, who have been of great emotional support to me. Special thanks to Ryan Young for his help in specimen collections, and Anne Conibear for helping me with computer modelling. To the lovely ladies of Lawrence Street for making my time spent in Grahamstown such a happy one, and especially to Jen for her prompt and thorough proof reading of this thesis.

Thank you to Rhodes University, Henderson and the National Research Foundation for funding my Masters degree.

Last but not least, thank you to my parents, Mick and Shirley, as well as Kirsten and Dawn for all your support and for always believing in me no matter how far away you are.

Chapter One
General Introduction

1.1 What are marine natural products?

Metabolites that do not appear to be involved in primary cellular functions (*e.g.* growth, energy transfer *etc.*) of the organism from which they are produced, are known as secondary metabolites, or natural products.[1] This production of 'non-essential' metabolites is neither energetically inexpensive nor do all organisms have the capacity to produce secondary metabolites. The production of secondary metabolites in the ocean is confined to a high proportion of marine invertebrates, plants, and microorganisms, and has not been reported from marine vertebrates.[1] Generally, the biosynthesis of specific secondary metabolites is restricted to a single species, or a few very closely related species, usually within the same genus.[1] The marine reef is a very competitive environment and the exact function of many marine natural products in the life of marine organisms is often unknown. Some of the roles for marine natural products may include chemical defense against predators (antifeedants); inter-species growth inhibition to reduce competition for space and nutrients; and intra-species chemical communication cues.[1, 2]

Oceans cover over 70% of the earth's surface, and comprise 95% of the earth's biosphere (the total volume available to life on earth).[1] The number of marine macro-organism species exceeds 2,000,000 while the total species diversity of marine micro-organisms is completely unknown.[3] The ocean possesses a significant variation in environmental conditions (*i.e.* light, temperature and pressure) along a vertical transect from the surface of the ocean to the ocean floor. Not unexpectedly, the diversity and even the size of marine life changes with this vertical environmental differentiation.[3] However, while the vertical transition in environmental conditions in the ocean is pronounced, the environmental conditions especially temperature, pressure and salinity at each defined depth have remained constant over a long period of time.[1] Sponges (Phylum: Polifera) are the oldest known multicellular life forms on the planet, diverging from metazoans over 600 million years ago.[4] Evolving in a stable marine, depth related, niche environment over hundreds of millions of years has enabled sponges and other marine invertebrates to divert energy from the day to day survival in a constantly changing environment, to the evolution of diverse protein mediated biosynthetic pathways for the production of a vast array of novel secondary metabolites.[1] The structures of marine natural products are therefore generally more chemically diverse than those produced by terrestrial plants and this is regularly reflected in reviews of marine natural products published annually in Natural Product Reports.[2]

Recently, Grabowski *et al.*[5] explored the concept of chemical space as it pertains to natural products and known drug compounds. They consequently showed that marine derived compounds have the broadest general coverage of this space, incorporating many drug relevant areas.[5] Bon and Waldmann[6] went further to explore the link between natural products and

protein space. Small molecule modulators of protein function are one of the driving forces in chemical biology research and drug discovery. Bon and Waldmann[6] draw attention to the fact that both protein folds and natural product scaffolds are highly conserved in nature. However, while changes in amino acid sequences may lead to changes in ligand binding sites in proteins, these binding sites will still conform to highly similar fold types.[5] Conversely, differentially substituted natural products, even within the same general structural class, can exhibit diverse biological activities. Therefore Bon and Waldmann[6] concluded that many natural products have evolved to interact with multiple proteins in order to illicit their biological functions and as an example they suggest that natural products responsible for toxicity reflect an ability to bind with multiple protein receptors. Similarly, Li and Vederas[7] have identified natural products as having privileged structures for drug discovery, through their production by enzymes, to interact with a broad range of functional proteins. They support their argument with evidence from the drug discovery process in which 7,000 polyketide natural products have yielded over 20 commercial drugs (0.3% hit rate) whereas the hit rate from high throughput screening of synthetic compound libraries is only at <0.001%. The link between marine natural products and new drug discovery is well established.[8] The problems of supply and variability have, however, hampered the development of marine natural products as novel pharmaceuticals and these challenges will be discussed in the next two Sections.

1.2 The challenge of supply

Marine natural products are routinely isolated in very small amounts *ca.* 0.1-10 mg/kg wet mass of marine invertebrate. The supply issue is most often encountered in the development of marine natural products as new pharmaceuticals where, for example, 1-5 kg per annum of an anti-cancer drug is required to meet the global demand for the drug once it is in clinical use.[9] Therefore, if the anti-cancer drug was isolated from a marine sponge this could require the non sustainable elimination of 3,000-16,000 metric tonnes of sponge per annum from the ocean which is obviously ecologically unacceptable.[9] Four possible strategies for overcoming the marine natural products supply problem are first, total synthesis; second, semi-synthesis; third, mariculture and fourth, fermentation of marine microbes. The chemical literature has many examples of how a combination of two or more of these four strategies have been used to resolve the supply challenge. Four selected examples will be presented here.

Currently there are only two marine natural products Ziconotide® (**1.1**) and Yondelis® (**1.2**) in clinical use, and a further 15 marine natural products in various phases of clinical development.[10] In this Section, we will briefly review the challenge of supply and how it was overcome for the two marine natural products in clinical use, one in clinical trials, and one in preclinical development.

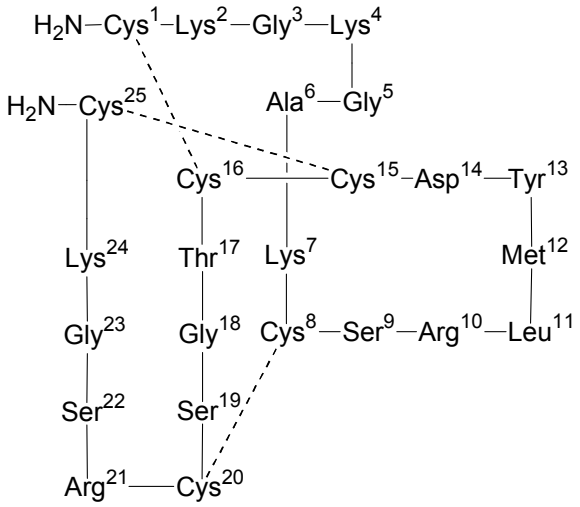

1.1

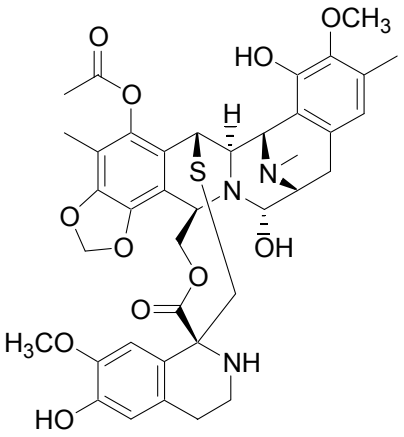

1.2

The ploypeptide, ω-conotoxin MVIIA (Ziconotide®, **1.1**) isolated from the marine cone snail *Conus magus*, was approved for clinical use in 2004, and was the first marine natural product to enter the market in over 25 years.[7, 11] Compound **1.1** is used in the treatment of chronic pain caused by spinal cord injuries, and is injected directly into the spinal column as its peptide structure would be digested if administered orally. The polypeptide structure of **1.1** may appear complex, however the total synthesis of this compound is achieved relatively simply through a series of peptide bond formations, allowing for the synthetic production of virtually unlimited amounts of the drug.[9] Chemical synthesis of natural product based pharmaceuticals is the ideal production method as it eliminates any adverse environmental impact. However, marine natural products often possess complex chemical structures, rich in chiral centers and their syntheses involve numerous individual reaction steps often rendering this method to resolve the supply problem practically impossible and economically non feasible.[12]

The second marine natural product currently in clinical use, **1.2**, Yondelis®, was introduced into clinical use in 2007 for the treatment of soft tissue sarcoma. Extracts from the sea squirt (ascidian, tunicate), *Ecteinascidia turbinata* were first found to have anti-tumor effects in 1969, but the active natural product, ecteinascidin-743 (ET-743, trabectedin, **1.2**) was only successfully isolated in low yields (1 g per metric tonne of ascidian) in 1990.[11] Mariculture of *E. turbinata* was used to obtain sufficient natural product for phase I and II clinical trials, however this method was not feasible for the production of larger quantities of **1.2** needed for phase III clinical trials, and eventual clinical use.[11] Although the natural product **1.2** has a complex chemical structure containing eight chiral centers, Corey *et al.*,[13] Endo *et al.*,[14] and Chen *et al.*[15] have all reported the total stereoselective synthesis of **1.2**. However, these syntheses all involved numerous synthetic

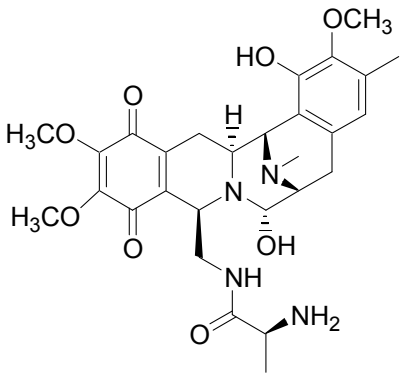

1.3

steps and were thus deemed economically nonviable for the commercial production of sufficient quantities of **1.2**. Cuevas *et al.*[16] noted that the structural features of **1.2** are very similar to cyanosafracin B (**1.3**) isolated from the bacterium *Pseudomonas fluorescens*, and suggested that the number of synthetic steps could be markedly reduced if **1.3** was used as a starting point in a semi-synthesis of **1.2**.[9] Compound **1.3** was accordingly produced through the fermentation of *P. fluorescens* and then used as a precursor in the semi-synthesis of **1.2**.[16] This semi-synthetic approach was a much more realistic method than total synthesis for the production of large quantities of **1.2** needed for phase III clinical trials, and eventual introduction into the market.[11]

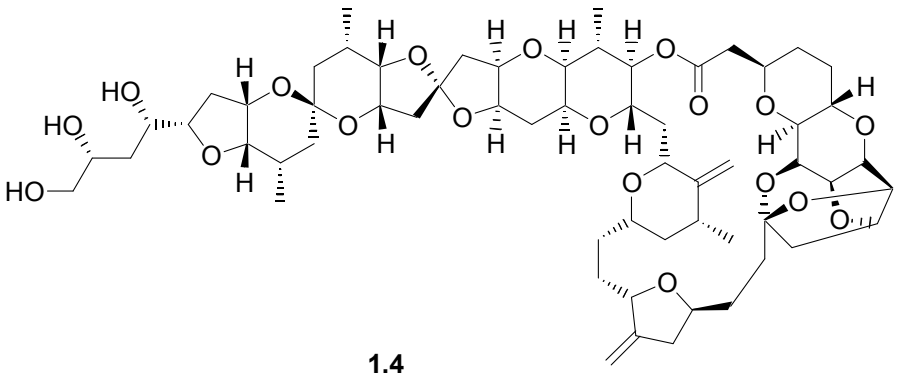

1.4

Halichondrin B (**1.4**), isolated from the sponge, *Lissodendoryx* sp. (300 mg per meteric tonne of sponge), is an extremely potent tubulin inhibitor.[12] *Lissodendoryx* sp. are rare deep water (-80 to -100 m) sponges found exclusively off the Kaikoura Peninsula, New Zealand.[17] The National Cancer Institute (NCI) commissioned a survey of the naturally occurring *Lissodendoryx* sp. populations of New Zealand and established that the estimated total biomass of *Lissodendoryx* sponge is approximately 289 tonnes, clearly indicating that wild harvest would never result in enough **1.4** for commercial use.[17] Mariculture of the *Lissodendoryx* sp. was subsequently carried out in Beatrix Harbour, New Zealand by the New Zealand Institute of Water and

Atmospheric Research (NIWA), in collaboration with the NCI.[17] *Lissodendoryx* sp. was successfully grown in mariculture, however, the overall yield of halichondrin B in the cultured sponge was not as high as that in the wild sponge.[17] Mariculture in general, requires a great deal of planning in terms of the positioning of the mariculture facility to ensure sustainability, as marine organisms are very susceptible to environmental changes and even seasonal changes will effect the growth of the sponge and their production of secondary metabolites.[17] Synthesis was once again believed to be the best option for the production of **1.4** for pre-clinical and clinical trials. Compound **1.4** has a complex structure containing 32 stereocenters and the first total synthesis of **1.4** developed by Kishi and co-workers,[18] required over 100 synthetic steps with an overall yield of less than 1%. In general an economically feasible drug synthesis should not exceed 30 synthetic steps.[12] The Japanese pharmaceutical company Eisai explored the possibility that smaller simpler analogs of **1.4** might still elicit the desired anti-tumor effect.[12] This structure-activity relationship study involved the preparation of over 200 analogues of **1.4** and resulted in the discovery of eribulin (E7289, **1.5**), a simplified analogue with 19 stereocenters, which exhibited improved cytotoxicity when compared with **1.4**.[12] This synthetic analogue is currently in phase III clinical trials for the treatment of metastatic breast cancer.[19] However the synthesis of **1.5** still requires more than 30 steps which makes its production for clinical use by synthesis possibly problematic and other options, as in the example of **1.2** described earlier, will possibly also need to be explored.[12]

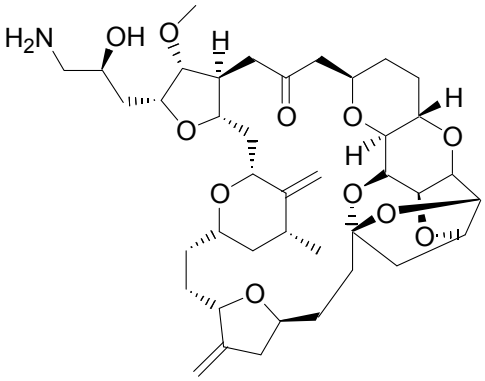

1.5

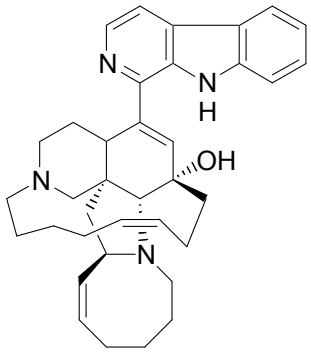

1.6

The manzamines, isolated from a number of different sponge species, are a group of promising alkaloid anti-malarial compounds in preclinical development.[20, 21] Manzamine A (**1.6**) was first isolated from the Caribbean sponge *Halicona* sp., and since then over 60 manzamine and related alkaloids have been isolated.[3, 21] Hill and co-workers[3] proposed that since the manzamines occur in a diverse range of unrelated sponges, these compounds may actually be produced by microbial (actinomycete) colonies within the sponge rather than the sponges themselves.[3] Isolation and culture of the different microbes contained in a sponge is required to determine

which symbiont is responsible for the production of the desired natural product. This can be challenging, as bacteria which inhabit sponges are often highly selective in terms of environmental conditions and often require the development of novel growth media for their successful culture.[9] However the advantages of successful microbial fermentation as a means of overcoming the marine natural product supply problem are enormous. Excitingly, Hill and co-workers[22] have succeeded in isolating the bacterium that produces **1.6**, which will hopefully provide the first steady supply of **1.6** and it's derivatives for further preclinical development.[22]

1.3 The challenge of variability

When a marine natural product is found to have promising bioactivity more of the secondary metabolite is required for further preclinical developments, hence a recollection of the marine organism is necessary. On recollection and attempted re-isolation of the bioactive metabolites, researchers are often met with changes in the concentrations of natural products, or even the diversity of the isolated compounds themselves. The marine environment is dynamic and so there are countless sources of variation in secondary metabolite production. Five of the most common possible sources of variability are taxonomic; genetic; microbial; seasonal and geographical and each of these will be discussed briefly in this Section.

Variability may arise if careful and concise taxonomic identification is not carried out during the initial collection of the marine invertebrate or algae. Organisms within the same genus often appear (to the untrained eye) to be similar or even identical, however the secondary metabolites produced by these related species may be dramatically different.[11] Many natural product chemists are not trained in taxonomy, and this lack of expertise can result in the unnecessary recollection of a particular species or even difficulty in re-identifying a species of interest for further study.[11]

As discussed earlier in Section 1.1, marine organisms have been continually evolving over millions of years to produce secondary metabolites that cater to their specific needs at a point in time. The enzymatic biosynthesis of these natural products is essentially controlled by the expression of a particular gene, or series of genes.[3] If the organism does not have a need for a particular secondary metabolite, gene expression can be switched off. For example, in as short a time as a decade, there has been the complete loss of expression of the once abundant secondary metabolite kahalalide A (**1.7**), originally isolated from a marine alga, *Bryopsis* sp..[3, 23] The reasons as to why *Bryopsis* are no longer producing **1.7** are unknown and this variation acts as a reminder to researchers, that the bioactive metabolites isolated today are the products of ongoing bio-organic evolution and may not necessarily persist into the future.[23]

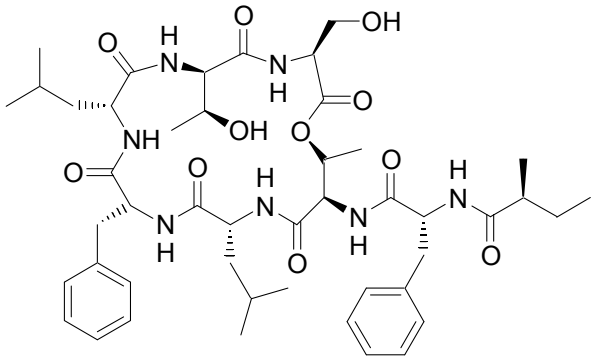

1.7

This genetic variability is possibly even more pronounced in marine microbes, as they have shorter life cycles enabling them to evolve and adapt to changing environments at a faster rate than marco-organisms.[23] As mentioned in Section 1.2 there is often a symbiosis between marine sponges and micro-organisms, and this is yet another source of variability. Micro-organisms have been found to constitute a considerable volume of a host sponge *e.g.* up to 40% of the volume of the sponge, *Xestospngia muta*, is made up of bacterial colonies.[22] Often there is a similarity in the microbial colonies found in sponges of different species, and from the same species in different geographical locations, which coupled with the fact that over 100 microbial species have been found to occur only in sponges, and not the surrounding seawater, suggests a long term symbiosis.[22] The exact role of marine microbes in the lives of sponges is unknown, however, there is evidence of possible parent-to-offspring transmission of microbes during sponge reproduction which again supports a positive symbiosis between sponge and microbe.[22] Individual sponges may differ in the proportion of microbial species present, creating a variation in the quantity or type of natural products isolated.[22]

Variability in the natural products produced by marine organisms is not solely due to evolutionary genetic advancement, and may occur throughout the life cycle of the organism due to seasonal changes. This seasonal effect was highlighted by Davies-Coleman and co-workers[24, 25] in a study of the sesquiterpene hydroquinone, rietone (**1.8**) isolated from the South African soft coral, *Alcyonium fauri*. A collection of *A. fauri* made in September 1994 afforded **1.8** in a 0.45% per dry mass of soft coral, which differed markedly from the 0.017% of **1.8** isolated from a new collection of *A. fauri* made a mere six month later in February 1995.[24] One of the many possible reasons for this seasonal variability may be an increased production of secondary metabolites for chemical defense during reproduction.[24]

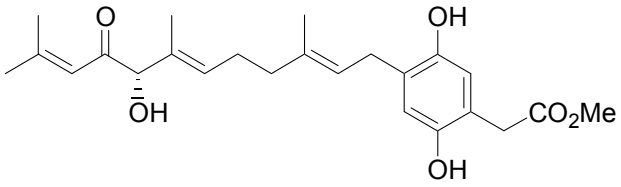

1.8

The geographical distribution of a marine organism can be another source of natural product variability, which arises due to changes in environmental conditions, available diet or even predators.[11] Nudibranchs (sea slugs) which sequester secondary metabolites from their diet are obviously susceptible to variation arising from a change in their dietary species at different geographical locations.[26] The South African nudibranch *Leminda millecra* has illustrated geographical variability in its sequestered secondary metabolite profile,[27, 28] and the geographical variability in secondary metabolites in this species will be discussed in detail in Chapter Three of this thesis.

1.4 Aims of this thesis

The aim of this thesis was to investigate the variability occurring in the secondary metabolites produced by three South African marine molluscs. We initially investigated variability in polypropionate natural products produced *via de novo* biosynthesis in the false limpet *Siphonaria capensis*, comparing the metabolites isolated from specimens of this species collected in 1998 with those isolated from specimens of the same species collected in the same location over ten years later. Over the last decade there have been improvements in the chromatographic methods used to isolate marine natural products and we were able to apply some of these new methods to our reinvestigation of the secondary metabolites of *S. capensis* and the other species in this study. *Siphonaria oculus* is closely related to *S. capensis* and our objective in studying the polypropionate secondary metabolites produced by this species was to explore the overlap of secondary metabolites in two similar species living in close proximity to each other.

Finally, we investigated the secondary metabolites in extracts made from a fresh collection of the nudibranch *Leminda millecra* from Algoa Bay. Our intention was to document possible variability in the sequestered metabolites occurring in this species a decade after the original collection also made in Algoa Bay. We also intended to increase our supply of cytotoxic prenylated toluhydroquinones and toluquinones reported to occur in these species.[28] These compounds are required for further mechanistic studies into the apoptosis of oesophageal cancer cells.

Chapter Two

Polypropionates from Two Species of South African *Siphonaria*

2.1 Introduction

2.1.1 General biology of *Siphonaria*

Marine molluscs of the genus *Siphonaria* (Sub-class: Pulmonata, Family: Siphonariidae), commonly known as false limpets, are shelled, air-breathing herbivores that are believed to have a marine ancestry and are possibly an evolutionary link between terrestrial and marine gastropod molluscs.[29, 30] *Siphonaria* species differ from true limpets (Sub-class: Prosobranchia, Families: Patellidae and Acmaedae) through the loss of their original gills.[30] Instead, the Siphonariidae, as with all pulmonates, have a lung cavity with a pneumostome on the right side of their body that allows for the intake of air whilst on land, along with a dorsal mantle that has evolved into an elaborate series of folds forming a secondary gill enabling *Siphonaria* to breathe when fully submerged in water.[30, 31] This ability to respire aerobically both in air and water enable siphonariids to inhabit intertidal zones and they are found along rocky coast lines in predominantly temperate regions.[30, 32]

Siphonariid limpets are able to fix themselves to rocks and clear a small area around themselves known as a home scar, which they defend.[30] In order to feed, siphonariids leave their home scars and are more easily displaced from rock surfaces by predators, however many species of *Siphonaria* are still avoided by predators implying an added chemical defence.[30] When disturbed, siphonariid limpets secrete a sticky white mucus from their lateral pedal glands.[30] The mucus released by *Siphonaria* is rich in polypropionates which are believed to deter predators, but little research has been done to confirm the role of polypropionates in chemical defence.[30, 33] McQuaid and co-workers[33] investigated the effectiveness of the mucus produced by *Siphonaria capensis* at deterring predators, and discovered that whelks and starfish are repelled, with the mucus effectively inducing a temporary paralysis of the tube foot-tissue of starfish.[33] On the other hand, tide pool fish were not completely deterred but showed a distaste for *S. capensis* as well as other food sources coated in a crude extract of the mucus.[33] *Siphonaria* have a radula that consists of rows of small weak teeth which limit siphonariids to grazing on predominantly soft macroalgae although lichens, blue-algae, microalgae and diatoms have also been found in their gut contents.[30, 33] The polypropionates contained in the siphonariids' toxic mucus are therefore believed to be biosynthesised *de novo* as the *Siphonaria* diet is neither focussed on specific species of algae or lichens nor rich in secondary metabolites.[30, 33]

2.1.2 Biosynthesis of polypropionate secondary metabolites

Polypropionate metabolites, made up of repeating 3 carbon propionate units, are also known to be produced by insects, bacteria, and fungi.[34] The polypropionate backbone of these compounds is believed to arise either due to the propionate elongation of a growing chain or the *S*-adenosyl methionine (SAM)-dependant methylation of an acetate derived chain.[34, 35] El-Sayed *et al*.[36] have shown that bacteria produce polypropionates using both pathways whilst fungi only utilise the acetate/SAM pathway to produce polypropionates.[35, 36]

Siphonariid polypropionate metabolites can be grouped into two classes according to their structures and stereochemistry at specific positions. Darias *et al.*[29] have categorised Class I polypropionates as polypropionates which are structurally mundane, *i.e.* consisting of a linear chain of at least three propionate subunits, where the stereogenic centres containing methyl groups along this chain all have an *S* configuration. Secondary metabolites within this class can have an acyclic structure like that of siphonarienone (**2.1**), or either a furanone ring moiety as in siphonarienfuranone (**2.2**) or 2-pyrone ring system *e.g.* pectinatone (**2.3**).[29]

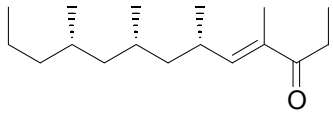

2.1

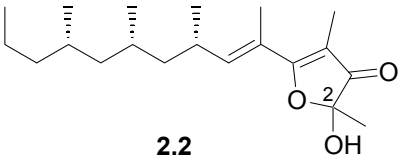

2.2

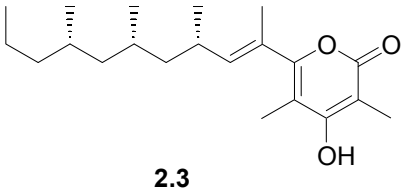

2.3

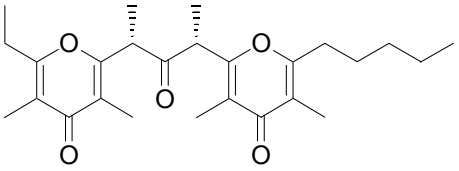

2.4

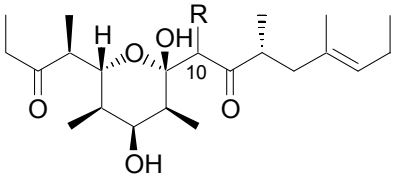

2.5 R = α-Me
2.6 R = β-Me

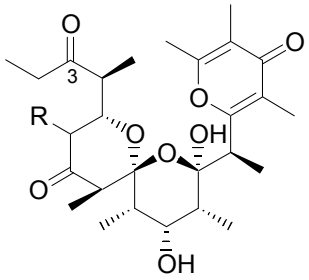

2.7 R = Me
2.8 R = Et

Siphonariid metabolites within Class II possess an identical configuration at only some of the comparable stereocenters and are usually comprised of a profuse polyoxygenated network that is frequently cyclised. On cyclisation, Class II polypropionates can either form γ-pyrone rings as in maurapyrone A (**2.4**) or a hemiacetal ring, *e.g.* denticulatins A (**2.5**) and B (**2.6**), or may even contain both ring systems as in siphonarin A (**2.7**) and B (**2.8**).[29] The complex arrangement of functional groups in the Class II polypropionate metabolites makes their biosynthesis more challenging to explain and it is therefore probably not surprising that at present, polypropionate biosynthesis has only been studied in two siphonariid species, both of which produce Class II type polypropionates.[37, 38] Both studies will be discussed here together with some recent biosynthetic work on polypropionates metabolised by a related marine sacoglossian mollusc which is likely to use similar biosynthetic pathways to produce these compounds.[35]

Manker *et al*.[37] investigated the biosynthesis of **2.5** and **2.6** by injecting [1-^{14}C]-acetate and [1-^{14}C]-propionate into specimens of *Siphonaria denticulata*. After six days of incubation, **2.5** and **2.6** were found to have incorporated the radioactive labelled propionate, whilst no significant amount of labelled acetate was incorporated which implies that *S. denticulate* utilises propionate derived biosynthesis exclusively (Scheme 2.1).[37]

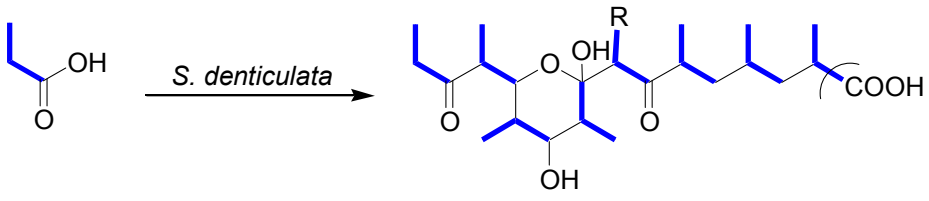

2.5 R = α-Me
2.6 R = β-Me

Scheme 2.1: Biosynthesis of denticulatins A (**2.5**) and B (**2.6**). (Note: Facile loss of CO_2 will afford **2.5** and **2.6**).[37]

Polypropionate biosynthesis was subsequently studied in the Australian siphonariid *Siphonaria zelandica*. Garson and co-workers[38] injected [1-^{14}C]-propionate into the foot tissue of *S. zelandica* and after four days of incubation the radio-labelled metabolites, **2.7** and **2.8** were isolated proving their propionate origin. Garson and co-workers[38] consequently proposed that **2.7** is assembled from an acetate starter unit followed by nine propionate units producing a hypothetical acyclic polypropionate precursor which subsequently cyclises, as shown in Scheme 2.2.

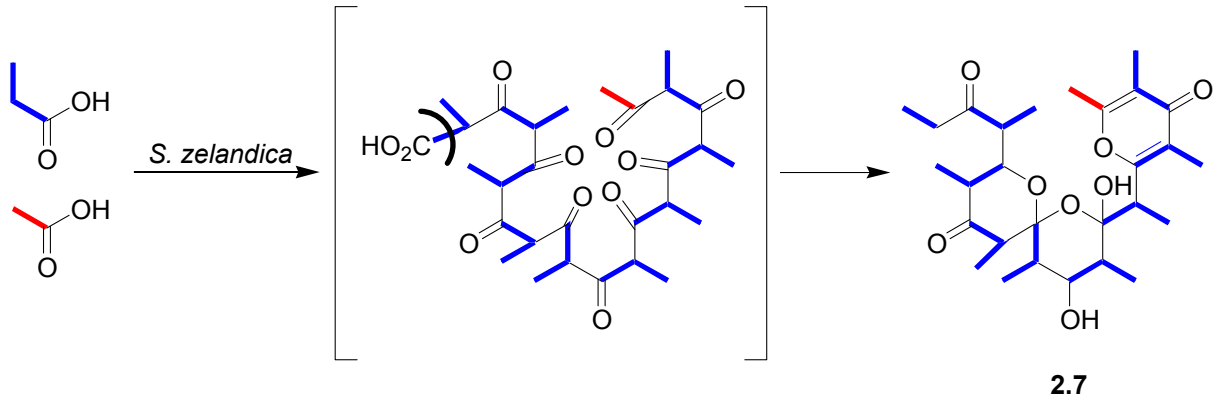

Scheme 2.2: Proposed biosynthesis of siphonarin A (**2.7**) *via* a putative pre-cyclisation intermediate.[38]

In a recent study, Cimino and co-workers[35] investigated the biosynthesis of polypropionates metabolites from the sacoglossian mollusc *Placida dendritica*. Three separate feeding experiments were performed, in which groups of *P. dendritica* were injected with the following precursors; sodium [1-^{13}C]-propionate, sodium [2-^{13}C]-acetate and sodium [1,2-$^{13}C_2$]-acetate. Placidene-A (**2.9**), placidene-C (**2.10**) and placidene-E (**2.11**) were chosen as model compounds in this study as their carbon skeletons suggested either regular propionate or mixed acetate/propionate biosynthetic pathways.[35] Analysis of the ^{13}C NMR spectrum of the purified compounds from the different feeding experiments allowed Cimino and co-workers[35] to establish that **2.9** was biosynthesised from propionate subunits exclusively whilst **2.10** and **2.11** also required incorporation of labelled acetate. Placidene-E incorporated a radio-labelled acetate starter unit and the chain was further elongated with the addition of propionate units before undergoing cyclisation. Compound **2.10**, however, was shown to be biosynthesised using an alternating acetate and propionate unit assembly as illustrated in Figure 2.1.[35]

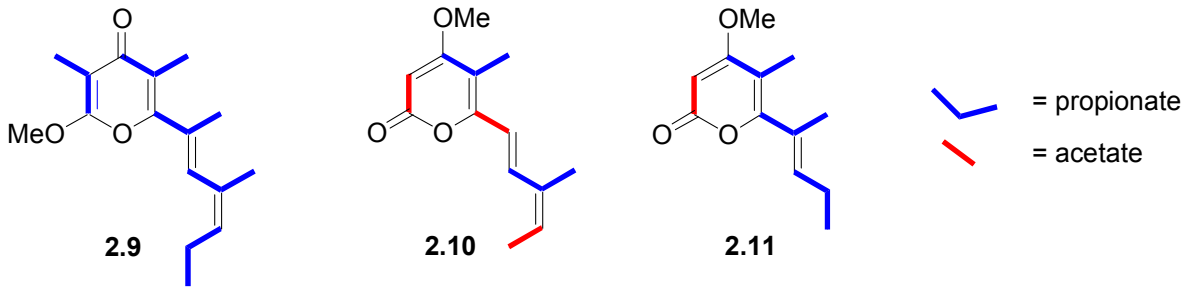

Figure 2.1: Distribution of acetate and propionate subunits in placidene A (**2.9**), C (**2.10**) and E (**2.11**).[35]

Biosynthetic investigations on siphonariid polypropionate metabolites have therefore shown that molluscs use propionate elongation of a growing chain rather than the *S*-adenosyl methionine (SAM)-dependant methylation of an acetate derived chain.[35, 37, 38]

2.1.3 Polypropionate metabolites isolated from *Siphonaria* species (1998-2010)

The marine polypropionate research field was last reviewed extensively in 1998 by Davies-Coleman and Garson[34] and later summarised by Garson, Darias and Davies-Coleman according to the geographical distribution of *Siphonaria* species.[29, 31, 32] Only three publications describing new polypropionate metabolites have been reported from *Siphonaria* species in the last twelve years and the isolation of these new polypropionate compounds is presented here in chronological order. The description of the new polypropionates isolated from *Siphonaria* species will be followed by a brief overview of two selected recent syntheses of siphonariid polypropionates. The first, a synthesis of capensifuranone (**2.12**) which confirmed the absolute stereochemistry of this compound is included because of the relevance of **2.12** to the re-investigation of the polypropionate metabolites produced by *Siphonaria capensis* discussed in Section 2.3.[39] The second synthesis of baconipyrone A (**2.13**), C (**2.14**) and siphonarin B **2.8** is included here because of the significant contribution this synthesis has made to our understanding of the biosynthesis of polycyclic and seemingly non-contiguous siphonariid polypropionates.[40]

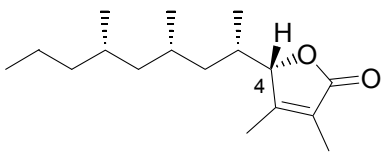

2.12

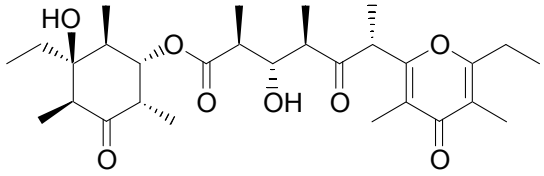

2.13

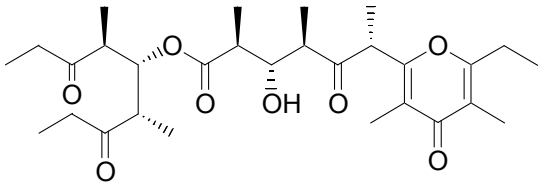

2.14

Rovirosa and co-workers[41] isolated a new polypropionate (**2.15**) and two known polypropionates, norsiphonarienolone (**2.16**) and furanone (**2.17**) from *Siphonaria lessoni* collected from the central coast of Chile.[41]

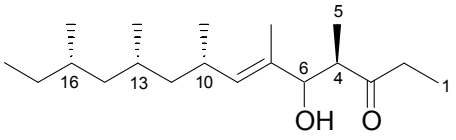

2.15

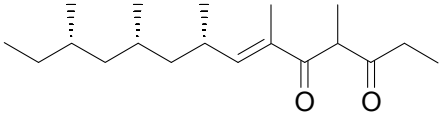

2.16

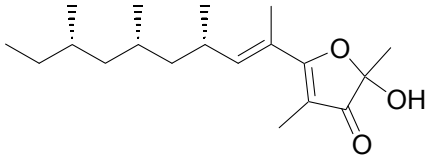

2.17

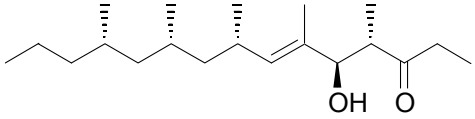

2.18

The ^{1}H and ^{13}C NMR data obtained for polypropionate **2.15** were similar to those obtained for siphonarienolone (**2.18**), a polypropionate previously isolated from *Siphonaria grisea* found in the Canary Islands.[42] Although the optical rotation observed for **2.15** ($[\alpha]_D$ = + 52.6^{o}) was different to that of **2.18** ($[\alpha]_D$ = + 19.6^{o}), the positive value for the rotation of **2.15** prompted Rovirosa *et al.*[41] to suggest a similar stereochemistry for **2.15** to that proposed for **2.18**.[41] The relative configuration at C-10, C-13 and C-16 in **2.15** was proposed by Rovirosa *et al*.[41] after comparison of the NMR data of **2.15** with those reported for polypropionates **2.16** and **2.17** previously isolated from *S. lessoni* by the same research group.[43] Surprisingly, given that the protons are on contiguous carbon atoms in an acyclic structure, the relative configuration at C-4 for **2.15** was determined spectroscopically using a ROESY NMR experiment which revealed a correlation between H-4 and H_3-5 tenuously suggesting a *syn* relationship between these protons.[41]

Two endemic South African *Siphonaria* species have also been investigated since the review by Davies-Coleman and Garson.[34] An initial investigation of *Siphonaria serrata* collected from the former Ciskei coast of South Africa afforded the known dihydrosiphonarins A (**2.19**) and B (**2.20**) and the new γ-pyrone siserrone A (**2.21**) as a minor metabolite, which the authors proposed may arise from a rearrangement of **2.19** (Scheme 2.3) .[44]

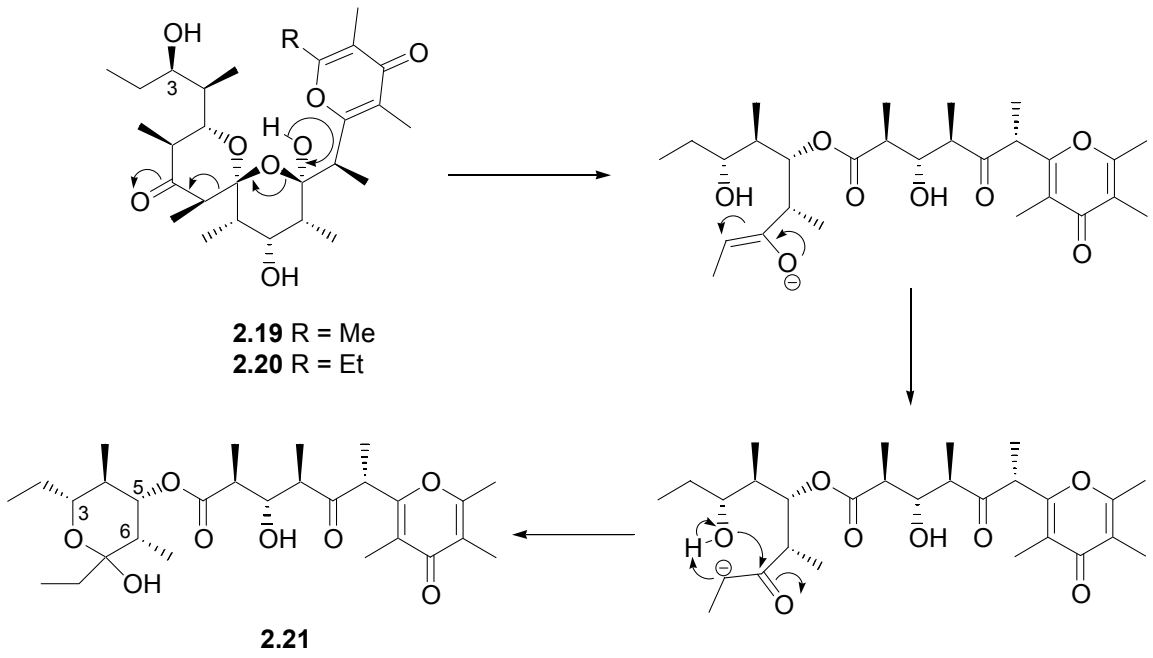

Scheme 2.3: Proposed mechanism for the formation of siserrone A (**2.21**) from dihydrosiphonarin A (**2.19**).[44]

Dihydrosiphonarins A and B were previously isolated from both *Siphonaria normalis* (Hawaii) and *Siphonaria lacinosa* (Australia).[29, 34] Interestingly, a second collection of *S. serrata* from the same location only resulted in the isolation of siserrone A and the structure for **2.21** was elucidated using NMR spectroscopy with the relative configuration of the cyclic hemiketal moiety assigned using the key ROESY NMR correlations between H-5 and H-6 placing the latter proton in an equatorial position. The large $J_{4,5}$ (11.2 Hz) coupling constant was indicative of a *trans* diaxial relationship between H-4 and H-5 whilst the relationship between H-5 and H-6 resulted in a smaller $J_{5,6}$ coupling constant (4.9 Hz) implying a *gauche* arrangement.[44]

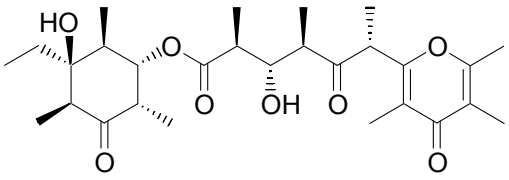

2.22

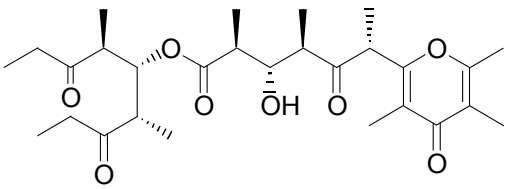

2.23

The majority of marine polypropionates have a contiguous backbone structure where the C_3 propionate subunits are adjacent to each other as described in section 2.1.2. However, **2.21** has a noncontiguous backbone structure similar to that of the baconipyrones A-D [**2.13**, **2.22**, **2.14**, and **2.23**] which are polypropionate esters previously isolated from *S. baconi* (Australia).[29] Faulkner and coworkers[45] have proposed that the noncontiguous polypropionate arrangement found in pyrones **2.13**, **2.22**, **2.14**, and **2.23** is derived biosynthetically *via* a retro-aldol rearrangement of another *S. baconi* metabolite, **2.7**, only differing from the dihydrosiphonarins **2.19** and **2.20** through oxidation of the secondary alcohol at C-3.[45] Compound **2.19** isolated from the first collection of *S. serrata* was therefore proposed to possibly be a similar precursor of the noncontiguous **2.21** as illustrated in Scheme 2.3,and this could also possibly explain why they were not isolated from the second collection.[44]

At the same time Davies-Coleman and co-workers[44] were contemplating the biosynthetic origin of **2.21**, Garson and co-workers[44] were encountering a similar rearrangement of **2.5** and **2.6**, previously isolated form *Siphonaria denticulata* (Australia)[29] and successfully synthesised by Paterson *et al.*.[46] Pure synthetic samples of **2.5** and **2.6,** which are C-10 epimers of each other, were found to interconvert on silica gel, which led Paterson *et al.*[46] to propose that *S. denticulata* produces a single polypropionate metabolite that epimerises at C-10 during chromatographic isolation.[46] In order to derivatise **2.5**, Brecknell *et al.*[44] attempted a Sharpless AD-mix asymmetric dihydroxlylation of **2.5**.[44, 47] The resultant unexpected product, however, was funiculatin A (**2.24**) a polypropionate previously isolated from *Siphonaria funiculata* (Australia).[48] Brecknell *et al.*[44] proposed that the mild basic conditions required for this dihydroxylation reaction had triggered a rearrangement of **2.5**. Interestingly, in the presence of base (K_2CO_3) **2.5** afforded the unstable non-contiguous polypropionate ester (**2.25**) which decomposed to the acid (**2.26**).[44]

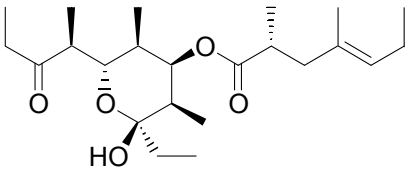

2.25

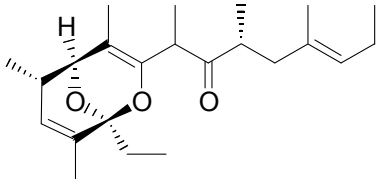

2.24

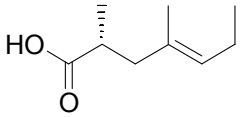

2.26

Suspicious that non-contiguous polypropionate esters may be artifacts of the isolation procedure Brecknell *et al.*[44] attempted to re-isolate the baconipyrones **2.13**, **2.22**, **2.14**, and **2.23**. After careful extraction, TLC and NMR examination of the extract from a fresh collection of *S. baconi* from Sorrento (Australia) indicated that none of the baconipyrones were detected, thus casting suspicion on their natural origin and providing further evidence to suggest that the natural product status of non-contiguous polypropionate esters should be viewed with caution.[44]

Recently, Beye and Ward[40] successfully synthesised a proposed precursor (**2.27**) for **2.13**, **2.14** and **2.8**.[40] Beye and Ward[40] proposed that the precursor **2.27** undergoes initial dual keto-enol tautomerism of the 7,9-diketone resulting in a labile stereocenter at C-8, which on further cyclisation via nucleophillic attack of the C-5 hydroxyl on the C-9 carbonyl will afford four possible diastereomers of the hemiacetal (**2.28**) (Scheme 2.4).[40] Attack of the C-5 hydroxyl on the C-7 carbonyl is not favoured because a four-membered ring, as opposed to a more energetically favourable six-membered ring, would be generated. Direct cyclisation of the more stable of the two 8*S* diastereomers (**2.28a**), in which all the alkyl substituents are equal, will produce **2.8** and this has been shown experimentally where **2.27** readily isomerised to the thermodynamically more stable siphonarin B (**2.8**), a process accelerated in the presence of imidazole.[40] Beyes and Ward[40] also proposed that any of the four hemiacetal diastereomers (**2.28a-d**) could afford **2.14** through retro-Claisen rearrangement. Compound **2.14**, in turn, could convert *via* aldol cyclisation to **2.13**. The formation of baconipyrones A and C from the dihydroxytetranone precursor **2.27** was shown experimentally when its cyclisation product **2.8**, treated with neutral alumina in refluxing ethanol, yielded a mixture of **2.13**, **2.14**, **2.27** and unreacted starting material.[40] The work of Beye and Ward[40] demonstrates that baconipyrones A and C can be derived from siphonarin **2.8** and precursor **2.27** under non enzymatic conditions again confirming that non-contiguous polypropionate esters are probably isolation artifacts.[40]

The second South African *Siphonaria* species to be investigated within the last 12 years is *Siphonaria capensis*.[49] Samples of *S. capensis* were collected on the south-east coast of South Africa, near the mouth of the Bushman's River.[49] Extraction and isolation of *S. capensis* secondary metabolites yielded C-2 epimeric mixtures of *E* and *Z* siphonarienfuranone (**2.2** and **2.29** respectively) previously isolated from *S. grisea*[42] and *S. pectinata*[29] as well as three novel polypropionates, capensinone (**2.30**), capensifuranone, **2.12**, and (2E, 4S, 6S, 8S)-2, 4, 6, 8-tetramethyl-2-undecenoic acid (**2.31**).[49] The NMR data for polypropionates **2.2** and **2.29** were consistent with those published previously, however the optical rotation of the *S. capensis* metabolite **2.2** ($[\alpha]_D$ +54) differed from the optical rotation reported by Nortre *et al.*[42] for siphonarienfuranone isolated form *S. grisea* ($[\alpha]_D$ +102).[49] Davies-Coleman and Beukes[49] proposed that the difference in optical rotation observed for the siphonarienfuranone isolated from

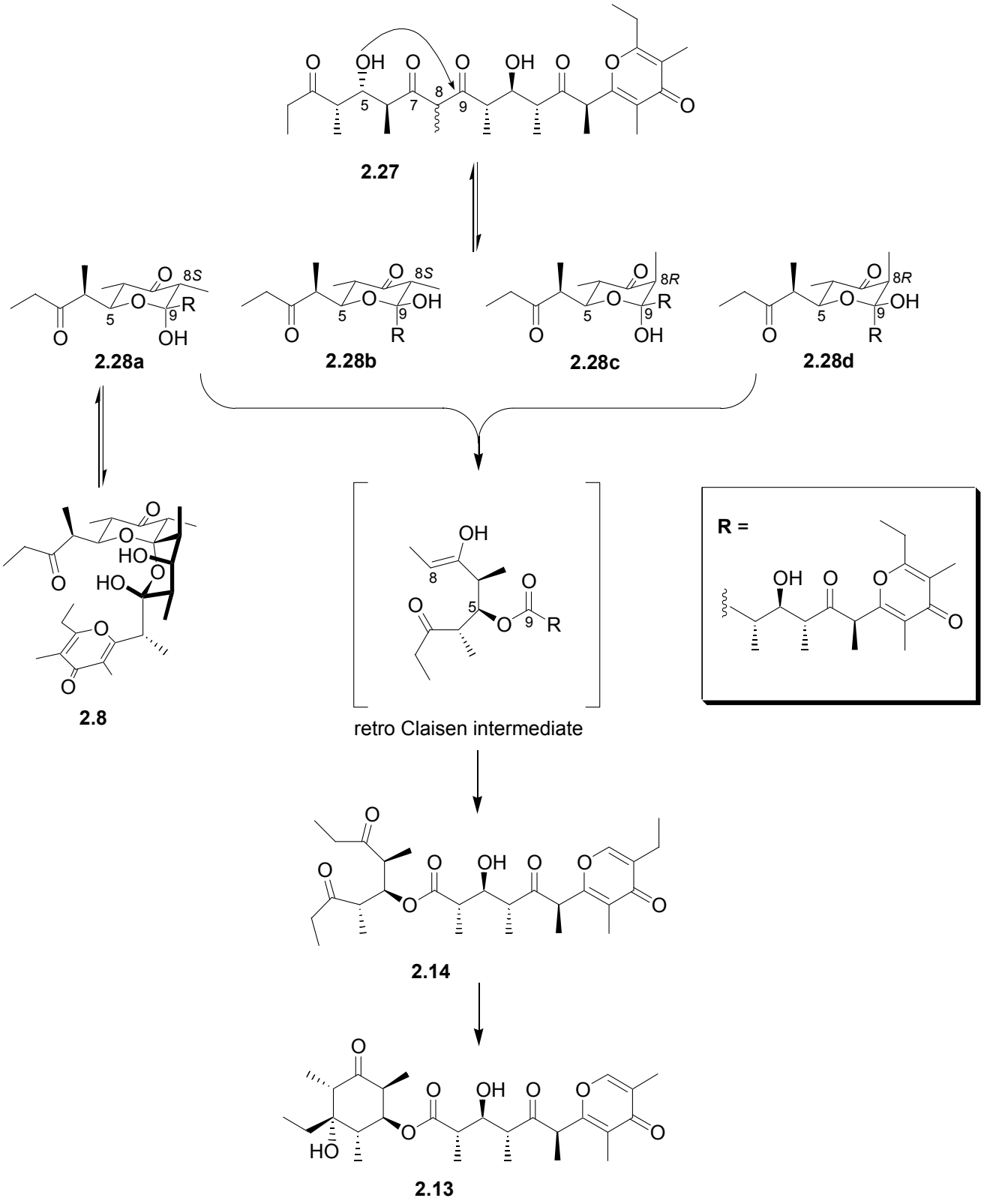

Scheme 2.4: The formation of baconipyrones A (**2.13**) and C (**2.14**) and siphonarin B (**2.8**) from a common precursor **2.27**.[40]

different *Siphonaria* species was possibly due to the slow isomerisation of polypropionate **2.2** to **2.29**.[49] Ruthenium tetroxide mediated oxidative cleavage of **2.2** gave (2S, 4S, 6S)-2,4,6 trimethylnonanoic acid, the optical rotation of which was consistent with published values, thus confirming the absolute configuration of the three chiral centres in the side chain of **2.2** and from biosynthetic arguments **2.29**.[49] Ruthenium tetroxide oxidative cleavage was also used to determine the absolute configuration of the acyclic chiral centres in **2.31**.[49]

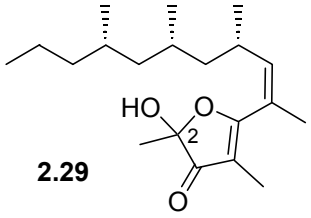

2.29

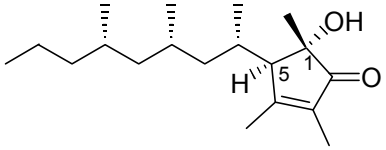

2.30

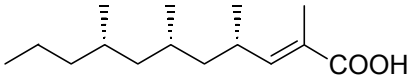

2.31

The structures of novel polypropionates **2.12** and **2.30** were determined from NMR data. The structure of capensinone is unusual in that it is the only marine polypropionate metabolite containing a cyclopentanone moiety.[49] The relative configuration at C-1 and C-5 in **2.30** was proposed by Davies-Colman and Beukes[49] after analysis of a series of 1D-NOE difference experiments.[49] However, the stereochemistry of C-4 in **2.12** could not be determined.[49]

Recently, however, Williams *et al*.[39] successfully synthesised **2.12** and its C-4 epimer (**2.32**) through a series of asymmetric conjugate addition reactions. The optical rotation and the ^{1}H and ^{13}C NMR data of synthetic capensifuranone were identical with those of **2.30** isolated from *S. capensis*. Williams *et al.*[39] therefore established an *S* configuration at C-4 in the natural product.[39]

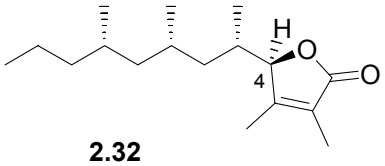

2.32

Capensinone and capensifuranone have an unusual vicinal arrangement of olefinic methyls in their cyclopentanone and furanone rings respectively, which disrupts the contiguous pattern of propionate subunits that is usually seen in siphonariid polypropionate metabolites.[49] The

biosynthesis of **2.30** and **2.12** is therefore unclear but Davies-Coleman and Beukes[49] proposed that the biosynthesis of **2.12** may involve the incorporation of an acetate unit into the polypropionate in a biosynthesis similar to that established by Cimino and co-workers[35], in the radio-labelling study of **2.10** isolated from the sacoglossian mollusc *Placida dendritica*.[35] A possible combination of five propionate subunits and an acetate unit is shown in Figure 2.2.[49] The possibility that **2.12** may be an artefact of the extraction procedures could also not be eliminated.[49]

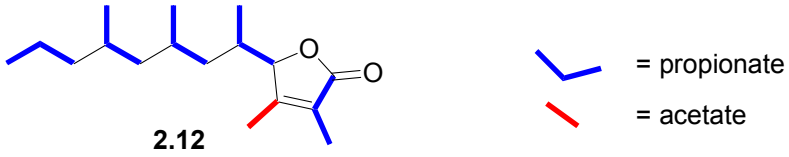

2.12

Figure 2.2: Proposed distribution of acetate and propionate units in **2.12**.[49]

2.2 Chromatographic material

The possibility of siphonariid metabolites rearranging to form artifacts during isolation using silica[40, 44, 46, 49] encouraged us to investigate alternative chromatographic media, *viz* poly(styrene-divinylbezene) (PSDVB) and DIOL. Background information about both these chromatography media is provided below.

2.2.1 Poly(styrene-divinylbezene) (PSDVB)

The initial fractionation of crude *Siphonaria* extracts utilised poly(styrene-divinylbezene) (PSDVB), a reverse-phase stationary phase. The numerous cross-linkages in the polymeric structure (Figure 2.3) of PSDVB make it a rigid, macroporous support to which metabolites are able to adsorb. The absence of polar sites in PSDVB ensures the separation of even the most polar metabolites such as quaternary ammonium salts and basic compounds without any threat of these metabolites irreversibly binding to the resin.[50] PSDVB can be used successfully throughout a large pH range (pH 1-13), it is inert in most organic solvents and can withstand very ionic solutions allowing for a wide range of potential applications.[51] As a general rule of thumb, we prepared chromatography columns of PSDVB resin in which 1 mL of resin was used for each 25 mg of extract.[52]

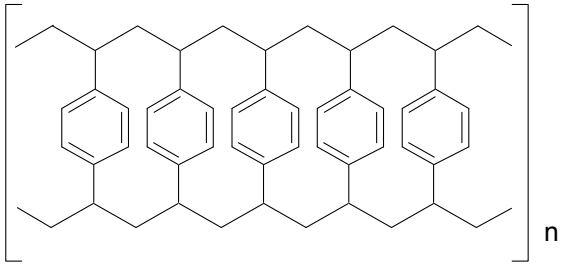

Figure 2.3: The chemical structure of the stationary phase poly(styrene-divinylbezene) (PSDVB).[51]

The dry PSDVB resin can by loaded into a standard open chromatography column without forming a slurry as the formation of air bubbles or the disruption for the column bed is not an issue in this adsorption chromatography method. The PSDVB resin is initially primed by washing with water to remove any fine resin particles, followed by three column volumes of the polar, water miscible solvent (normally the solvent used in extraction, *i.e*. methanol or acetone).

The general technique employed to initially adsorb all the non-polar, semi-polar, and polar metabolites, from the crude extract onto the PSDVB resin, is known as cyclic loading and was first developed in 1996 by West and Northcote, in the fractionation of crude extracts of the New Zealand sponge *Mycale hentscheli*.[51] A typical PSDVB chromatography column is depicted in Figure 2.4.

In the process of cyclic loading (Figure 2.4), an acetone or methanol solution of the crude extract is initially loaded onto the column and allowed to pass slowly through the PSDVB resin, ensuring maximum interaction and therefore adsorption of the non-polar metabolites contained in the extract onto the PSDVB beads.[51] The eluent is collected and diluted with water to approximately 50% of the original organic concentration and passed through the same column again, with metabolites of mid-polarity adhering to the PSDVB resin during this second loading.[52] This process of dilution and re-loading is continued, allowing more polar metabolites to be sequentially adsorbed until the “organic” concentration of eluent collected has been diluted with water to 12.5% of the original extract. At this stage, the eluent will often appear much paler than the crude extract loaded initially, indicating that majority of the compounds of interest have been adsorbed on the PSDVB resin beads.[52]

Normally, if a large volume of water is added to a crude marine extract, any non-polar fats, steroids or triglycerides present immediately precipitate out of solution, but since the crude extract has passed through the PSDVB resin before water is added, all of these non-polar metabolites are adsorbed on to the PSDVB resin beads. However, care must still be taken when the aqueous

dilutions are made to prevent a precipitate forming. In the event that a precipitation does from on dilution, the original organic solvent used in extraction can be added until the precipitate re-dissolves, and the aqueous solution passed through the PSDVB column before continuing with the dilutions as previously described.[52]

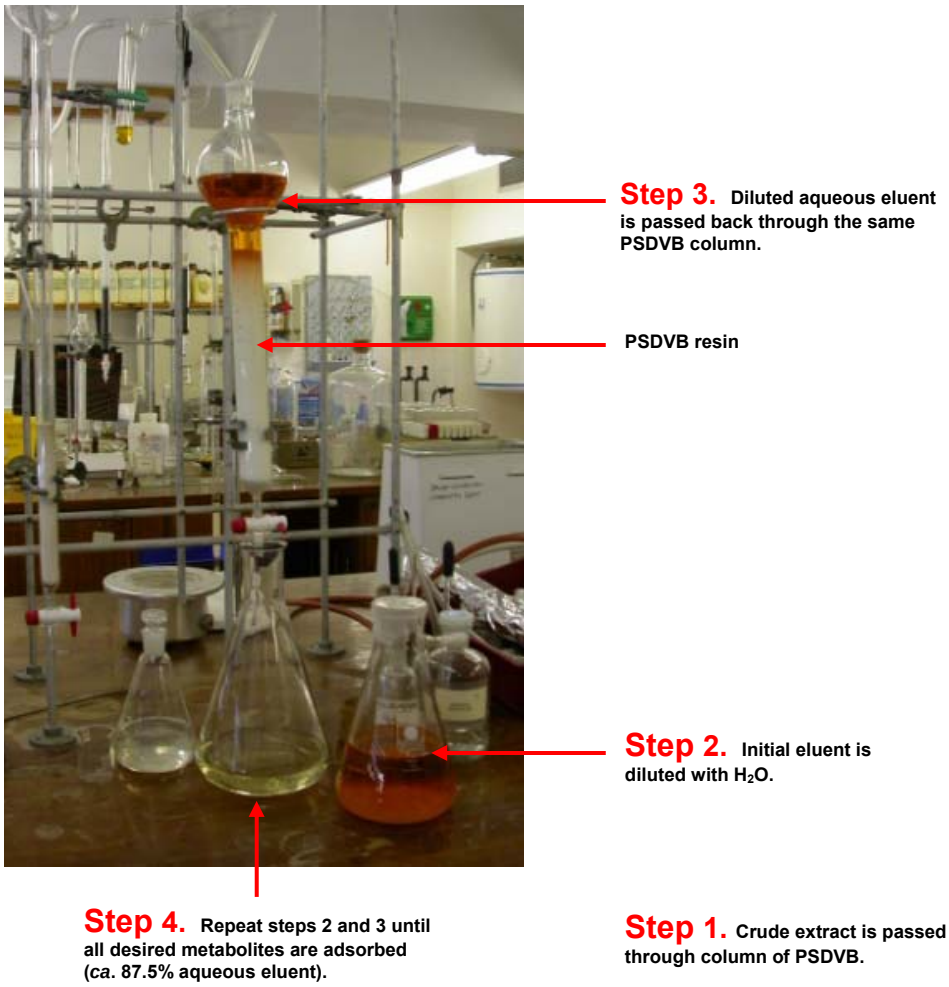

Figure 2.4: Photograph illustrating the process of cyclic loading using PSDVB stationary phase.

Once the PSDVB column has been loaded, it is washed with three column volumes of water to remove any inorganic salts (seawater contains *ca.* 3.5% sodium chloride). The column is then eluted with aqueous acetone or methanol, in aliquots of decreasing polarity.[52] This elution regime will result in the most polar metabolites eluted first and the least polar metabolites last. Usually, the highest proportion or biologically active metabolites are found within the mid-polar fractions and the unwanted sterols and fatty acids occur in the non-polar fractions with the organic salts, sugars and proteins emerging in the polar fractions.[51]

Fractions containing mixtures of water and organic solvents are difficult to reduce *in vacuo* on a rotary evaporator due to their potential to 'bump' when placed under vacuum. To overcome this problem, a procedure known as back-loading can be used. Back-loading is a variation on cyclic-loading where that eluted fraction is cyclic-loaded back onto a smaller PSDVB column and eluted with a smaller volume of pure organic solvent, effectively concentrating the fraction and facilitating the removal of solvent *via* rotary evaporation.

The increasing volumes occurring with each dilution often mean that one is working with very large volumes, which is time consuming and requires large glassware. However, this method eliminates the need to concentrate the crude extract and avoids liquid-liquid partitioning, making the method a milder form of initial fractionation.[52] PSDVB is commercially available under the trade name Diaion HP-20 and is manufactured in two grades, fine (HP-20) and super fine (HP-20ss). The PSDVB resin used throughout this research was HP-20 and will be referred to as such from here on.

2.2.2 DIOL

DIOL is a derivative of silica where a portion of hydroxyl groups on the silica are replaced by propanediol groups, which effectively reduces the polarity of the stationary phase.[53] Therefore the dipole-dipole interactions between solute and stationary phase occurring with DIOL chromatography are reduced, ensuring that fewer polar compounds bind irreversibly when compared to a normal silica stationary phase.[53] DIOL is more suitable for the chromatography of marine extracts and fractions, given the often more polar characteristics of marine secondary metabolites.

2.3 *Siphonaria capensis*

2.3.1 Recollection and re-isolation of *Siphonaria capensis* metabolites

In May 2009 a collection of specimens of *Siphonaria capensis* was made by hand, along the Kenton coastline near the mouth of the Kareiga River (Figure 2.5). *S. capensis*, commonly known as the Cape false-limpet, are identifiable by their characteristic oval shell that is slightly swollen on one side and their low and flat ribs that run from an almost central apex down to a smooth or slightly scalloped margin (Figure 2.5).[54] *S. capensis* is the most common of the nine recognised southern African *Siphonaria* species and is found in the intertidal zones along the Namibian, South African and southern Mozambique coastlines, where it occurs in communities of >100,000 individuals.[33]

Figure 2.5: Collection of *Siphonaria capensis*, made by Dr W. Popplewell and myself, from the rocky intertidal zone along the Kenton coast line.

Specimens (2114 individuals) of *S. capensis* were steeped in acetone overnight, sonicated and the solvent removed before being steeped in acetone overnight again. The two acetone extracts were combined and cyclic-loaded onto a column of HP-20 resin. The HP-20 column was eluted sequentially with 20%, 40%, 60%, 80% aqueous acetone and finally 100% acetone. The ^{1}H NMR spectra of crude fractions obtained from the initial HP-20 chromatography are shown in Figure 2.6. When choosing a fraction for further purification, particular attention was paid to the presence of methyl doublets in the region δ_H 0.8-2.0 ppm (a characteristic feature of polypropionate metabolites) in addition to olefinic peaks around 5.2-6.3 ppm in the ^{1}H NMR spectra.

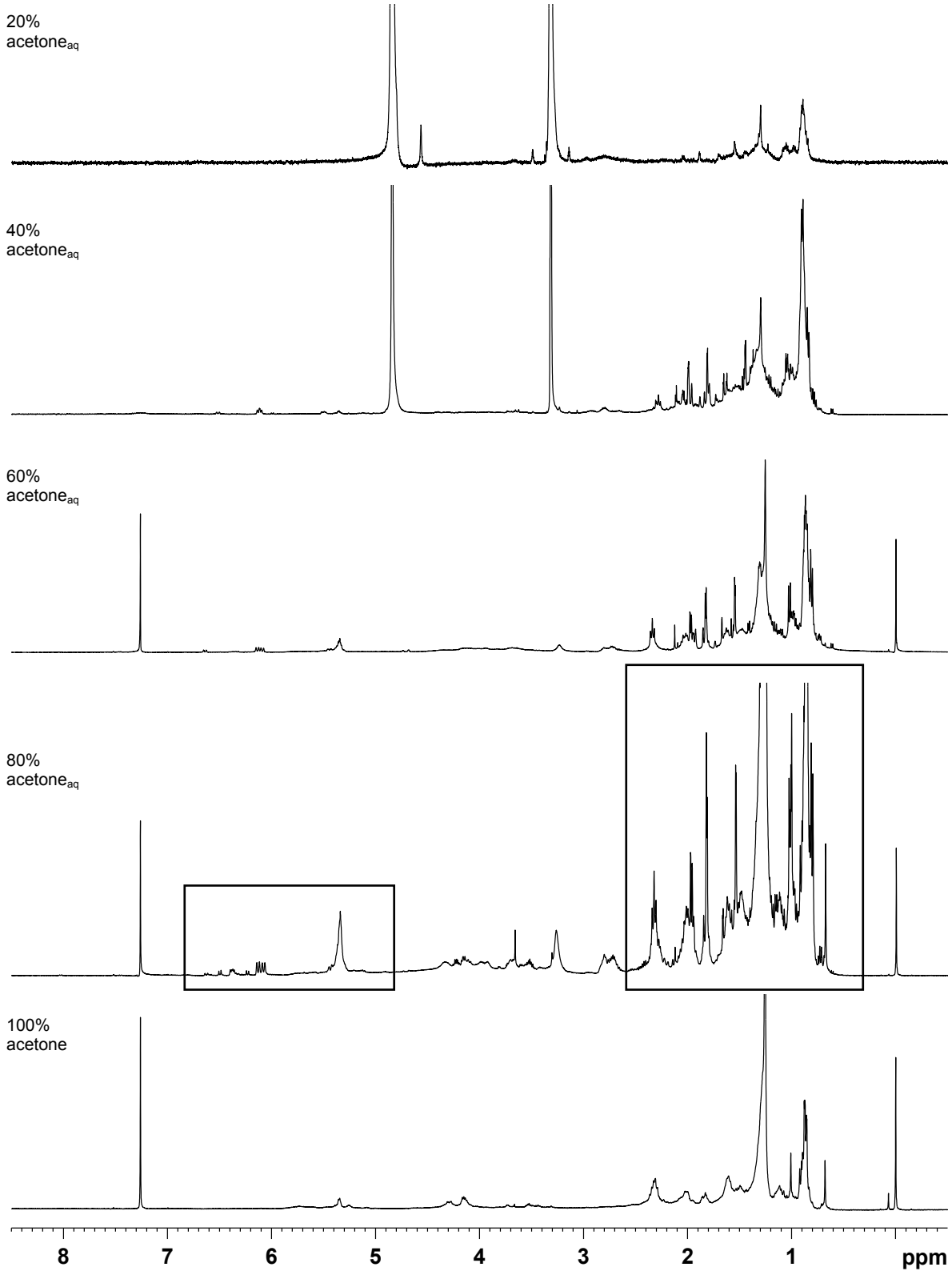

Figure 2.6: ^{1}H NMR (600 MHz) spectra of crude fractions eluted from HP-20 resin. Boxes highlight areas of interest.

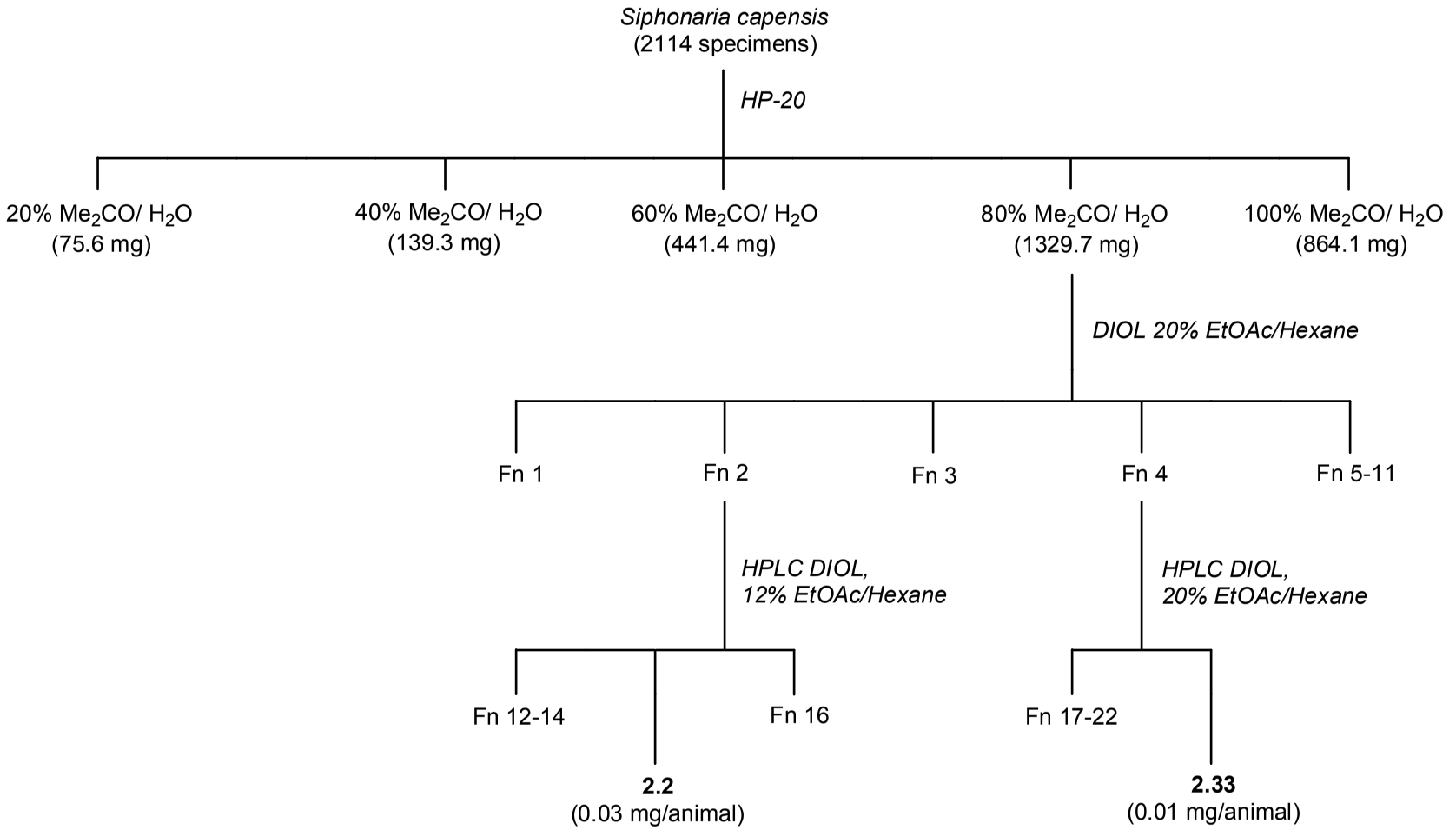

Scheme 2.5: Chromatography protocol used to isolate *Siphonaria capensis* metabolites

Of the five crude *S. capensis* fractions, the 80% aqueous acetone fraction was chosen for further chromatography based on its ^{1}H spectra and relatively large mass (1329.7 mg). The 80% aqueous acetone fraction was purified further through an open chromatography using a stationary phase of propanediol-bonded silica (DIOL) as illustrated in Scheme 2.5. Analysis of the ^{1}H NMR spectra of the second DIOL fraction revealed the presence of the characteristic polypropionate peaks and was further purified *via* normal phase HPLC (12% ethyl acetate/hexane) on DIOL to yield the known siphonariid metabolite *E*-siphonarienfuranone (**2.2**, 0.03 mg/animal) previously isolated from *S. capensis*[49] and *S. grisea*[42]. Comparison of the ^{1}H and ^{13}C NMR data of **2.2** to those reported in the literature[49] initially confirmed the structure of **2.2** (Table 2.1).

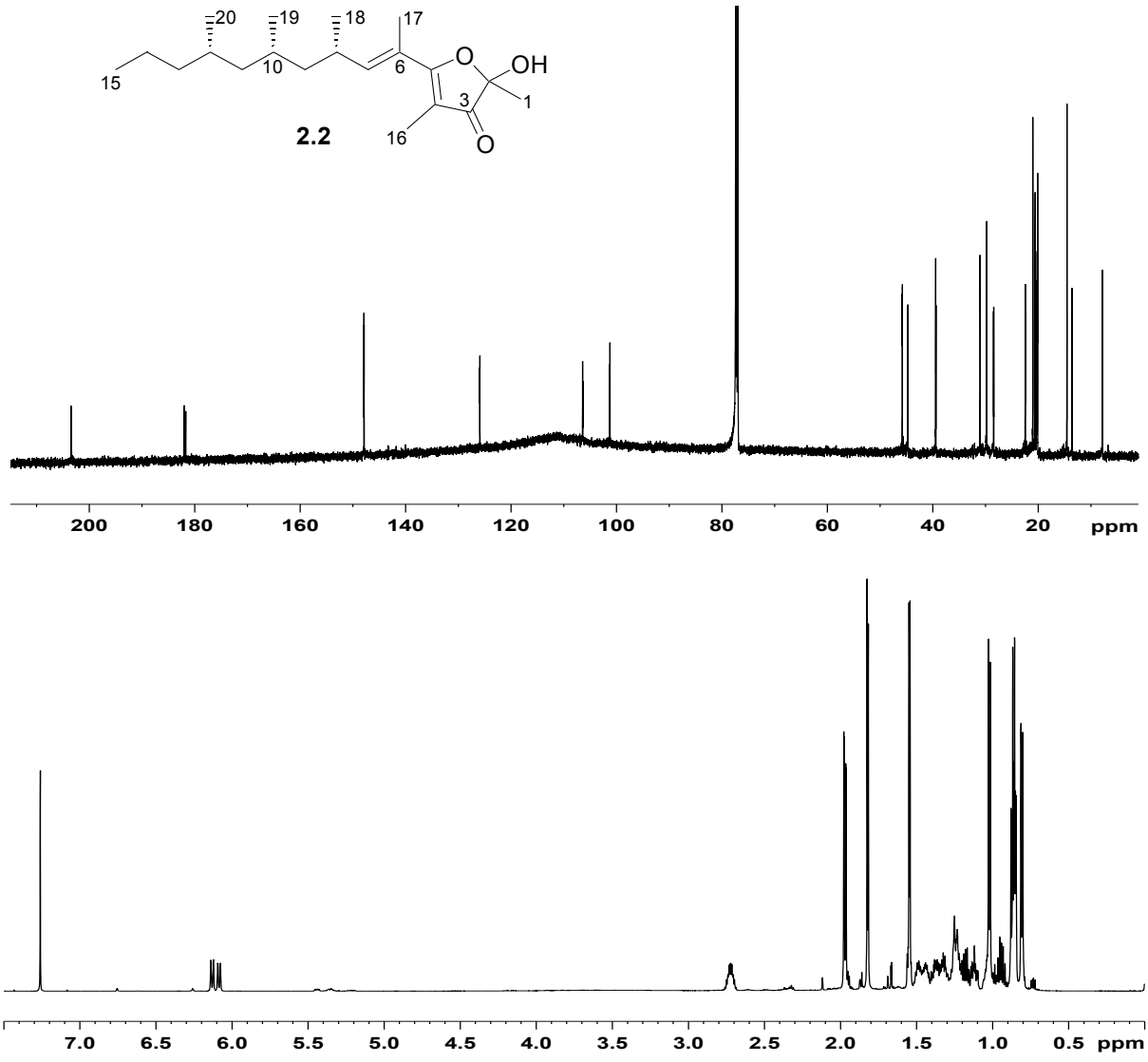

Figure 2.7: ^{1}H ($CDCl_3$ 600 MHz) and ^{13}C (150 MHz) NMR spectra of siphonarienfuranone (**2.2**).

Table 2.1: ^{1}H (600 MHz) and ^{13}C NMR (150 MHz) data obtained in $CDCl_3$ for **2.2** alongside those obtained previously by Beukes and Davies-Coleman.[49]

	2.2		Literature data[49]	
Position	δ_C ppm	δ_H ppm (int., mult., *J*/Hz)	δ_C ppm	δ_H ppm (int., mult., *J*/Hz)
1	22.4/22.5	1.54/1.55 (3H, s)	22.27/22.30	1.53 (3H, d, 6.6)
2	101.2/101.3	-	101.09/ 101.14	-
3	203.4/203.5	-	203.2/203.3	-
4	106.4	-	106.2/106.3	-
5	181.7/182.0	-	181.5/181.8	-
6	125.9	-	125.7/125.8	-
7	147.8/147.9	6.07/6.13 (1H, d,10.0)	147.6/147.7	6.10/6.13 (1H, d,10.0)
8	31.0	2.72 (1H, m)	30.9	2.70 (1H, m)
9a	44.7	1.13 (1H, m)	45.6	0.94 (1H, m)
9b		1.39 (1H, m)		1.38 (1H, m)
10	28.4/28.5	1.45 (1H, m)	29.7	1.47 (1H, m)
11a	45.7/45.8	0.94 (1H, m)	44.59/44.61	1.47 (1H, m)
11b		1.19 (1H, m)		1.10 (1H, m)
12	29.8	1.50 (1H, m)	28.33/28.30	1.44 (1H, m)
13a	39.4	1.04 (1H, m)	39.2/39.3	1.02 (1H, m)
13b		1.24 (1H, m)		1.23 (1H, m)
14a	20.1	1.25 (1H, m)	19.9	1.23 (1H, m)
14b		1.34 (1H, m)		1.30 (1H, m)
15	14.5	0.86/0.87 (3H, t, 6.8)	14.4	0.86 (3H, m)
16	7.8	1.82/1.83 (3H, s)	7.6	1.80 (3H, s)
17	13.5/13.6	1.96/1.98 (3H, d, 1.1)	13.37/13.41	1.95 (3H, d, 5.4)
18	21.0	1.02 (3H, d, 6.7)	20.84	1.02 (3H, d, 6.6)
19	20.6	0.85 (3H, d, 6.4)	20.4	0.85 (3H, m)
20	20.2/20.3	0.81 (3H, d, 6.5)	20.0/20.1	0.80 (3H, d, 6.6)

The duplication of the olefinic signal at δ 6.07/6.13 (1H, d, *J* = 10.0 Hz, H-7) as well as the methyl signals at δ 0.86/ 0.87 (3H, t, *J* = 6.8 Hz, H_3-15), 1.54/1.55 (3H, s, H_3-1), 1.82/1.83 (3H, s, H_3-16) and 1.96/1.98 (3H, d, *J* = 1.1 Hz, H_3-17) in the ^{1}H NMR spectra (Figure 2.7) suggested that the sample of **2.2** was a mixture of C-2 epimers. A combination of HSQC and COSY correlations were used to confirm the structure of the polypropionate side chain. The two and three bond HMBC correlations (Figure 2.8) between the H_3-17 proton doublets (δ 1.96/1.98) and C-5, C-6, and C-7 positioned this side chain at C-5 on the furanone ring as expected. The

position of the remaining two deshielded methyl groups at C-2 and C-4 was confirmed through two and three bond HMBC correlations from the methyl protons to the relevant adjacent carbons (Figure 2.8).

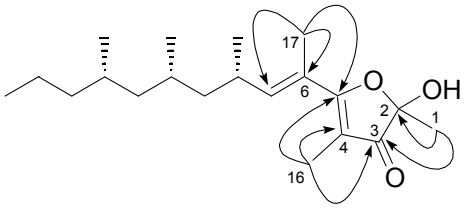

2.2

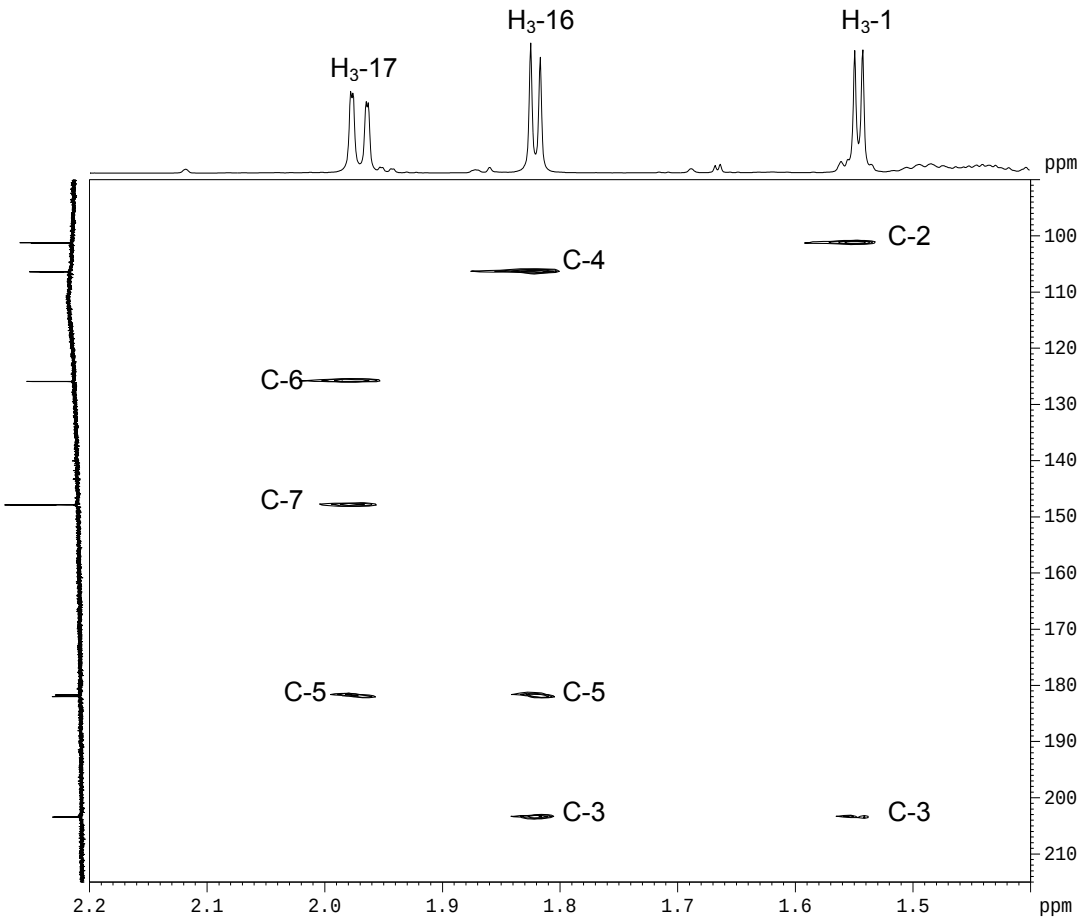

Figure 2.8: A region (F1 = δ 1.4-2.2 ppm; F2 = δ 90-205 ppm) of the gHMBC spectrum ($CDCl_3$, 600 MHz) of **2.2**. The accompanying structure shows the key HMBC correlations used to confirm the positioning of the furanone ring substituents of **2.2**.

Interestingly, the optical rotation measured for **2.2** ($[\alpha]_D^{20}$ +95) isolated in our study of *S. capensis*, while differing from that previously obtained by Beukes and Davies-Coleman[49] of *S. capensis* ($[\alpha]_D$ +54),[49] compares favourably with that reported by Norte *et al.* from *S. grisea* ($[\alpha]_D$ +102)[42] Paradoxically, **2.29** was not isolated from our latest collection of *S. capensis*. Norte *et al.*[42] and Beukes and Davies-Coleman[49] have observed that when *E* siphonarienfuranone is left to stand in solution, it slowly isomerises to **2.29** suggesting that **2.29** may be an artifact and not a natural siphonariid metabolite. Throughout our re-investigation of *S. capensis* great care was taken to ensure that all NMR data were obtained promptly and samples were refrigerated to reduce isomerisation. Our use of milder chromatography media could also have contributed to the absence of **2.29** in our study of *S. capensis*.

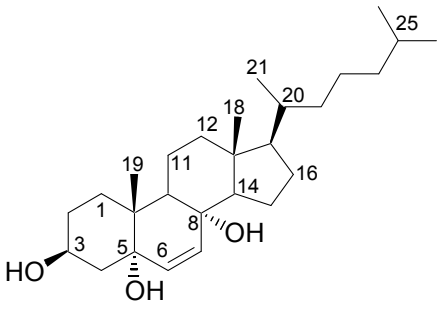

2.33

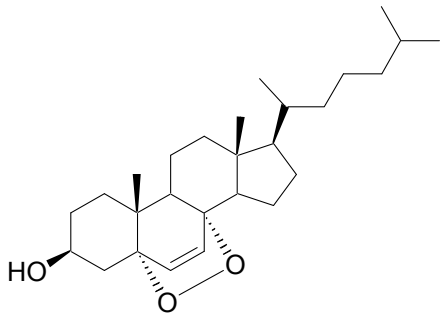

2.34

The non-polypropionate metabolite cholest-7-en-3,5,7-triol (**2.33**, 0.01 mg/animal) was also isolated from fraction 4, after normal phase HPLC (20% ethyl acetate/hexane) on a DIOL column (Scheme 2.5). The molecular formula of **2.33** ($C_{27}H_{46}O_3$) was deduced from ^{13}C and ^{1}H NMR and supported by LREIMS, which implied five degrees of unsaturation. The two deshielded resonances at δ_C 130.8 and 135.4 in the ^{13}C NMR spectrum of **2.33** (Figure 2.9) and information from the associated DEPT 135 experiment indicated the presence of a disubstituted olefin accounting for one of the degrees of unsaturation. The IR spectrum contained three broad bands (ν_{max} 3534, 3398, 3241 cm^{-1}) consistent with the presence of hydroxyl functionalities. The lack of any IR bands in the carbonyl region implied that the other four degrees of unsaturation could be attributed to a tetracyclic system. The presence of 27 carbons and the tetracyclic nature of **2.33** provided ample evidence for us to suggest that **2.33** was a steroid. The mass spectrometry data and two key oxygenated, quaternary, deshielded ^{13}C NMR resonances at δ_C 79.5 and 82.2 led us to compare our NMR data for **2.33** with those acquired by van Wyk *et al.*[52] for cholest-7-en-3,5,7-triol recently isolated from the unrelated pulmonate mollusc *Trimusculus costatus* (Table 2.2). The initial ^{1}H and ^{13}C NMR chemical shift assignments, made by analogy, were subsequently confirmed where necessary by a series of 2D NMR experiments (COSY and HMBC). Optical rotation data ($[\alpha]_D^{20}$ +7, lit.[52] +4) unequivocally confirmed the cholest-7-en-3,5,7-triol structure of

2.33 from *S. capensis*. Compound **2.33** has not been isolated previously from any other *Siphonaria* species.

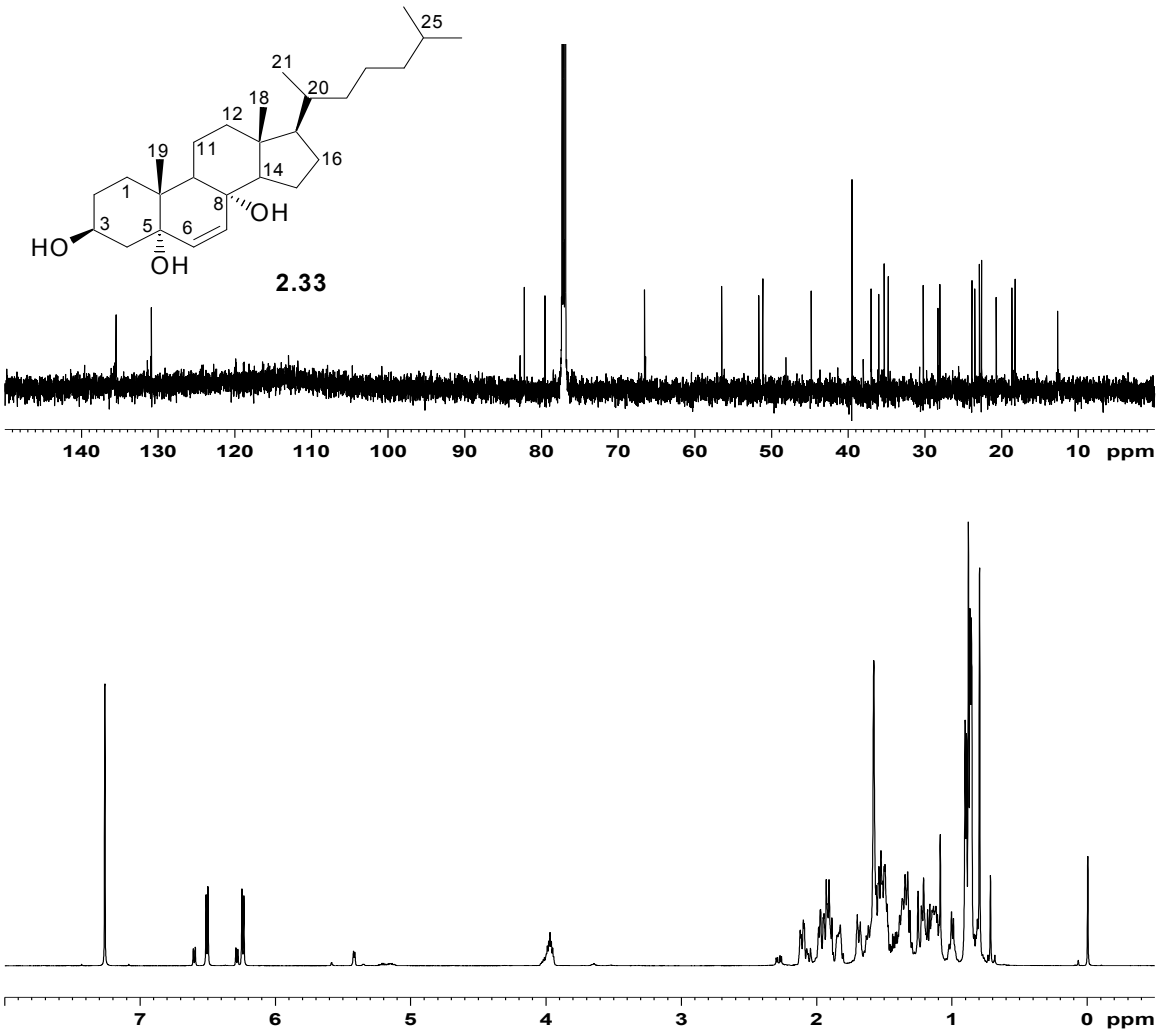

Figure 2.9: ^{1}H ($CDCl_3$, 600 MHz) and ^{13}C ($CDCl_3$, 150 MHz) NMR spectra of **2.33**

There are two small, extra olefinic resonances at δ_H 6.30 (d, 8.6) and 6.60 (d, 8.6) in the ^{1}H NMR spectrum, and olefinic signals at δ_C 131.0 and 135.6 as well as an extra, small, quaternary, oxygenated resonance at δ_C 82.8 in the ^{13}C NMR spectrum (Figure 2.9). This duplication of signals suggested the presence of a second minor metabolite in the sample of **2.33** isolated from *S. capensis*. The shifts of these smaller resonances are consistent with data obtained for the epidioxysterol (**2.34**), a common marine metabolite previously isolated from tunicates, bivalves, and sea anemones.[55-57] The ratio of **2.33** to **2.34** (5:1) was determined by integration of the ^{1}H NMR data. This cyclic peroxide is possibly the precursor of **2.33**.

Table 2.2: ^{1}H (600 MHz) and ^{13}C (150 MHz) NMR data obtained in $CDCl_3$ for **2.33** isolated from *S. capensis* and *T. costatus*.[52]

	2.33		Literature data[52]	
Position	δ_C ppm	δ_H ppm (int., mult., *J*/Hz)	δ_C ppm	δ_H ppm (int., mult., *J*/Hz)
1β	34.7	1.69 (1H, ddd, 13.5, 6.9, 3.5)	34.7	1.67 (1H, ddd, 13.5, 6.9, 3.5)
1α		1.95 (1H, m)		1.95 (1H, m)
2β	30.2	1.52 (1H, m)	30.1	1.51 (1H, m)
2α		1.83 (1H, m)		1.82 (1H, m)
3	66.5	3.97 (1H, m)	66.4	3.95 (1H, m)
4β	37.0	1.91 (1H, m)	36.9	1.88 (1H, dd, 13.8, 11.7)
4α		2.11 (1H, ddd, 13.8, 5.0, 2.0)		2.09 (1H, ddd, 13.8, 5.0, 1.9)
5	82.2	-	82.1	-
6	135.4	6.24 (1H, d, 8.5)	135.4	6.22 (1H, d,8.5)
7	130.8	6.50 (1H, d, 8.5)	130.7	6.49 (1H, d, 8.5)
8	79.5	-	79.4	-
9	51.6	1.53 (1H, m)	51.6	1.54 (1H, dd, 12.2, 4.6)
10	37.0	-	36.9	-
11a	20.7	1.42 (1H, m)	20.6	1.42 (1H, m)
11b		1.61 (1H, m)		1.61 (1H, m)
12a	39.5	1.17 (1H, m)	39.4	1.17 (1H, m)
12b		1.96 (1H, m)		1.95 (1H, m)
13	44.7	-	44.7	-
14	51.1	1.49 (1H, m)	51.0	1.48 (1H, m)
15a	23.5	1.20 (1H, m)	23.4	1.20 (1H, m)
15b		1.48 (1H, m)		1.48 (1H, m)
16a	28.3	1.37 (1H, m)	28.2	1.36 (1H, m)
16b		1.91 (1H, m)		1.92 (1H, m)
17	56.4	1.18 (1H, m)	56.4	1.17 (1H, m)
18	12.7	0.79 (3H, s)	12.6	0.78 (3H, s)
19	18.2	0.88 (3H, s)	18.1	0.86 (3H, s)
20	35.3	1.35 (1H, m)	35.2	1.36 (1H, m)
21	18.6	0.90 (3H, d, 6.5)	18.6	0.88 (3H, d, 6.5)
22a	36.0	1.01 (1H, m)	35.9	1.01 (1H, m)
22b		1.32 (1H, m)		1.32 (1H, m)
23a	23.9	1.15 (1H, m)	23.8	1.14 (1H, m)
23b		1.33 (1H, m)		1.32 (1H, m)
24	39.4	1.14 (2H, m)	39.4	1.14 (2H, m)
25	28.0	1.51 (1H, m)	28.0	1.51 (1H, m)
26	22.9	0.87 (3H, d, 8.5)	22.8	0.85 (3H, d, 6.6)
27	22.6	0.86 (3H, d, 8.5)	22.5	0.84 (3H, d, 6.6)

Trimusculus sp. (Sub-class: Pulmonata, Family: Trimusculidae), are shelled molluscs commonly found in densely aggregated colonies under rocks in the inter-tidal zones along the south and east coast of South Africa. *T. costatus*, like *Siphonaria* sp. have an evolved mantle cavity that acts as both a lung and a gill, allowing them respire in and out of water.[54, 58] *S. capensis* feeds mainly on macroalgae whilst *T. costatus* filter feeds on phytoplankton trapped in a net of mucus which they secrete from their mantle glands.[30, 54] This difference in dietary preferences would imply that the presence of **2.33** in both organisms is due to *de novo* biosynthesis rather than **2.33** being classified as a sequestered metabolite. *Trimusculus* species also produce a second, diterpene rich mucus secreted from numerous subepithelial glands in the mantle and sides of the foot that serves as a chemical defence against predators.[58] The role of **2.33** in the biology of *T. costatus* is unknown, and no assumptions can therefore be made as to why this compound is also produced by *S. capensis*.

2.4 *Siphonaria oculus*

2.4.1 Collection and isolation of *Siphonaria oculus* metabolites

Siphonaria oculus is commonly known as the “eyed false limpet” due to the appearance of a white bar across the apex of its shell, known as an ‘eye-spot’ (Figure 2.10).[54] The foot of *S. oculus* species is dotted with fine white spots and the shells of individuals have a distinct rib pattern that alternates between small and large ribs that project slightly from the margin creating a rough edge.[54] *S. oculus* colonies occur along the southern coast of South Africa and are most commonly found on sheltered rocks along the banks of coastal rivers or in the mid shore intertidal zone.[54]

Figure 2.10: Colony of *Siphonaria oculus* found on the banks of the Kariega River.

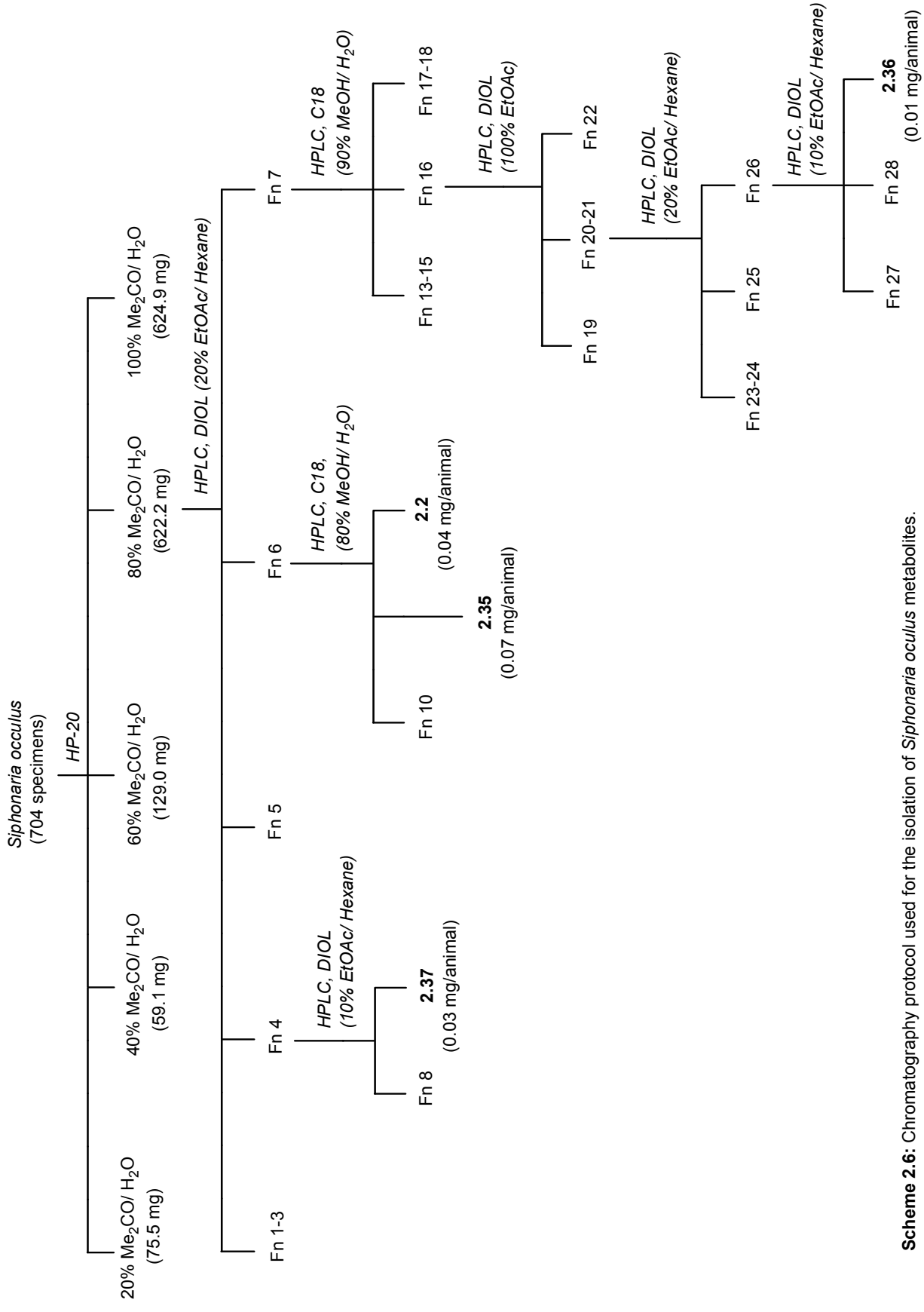

Scheme 2.6: Chromatography protocol used for the isolation of *Siphonaria oculus* metabolites.

In August 2009 a collection of *S. oculus* specimens (704) was made by hand, near Terrivonne Wharf on the Kariega River. The collection site was 3 km up river of the intertidal site where the collection of *S. capensis* was made. The specimens of *S. oculus* were steeped in acetone as described previously in Section 2.3 before being subjected to the chromatography protocol outlined in Scheme 2.6, leading to the isolation of three new siphonariid metabolites (**2.35**, **2.36**, and **2.37**) and the known polypropionate siphonarienfuranone (**2.2**).

Reverse phase HPLC (80% methanol/water) of fraction 6, on a C-18 stationary phase, yielded the new polypropionate **2.35** (0.07 mg/animal) and siphonarienfuranone (**2.2**, 0.04 mg/animal). The spectroscopic data obtained for **2.2** was consistent with both the literature data[42, 49] and the data obtained for **2.2** re-isolated from *S. capensis*. The molecular formula of **2.35** was established from HREIMS data as $C_{20}H_{32}O_3$ which implied five degrees of unsaturation. The characteristic bands at 3339 and 1686 cm^{-1} in the IR spectra of **2.35** indicated the presence of hydroxyl and carbonyl functionalities respectively.

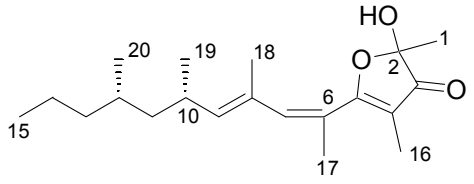

2.35

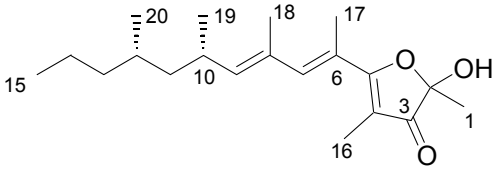

2.36

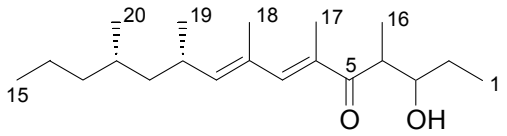

2.37

Inspection of the ^{13}C NMR (Figure 2.11) and DEPT 135 spectra obtained for **2.35** revealed quaternary carbon signals at δ_C 102.0, 108.5, 184.8, and 202.8/202.9 suggesting the presence of a furanone moiety consistent with that found in **2.2**. This unsaturated ring system accounted for three of the five double bond equivalents and the remaining two degrees of unsaturation were accordingly assigned to two olefinic groups in a side chain confirmed by the presence of deshielded signals in the ^{13}C NMR spectra (δ_C 122.8/123.0, 130.7, 139.9/140.0, 141.5/141.8) and olefinic proton resonances [δ_H 5.20/5.23 (d, *J* = 9.8 Hz) and 6.26 (d, *J* = 1.2 Hz)] in the ^1H NMR spectrum. Correlations observed in a two-dimensional COSY NMR experiment (Figure 2.12 and Table 2.3) from the olefinic proton (δ_H 5.20/5.23, d, *J* = 9.8 Hz) through to the methyl protons (δ_H 0.85, t, *J* = 7.2 HZ) indicated the presence of a contiguous seven carbon chain with two methyl substituents, δ_H 0.79 (d, *J* = 6.20 Hz) and 0.87/0.85 (d, *J* = 6.5 Hz). The methylene envelope in

the ^{1}H NMR spectra also contained four other methyl proton signals, three of which were deshielded olefinic methyls at δ_H 1.52/1.53 (s), 1.69 (s) and 1.97/1.98 (d, *J* = 1.5 Hz). The duplication of the resonance for the olefinic methyl on the furanone ring (H_3-16, δ_H 1.52/1.53) in **2.35** arises from the presence of C-2 epimers of this compound. Further duplication of the proton and carbon resonances (with the exception of C-2) assigned to the furanone ring were also observed. The remaining methyl singlet (δ_H 1.55/1.56) was assigned to the methyl moiety attached to the hemiacetal carbon (δ_C 102) of the furanone ring.

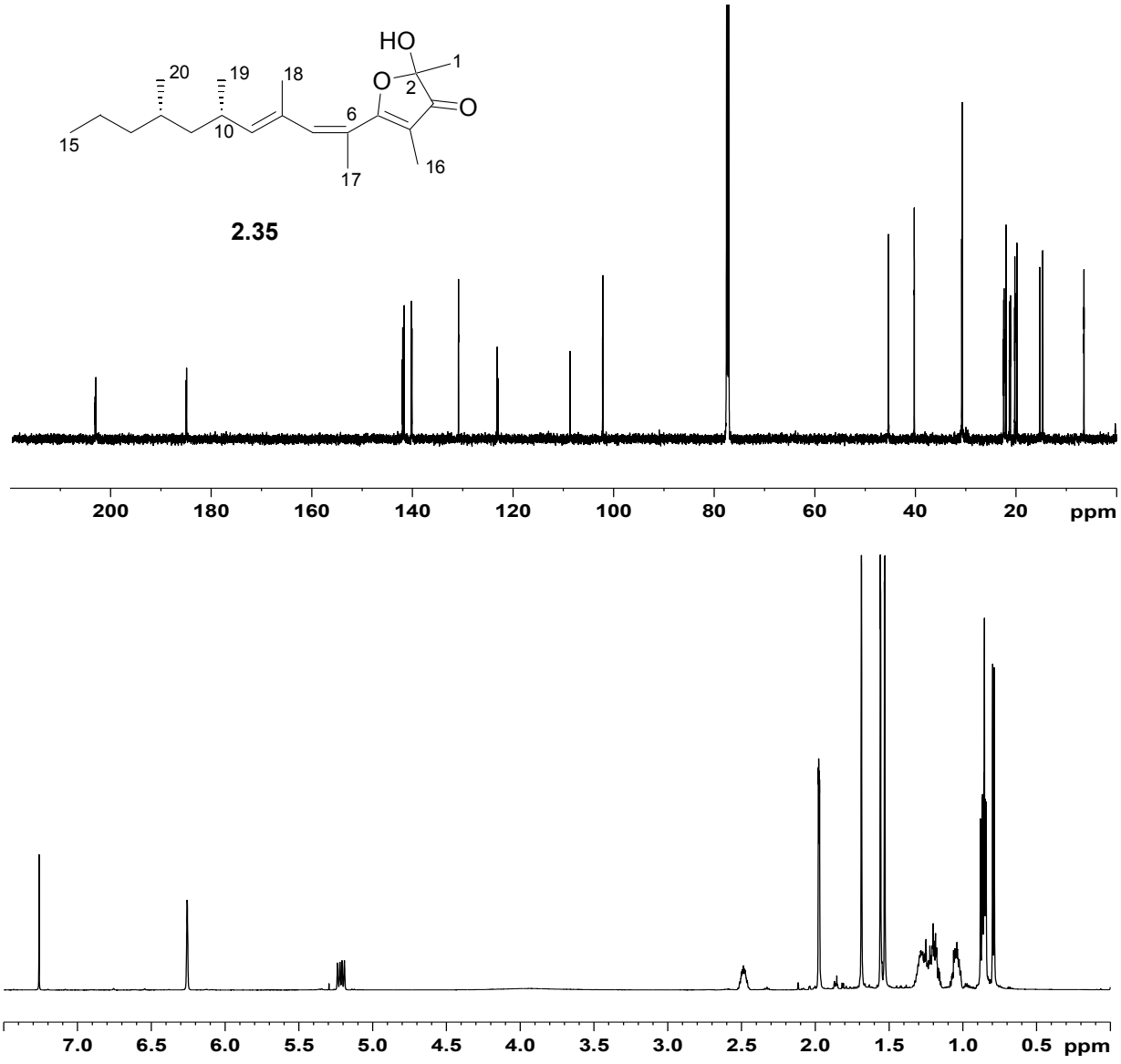

Figure 2.11: ^{1}H ($CDCl_3$, 600 MHz) and ^{13}C ($CDCl_3$, 150 MHz) NMR spectra obtained for **2.35**.

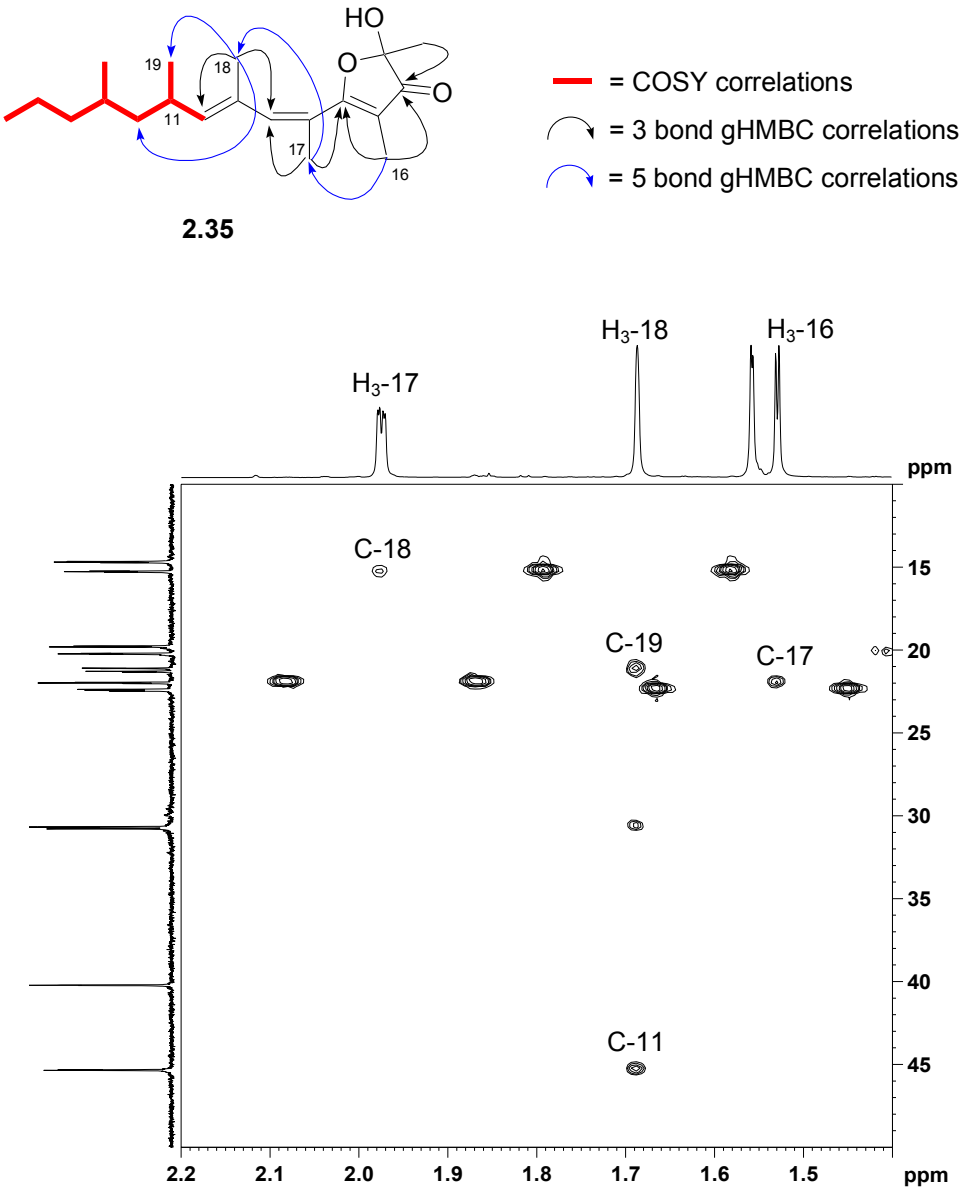

Figure 2.12: A region (F1 = δ 1.4-2.2 ppm; F2 = δ 10-50 ppm) of the gHMBC spectrum ($CDCl_3$, 600 MHz) of **2.35** illustrating the five bond gHMBC correlations. The accompanying structure shows the key gHMBC and COSY correlations used to elucidate the structure of **2.35**.

The methyl group positions and that of the side chain were determined through three bond gHMBC correlations from the methyl protons to the relevant surrounding carbon atoms (Figure 2.12 and Table 2.3). For example, the three bond gHMBC correlation evident between H_3-1 (δ_H 1.55/1.56) and C-3 as well as those observed between H_3-16 (δ_H 1.52/1.53) and C-3 and C-5 confirmed the position of these methyl groups on the furanone ring. Further ^3J gHMBC correlations between H_3-17 (δ_H 1.97/1.98) and C-5 and C-7 as well as those between H_3-18 (δ_H 1.69) and C-7 and C-9 finalised the structural assignment of the polypropionate side chain and confirmed its position at C-5 of the furanone ring.

Table 2.3: ^{1}H ($CDCl_3$, 600 MHz), ^{13}C ($CDCl_3$, 150 MHz) and 2D NMR data obtained for **2.35**.

Position	δ_C ppm	δ_H ppm (int., mult., *J*/Hz)	gHMBC	COSY
1	22.2/22.3	1.55/1.56 (3H, s)	C-2, C-3, C-16	
2	102.0			
3	202.8/202.9			
4	108.5			
5	184.8			
6	122.8/123.0			
7	139.9/140.0	6.26 (1H, d, 1.2)	C-5, C-9, C-17, C-18	H-9, H_3-17, H_3-18
8	130.7			
9	141.5/141.8	5.20/5.23 (1H, d, 9.8)	C-7, C-11, C-18	H-7, H-10, H_3-18
10	30.5	2.49 (1H, m)	C-8, C-9, C-11, C-12, C-19	H-9, H-11a, H-11b, H_3-19
11	45.2	1.05 (1H, m)	C-9, C-10, C-12, C-13, C-19, C-20	H-10, H-12
		1.21 (1H, m)	C-9, C-10, C-12, C-13, C-19, C-20	H-10, H-12
12	30.6	1.28 (1H, m)	C-10, C-11, C-13	H-11a, H-11b, H-13a, H-13b, H_3-20
13	40.1	1.06 (1H, m)	C-11, C-12, C-15, C-20	H-12, H-14a, H-14b
		1.19 (1H, m)	C-11, C-12, C-15, C-20	H-12, H-14a, H-14b
14	20.1	1.23 (1H, m)	C-12, C-13, C-15	H-13a, H-13b, H_3-15
		1.29 (1H, m)	C-12, C-13, C-15	H-13a, H-13b, H_3-15
15	14.5/14.6	0.85 (3H, t, 7.2)	C-13, C-14	H-14a, H-14b
16	6.3/6.4	1.52/1.53 (3H, s)	C-3, C-4, C-5, C-6, C-7, C-17	
17	21.8/21.9	1.98/1.97 (3H, d, 1.5)	C-4, C-5, C-6, C-7, C-8, C-16, C-18	H-7
18	15.1/15.2	1.69 (3H, s)	C-6, C-7, C-8, C-9, C-10, C-11, C-19	H-9
19	21.0/21.2	0.87/0.85 (3H, d, 6.5)	C-9, C-10, C-11, C-12	H-10
20	19.6/19.7	0.79 (3H, d, 6.2)	C-10. C-11. C-12.C-13.	H-12

Paradoxically, unexpected five bond gHMBC correlations were also observed (Figure 2.12). The gHMBC experiment is optimised for three bond correlations[59] and although five bond correlations are unusual they have been observed before in our laboratory in highly conjugated marine compounds *e.g.* pyrroloiminoquinones metabolites from latrunculid sponges.[60] The presence of ^{5}J gHMBC correlations confirms the conjugate arrangement of the olefinic groups contained in **2.35**. The assignment of a *Z* configuration to the Δ^{6} olefin in **2.35** will be discussed later.

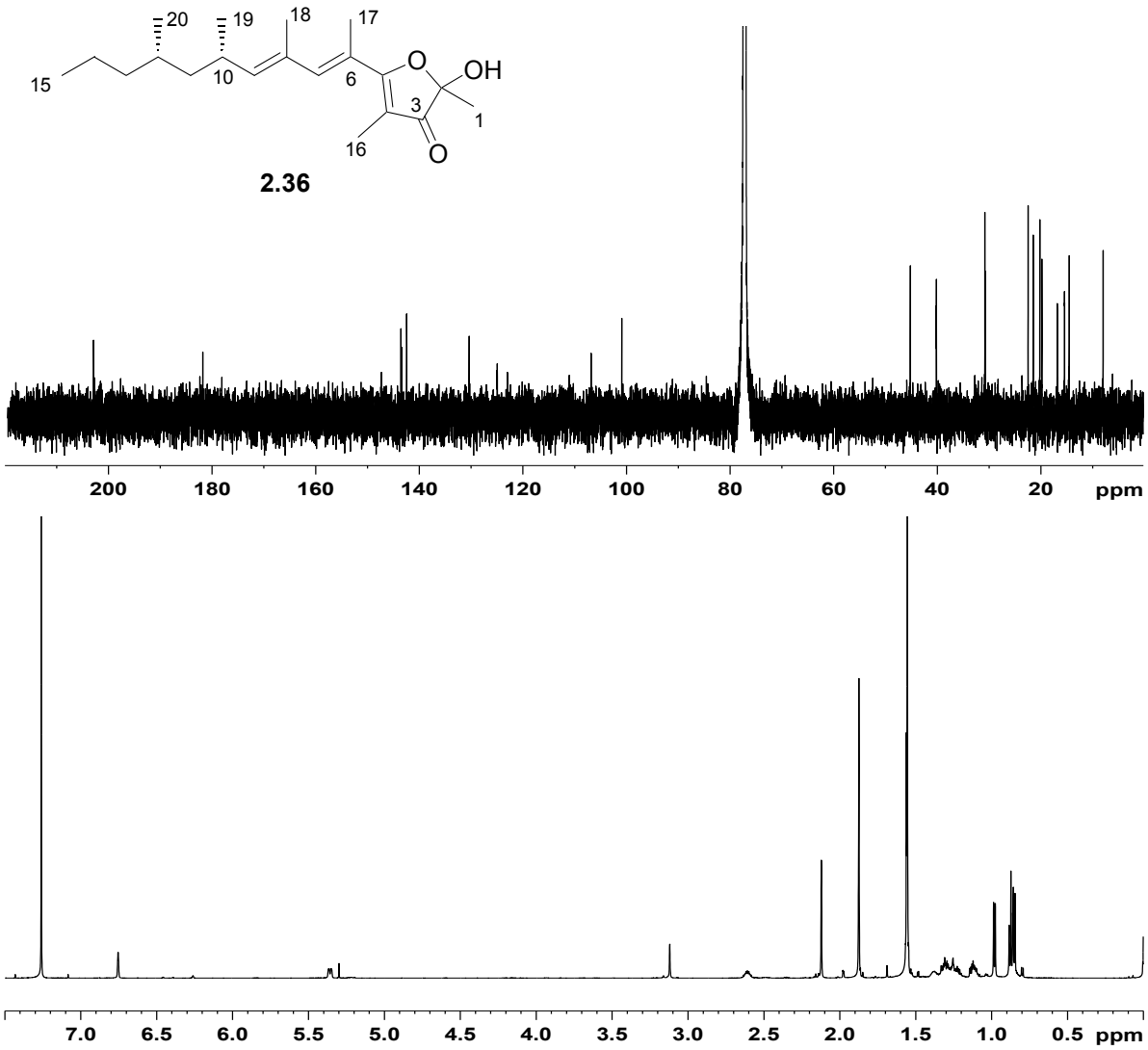

2.36

Figure 2.13: ^{1}H ($CDCl_3$, 600 MHz) and ^{13}C ($CDCl_3$, 150 MHz) NMR spectra obtained for **2.36.**

The polypropionate **2.36** (0.01 mg/animal) was isolated from fraction 7 (Scheme 2.6) after a series of normal phase and reverse phase HPLC purification steps. The molecular formula of **2.36** was determined through HREIMS data as $C_{20}H_{32}O_3$ *i.e.* isomeric with **2.35**. The IR spectrum of **2.36** was consistent with that obtained for **2.35** and suggested the presence of hydroxyl and

carbonyl functionalities (ν_{max} 3429 and 1634 cm^{-1} respectively). The quaternary carbon signals at δ_C 100.9, 106.8, 181.8, and 202.9 in the ^{13}C NMR and DEPT 135 spectra, as well as the methyl proton signals at δ_H 1.56, and 1.87 in the ^{1}H NMR (Figure 2.13) were also consistent with the 2-hydroxy-2,3 dihydro-2,4 dimethylfuran-3-one system of **2.2** and **2.35**.

Table 2.4: ^{1}H ($CDCl_3$, 600 MHz), ^{13}C ($CDCl_3$, 150 MHz) and 2D NMR data obtained for **2.36**.

Position	δ_C ppm	δ_H ppm (int., mult., *J*/Hz)	gHMBC	COSY
1	22.5	1.56 (3H, s)	C-2. C-3	H-OH
2	100.9			
3	202.9			
4	106.8			
5	181.8			
6	124.9			
7	142.4	6.75 (1H, s)	C-5, C-9, C-17, C-18	H-9, H_3-17, H_3-18
8	130.3			
9	143.4/143.5	5.36 (1H, d, 9.7)	C-7, C-11, C-18, C-19	H-7, H-10, H_3-18
10	30.8	2.61 (1H, m)	C-8	H-9, H-11a, H-11b, H_3-19
11	45.2	1.13 (1H, dd, 9.0, 4.5)	C-9, C-10, C-12, C-13, C-19, C-20	H-10, H-11b, H-12
		1.32 (1H, dd, 9.3, 4.0)	C-9, C-10, C-12, C-13, C-19, C-20	H-10, H-11a, H-12
12	30.7	1.38 (1H, m)	C-14	H-11a, H-11b, H-13a, H-13b, H_3-20
13	40.2	1.12 (1H, m)	C-11, C-12, C-15, C-20	H-12, H-13b, H_2-14
		1.24 (1H, m)	C-11, C-12, C-15, C-20	H-12, H-13a, H_2-14
14	20.2	1.31 (2H, m)	C-12, C-13, C-15	H-13a, H-13b, H_3-15
15	14.5	0.87 (3H, t, 7.2)	C-13, C-14	H_2-14
16	8.0	1.87 (3H, s)	C-3, C-4, C-5	
17	15.4	2.12 (3H, br. s,)	C-5, C-6, C-7, C-8	H-7
18	16.8	1.88 (3H, br. s)	C-6, C-7, C-8, C-9, C-17, C-19	H-7, H-9
19	21.5	0.98 (3H, d, 6.7)	C-9, C-10, C-11	H-10
20	19.8	0.85 (3H, d, 6.4)	C-11, C-12, C-13	H-12

The presence of the olefinic carbon signals at δ_C 124.9, 130.3, 142.4, and 143.4/143.5 and deshielded olefinic methyl proton resonances at δ_H 1.88 and 2.12 in the ^{13}C and ^{1}H NMR spectra obtained for **2.36** account for the two remaining degrees of unsaturation. COSY correlations were used to position the two methyl groups (δ_H 0.85 (d, *J* = 6.4) and 0.98 (d, *J* = 6.7) along the contiguous, saturated, carbon chain. Three and five bond gHMBC correlations were used to position the olefinic groups in the side chain and to establish where the side chain was positioned on the furanone ring. These correlations and others to support the proposed structure are provided in Table 2.4.

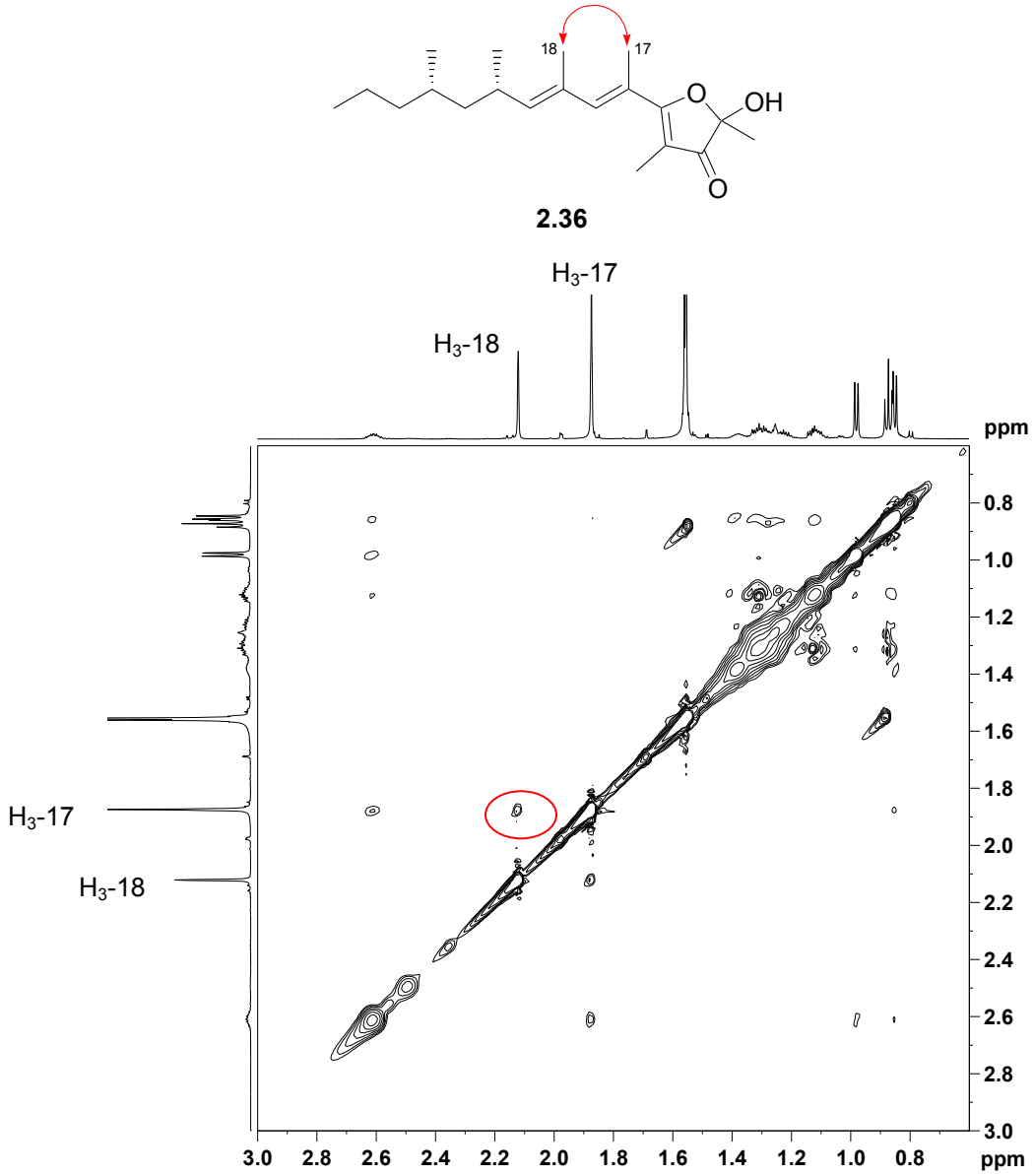

2.36

Figure 2.14: A region of the NOESY spectra (F1 = 0.6-3.0 ppm) obtained for **2.36**. The accompanying structure illustrates the NOESY correlation used to determine the geometry of the isomer.

After the structural elucidation of **2.36** from the 2D NMR, it was apparent that this compound was a geometric isomer of **2.35**. To confirm this and to establish at which olefin this isomerisation occurs, NOESY NMR data were acquired for both **2.35** and **2.36**. Figure 2.14 shows the upfield section (δ_H 0.60-3.00) of the NOESY spectrum obtained for **2.36**. There is a clear NOESY correlation between the methyl protons of H_3-17 (δ 2.12) and H_3-18 (δ 1.88) in the NOESY spectrum of **2.36**, whilst no correlation was observed between the methyl protons at the same positions in **2.35**. This implied that the methyl substituents at C-6 and C-8 are in relatively close proximity to each other in **2.36** and not **2.35**, indicating that **2.36** has an *E, E* structure whilst **2.35** has a *Z, E* structure.

Fraction 4 (Scheme 2.6) yielded a new polypropionate 2-hydroxy-4,6,8,10,12-pentamethyl-pentadeca-6,8-dien-5-one (**2.37**, 0.03 mg/animal, $[\alpha]_D^{19}$ +61) after normal phase HPLC (10% ethylacetate/hexane) on DIOL. The molecular formula of **2.37** ($C_{20}H_{36}O_2$) established from HREIMS data indicated three double bond equivalents. The ^{13}C and ^{1}H NMR spectra of **2.39** are presented in Figure 2.15. The deshielded ^{13}C NMR chemical shift (δ_C 208.7 ppm) and the IR absorbance (ν_{max} 1639 cm^{-1}) suggested the presence of a ketone which would account for the one of the three double bond equivalents.

The two remaining degrees of unsaturation were accounted for by four olefinic signals in the ^{13}C NMR spectrum of **2.37** (δ_C 134.7, 144.7, 130.8 and 144.5 ppm) establishing that there were two vinylic moieties within the carbon chain. A broad absorption at 3422 cm^{-1} in the IR spectrum as well as an oxymethine signal at δ 76.1 ppm in the ^{13}C NMR spectrum indicated the presence of a hydroxyl functionality. The methylene region of the ^{1}H NMR spectrum of **2.37** contained seven methyl proton signals, two of which were triplets at δ 0.87 (t, *J* = 7.2 Hz) and 0.98 (t, *J* = 7.4 Hz) placing them at either end of the 15 carbon chain. The downfield shift of two of the methyl resonances at δ 1.89 (d, *J* = 1.0 Hz) and 1.94 (d, *J* = 1.0 Hz) suggested that they were olefinic methyl groups. The remaining unassigned doublet methyl proton signals at δ 0.85 (d, *J* = 6.5 Hz), 0.98 (d, *J* = 6.6 Hz) and 1.18 (d, *J* = 7.2 Hz) were positioned along the carbon chain using HSQC and COSY experiments. COSY correlations established the presence of two contiguous propionate chains, separated possibly by the quaternary carbons of the ketone and olefinic groups as illustrated in Figure 2.16.

The position of these two chains relative to the carbonyl and olefinic moieties was established through ^{3}J and ^{5}J bond gHMBC correlations (Figure 2.16 and Table 2.5). Three bond gHMBC correlations between the methyl protons at δ_H 1.18 and the oxymethine carbon (δ_C 76.1) and the carbonyl carbon (δ_C 208.7) positions this methyl and its propionate chain adjacent to the ketone carbonyl (C-5). Further three bond gHMBC correlations between the first olefinic methyl protons

at δ_H 1.94 and C-5 and C-7 and the second olefinic methyl protons at δ_H 1.89 and C-7 and C-9 placed them at C-17 and C-18 respectively and established the conjugate arrangement of the ketone and the Δ^6 and Δ^8 olefins. This conjugate arrangement was confirmed by the gHMBC correlations observed between the methyl protons on C-17 (δ_H 1.94) and C-16 and C-8 as well as those between the protons on methyl C-18 (δ_H 1.89) and C-11 and C-19. Although these are unexpected ^5J HMBC correlations, we have clearly established their usefulness in the structure elucidation of **2.35** and **2.36**.

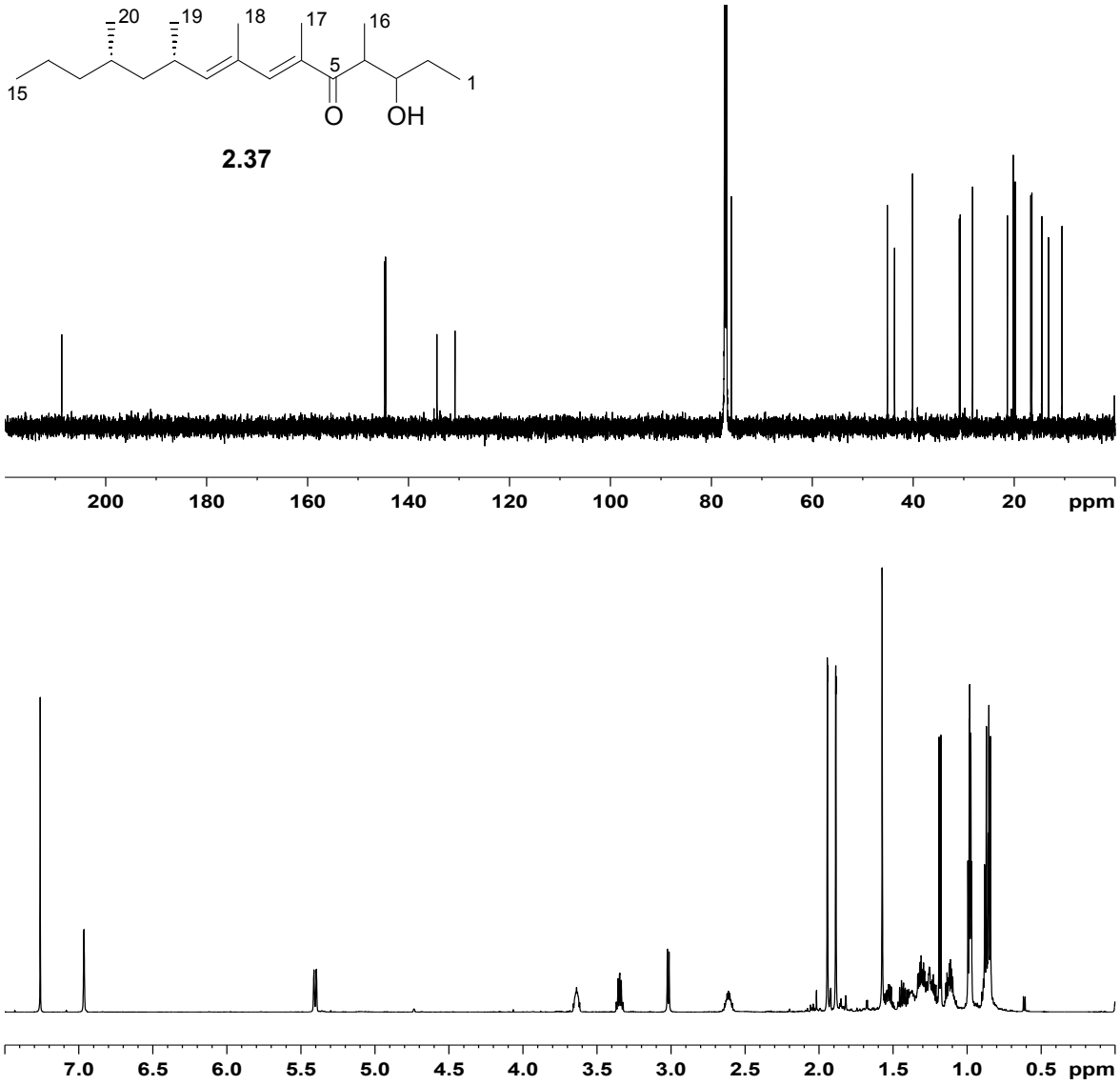

2.37

Figure 2.15: ^{1}H ($CDCl_3$, 600 MHz) and ^{13}C ($CDCl_3$, 150 MHz) NMR spectra obtained for **2.37.**

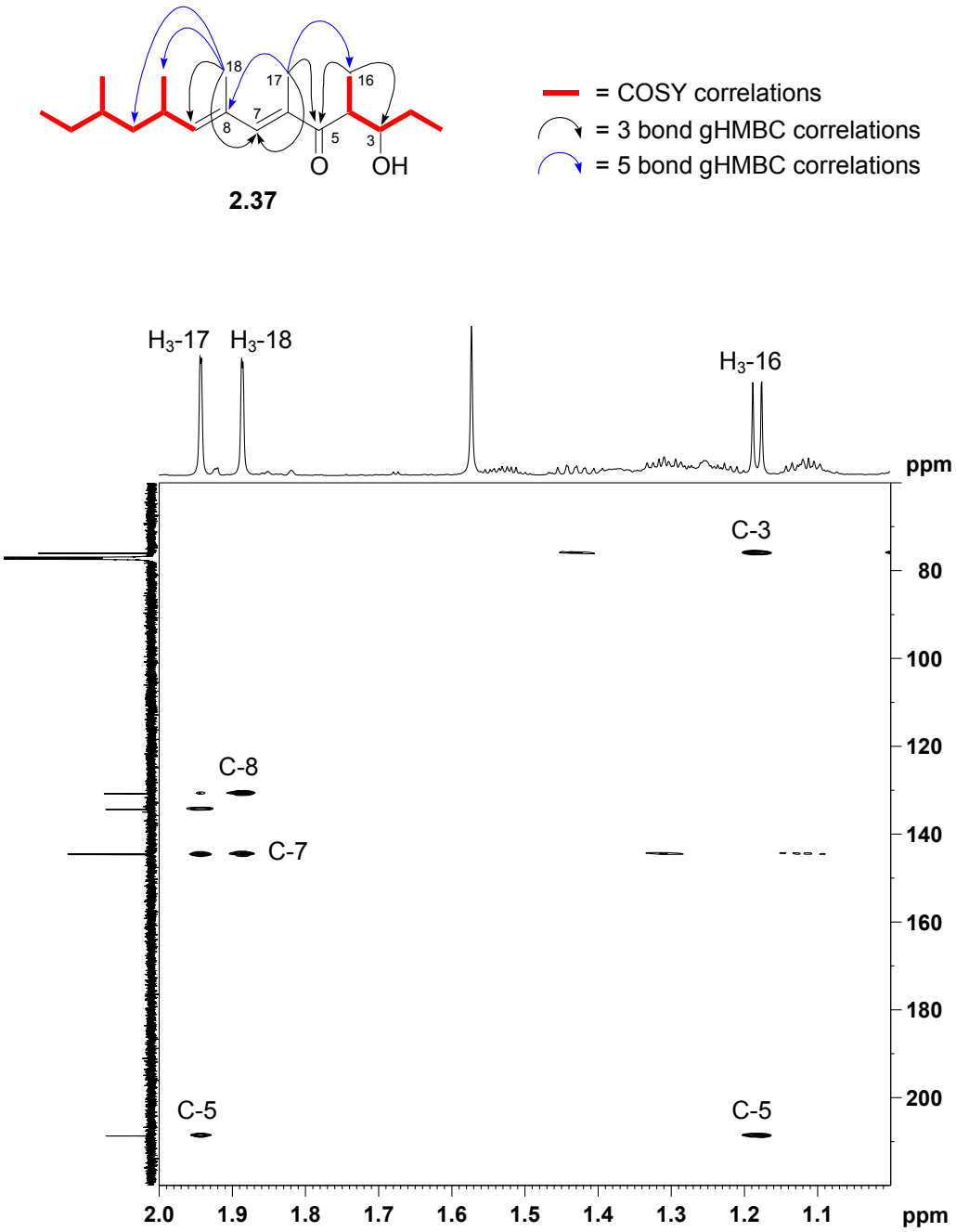

Figure 2.16: A region (F1 = δ 1.0-2.0 ppm; F2 = δ 60-220 ppm) of the gHMBC spectrum ($CDCl_3$, 600 MHz) of **2.37**. The accompanying structure shows the key gHMBC and COSY correlations used to elucidate the structure of **2.37**.

Table 2.5: ^{1}H ($CDCl_3$, 600 MHz), ^{13}C ($CDCl_3$, 150 MHz) and 2D NMR data obtained for **2.37**.

Position	δ_C ppm	δ_H ppm (int., mult., *J*/Hz)	gHMBC	COSY
1	10.5	0.98 (3H, t, 7.4)	C-2, C-3	H-2a, H-2b
2	28.2	1.44 (1H, m)	C-1, C-3, C-4	H-1, H-2b, H-3
		1.53 (1H, m)	C-1, C-3, C-4	H-1, H-2a, H-3
3	76.1	3.64 (1H, m)	C-1, C-2, C-4, C-5, C-16	H-2a, H-2b, H-4
4	43.7	3.35 (1H, quin, 6.8)	C-2, C-3, C-5, C-16	H-3, H_3-16
5	208.7			
6	134.4			
7	144.7	6.96 (1H, s)	C-5, C-6, C-9, C-17, C-18, C-19	H-9, H_3-17, H_3-18
8	130.8			
9	144.5	5.40 (1H, d, 9.7)	C-7, C-10, C-11, C-12, C-18, C-19	H-7, H-10, H_3-18
10	30.8	2.61 (1H, m)	C-8, C-9, C-11, C-12, C-19	H-9, H-11a, H-11b, H_3-19
11	45.1	1.13 (1H, m)	C-8, C-9, C-13, C-19	H-10, H-11b, H-12
		1.31 (1H, m)	C-8, C-9, C-13, C-19	H-10, H-11a, H-12
12	30.7	1.38 (1H, m)	C-10, C-14	H-11a, H-11b, H-13a, H-13b, H_3-20
13	40.1	1.11 (1H, m)	C-11, C-12, C-15, C-20	H-12, H-13b, H_2-14
		1.24 (1H, m)	C-11, C-12, C-15, C-20	H-12, H-13a, H_3-15
14	20.2	1.32 (2H, m)	C-12	H-13a, H_3-15
15	14.5	0.87 (3H, t, 7.2)	C-13, C-14	H-13b,H_2-14
16	16.5	1.18 (3H, d, 7.2)	C-3, C-4, C-5	H-4
17	13.2	1.94 (3H, d, 1.0)	C-5, C-6, C-7, C-8, C-16	H-7
18	16.7	1.89 (3H, d, 1.0)	C-7, C-8, C-9, C-11, C-19	H-7, H-9
19	21.4	0.98 (3H, d, 6.6)	C-9, C-10, C-11	H-10
20	19.8	0.85 (3H, d, 6.5)	C-11, C-12, C-13	H-12

The absolute configuration of the chiral carbons at C-10 and C-12 were assigned, as *S* through comparison with polypropionates of similar structures previously isolated from other *Siphonaria* species, all of which have an *S* configuration at the methyl containing chiral centres in the propionate chain. However, the stereochemical configuration of the other chiral centres in **2.37** could not be assigned from biosynthetic arguments. Fortunately, the secondary alcohol functionality at C-3 in **2.37** provided an opportunity for us to attempt to assign the absolute configuration at this position using the modified Mosher's method.[61]

In 1969 Mosher introduced the chiral esterifying reagent 2-methoxy-2-phenyl-2-(trifluoromethyl)acetic acid (MTPA), with the added advantage that it does not contain a proton α to the carbonyl group which makes racemisation during esterification impossible.[61, 62] During the preparation of Mosher's esters and amides, an enantiomerically pure acid chloride of Mosher's reagent is reacted with either a primary or secondary alcohol or amine in the substrate.[62] Dale and Mosher[61] proposed that the most stable arrangement of the MTPA ester or amide in solution, as illustrated in Figure 2.17, is where the trifluoromethyl, ester carbonyl and oxymethine or aminomethine proton moieties lie in the same plane.[61, 63] In this conformation, the diamagnetic effect of the benzene ring on the protons of the alkyl chain on the same side of this moiety, will cause their ^{1}H NMR signals to shift upfield, whilst the protons on the other alkyl chain are deshielded by the methoxy moiety, shifting their ^{1}H NMR signals downfield.[63]

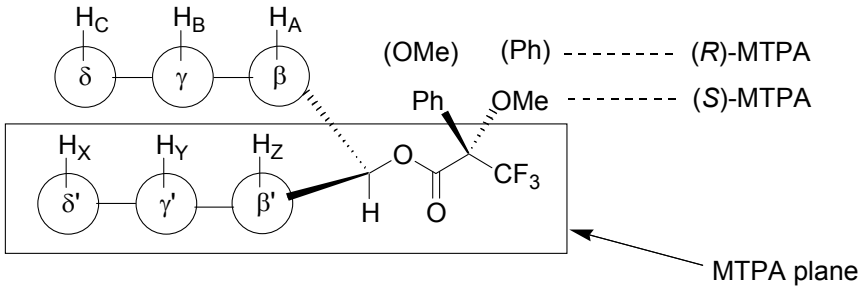

Figure 2.17: Conformation of (*R*)- and (*S*)-MTPA esters derived from a secondary alcohol.

When Mosher originally developed this spectroscopic method, the NMR instruments available operated in the 60-100 MHz range which made it almost impossible to completely assign the protons of a complex compound. To overcome this problem, lanthanide and ^{19}F NMR shift reagents were used to determine the shift differences occurring at the CF_3 (^{19}F) and OMe (^{1}H) functionalities.[63] This however meant that only two data points were available when determining the absolute configuration which obviously reduced the reliability of this method.[63] The modified Mosher's method was developed with the invention of high field, Fourier Transform NMR spectrometers, which allow one to completely assign the ^{1}H chemical shifts of even complex

molecules, increasing the number of data points available.[63] In the modified Mosher's method, all the proton signals in both the (*R*)- and (*S*)- MTPA esters are assigned and then the $\Delta\delta$ values (difference in chemical shift) of these protons are obtained using the formula $\Delta\delta = \delta_S - \delta_R$. The protons with positive $\Delta\delta$ values are placed on the right side and those with negative $\Delta\delta$ values on the left of the molecular model illustrated in Figure 2.18. The absolute values of $\Delta\delta$ are often proportional to the distance from the MTPA moiety and this can be used to check the validity of the model, which will indicate the absolute configuration of the compound. [63]

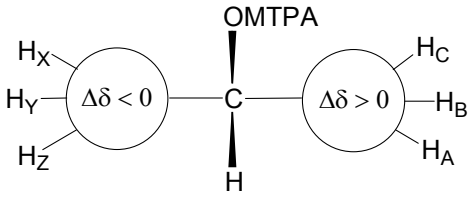

Figure 2.18: The model used to determine the absolute configurations of secondary alcohols using the modified Mosher's method. [63]

The modified Mosher's method has been used to successfully determine the absolute configuration of numerous marine metabolites. However, because of the small quantity of **2.37** available, a trial reaction was deemed necessary to practise the preparation of Mosher's esters on small quantities of alcohol (<5 mg). Hexanol was chosen for the trial reaction due to its alcohol functionality and availability. The (*S*)-MTPA ester of hexanol (**2.38**) was prepared and the ^{1}H and ^{13}C NMR spectra obtained are shown in Figure 2.19. On inspection of the ^{13}C NMR, the appearance of four signals in the aromatic region (*ca.* δ_C 120-140) confirmed the presence of a phenyl moiety, whilst the quartet at 123.3 (q, $^{1}J_{CF}$ =288 Hz) is consistent with the presence of the trifluoromethyl functionality in the sample of **2.38**. The ^{3}J gHMBC correlation (Figure 2.20) observed between proton on C-1 of hexanol and the carbonyl moiety at C-1' of the MTPA group confirmed the successful formation of the ester linkage.

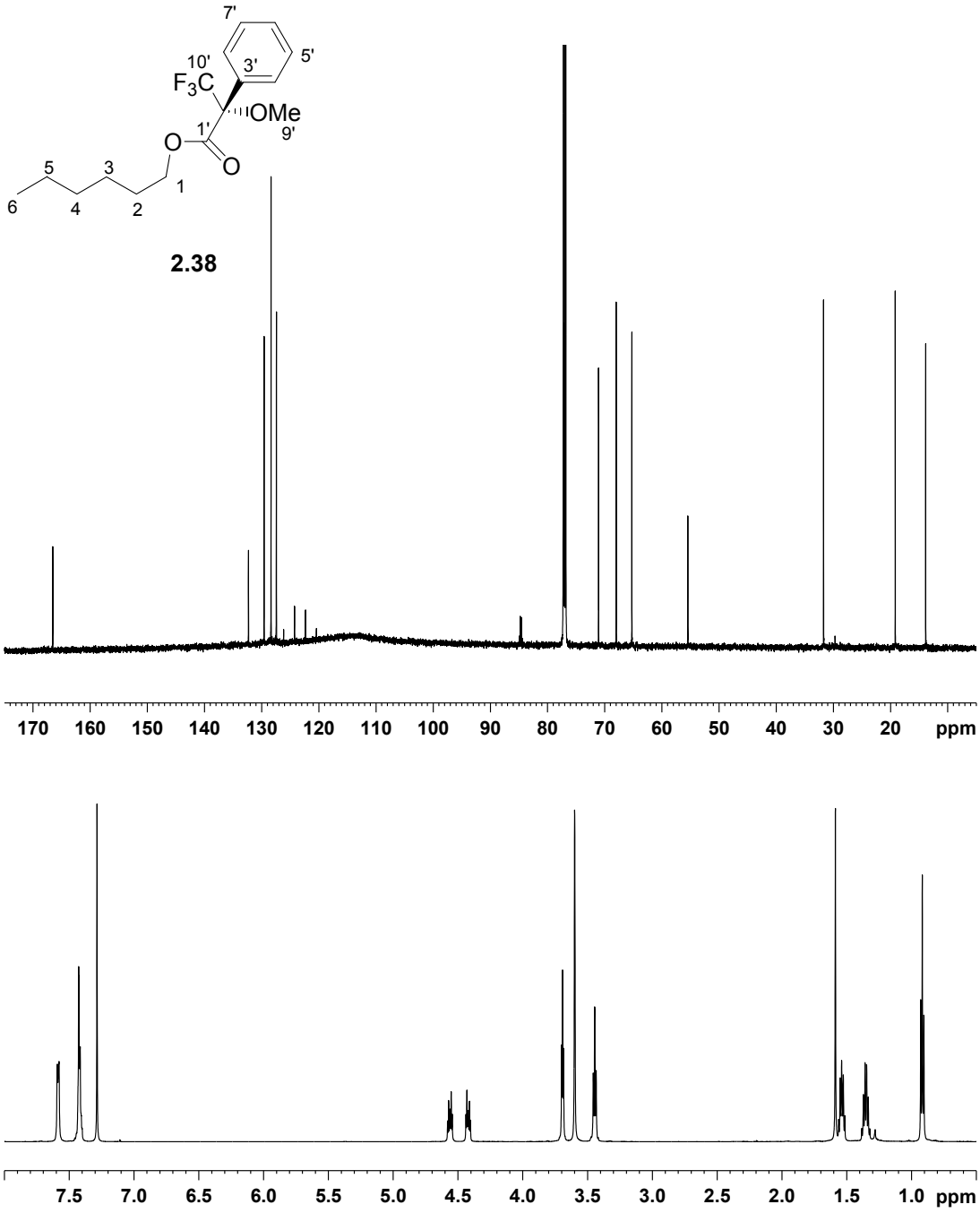

Figure 2.19: ^{1}H ($CDCl_3$, 600 MHz) and ^{13}C ($CDCl_3$, 150 MHz) NMR spectra obtained for **2.38**.

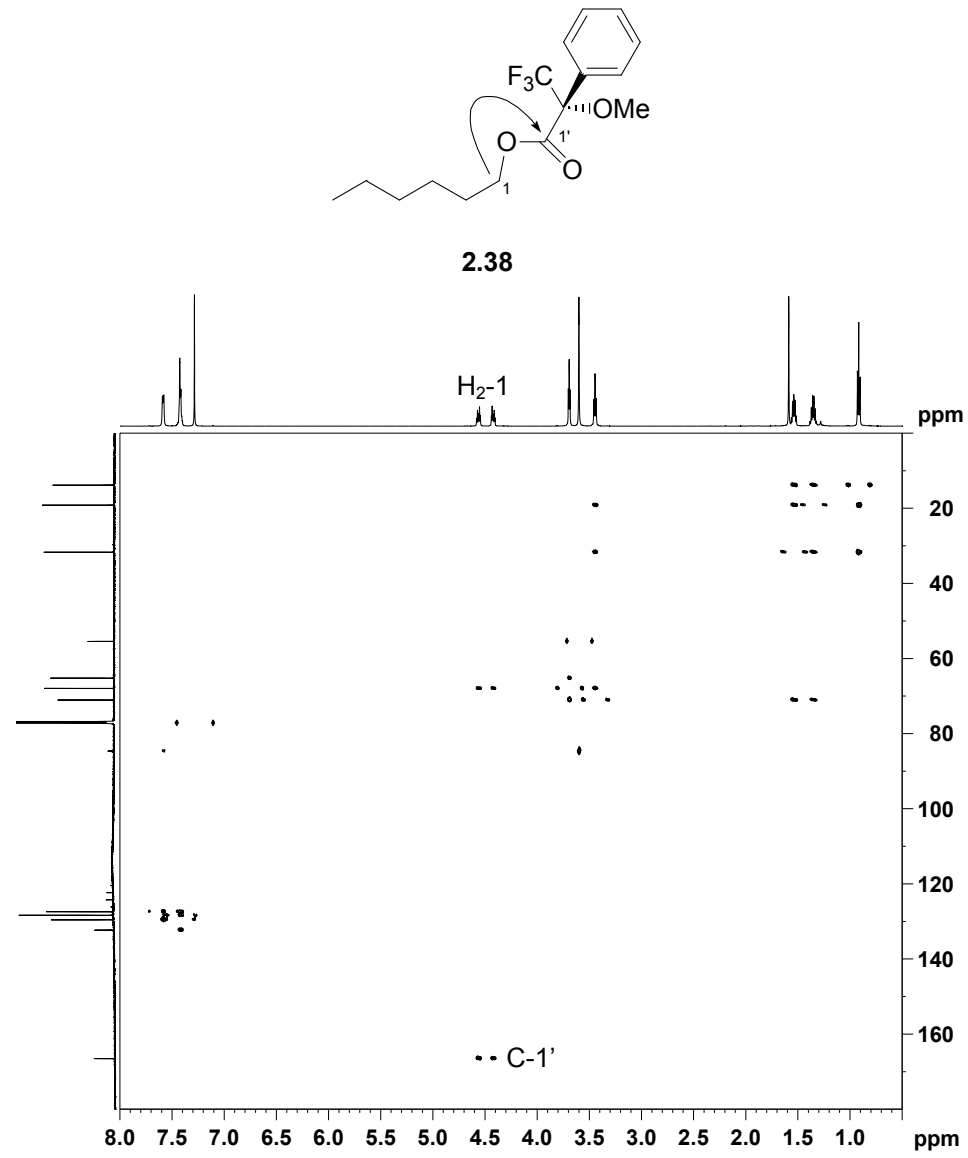

Figure 2.20: The gHMBC spectrum obtained for **2.38**. The accompanying structure illustrates the correlation used to confirm the formation of the MTPA ester.

The success of this trial reaction encouraged us to attempt the preparation of the (*R*)- and (*S*)-MTPA esters of the polypropionate **2.37**. The attempted esterification was carried out using exactly the same procedure as the trial reaction, but on inspection of the ^{1}H and ^{13}C NMR spectra of both the (*R*)- and (*S*)-MTPA products, it was clear that although there was evidence of new aromatic and methoxy signals, the signals assigned to the hydroxyl proton (δ_H 3.02) remained unchanged (Figure 2.21), implying that the attempted Mosher's esterification had resulted in a mixture of unreacted starting materials. It is possible that a strong hydrogen bond between the

hydroxyl proton and carbonyl at C-5 might have impeded the esterification reaction. The appearance of the hydroxyl proton as a doublet (J = 7.3 Hz) and not a broad singlet might suggest that proton exchange is reduced because of hydrogen bonding to the C-5 carbonyl (Figure 2.21). Unfortunately, we were unable to retrieve the unreacted polypropionate and other methods of establishing the absolute configuration were not investigated.

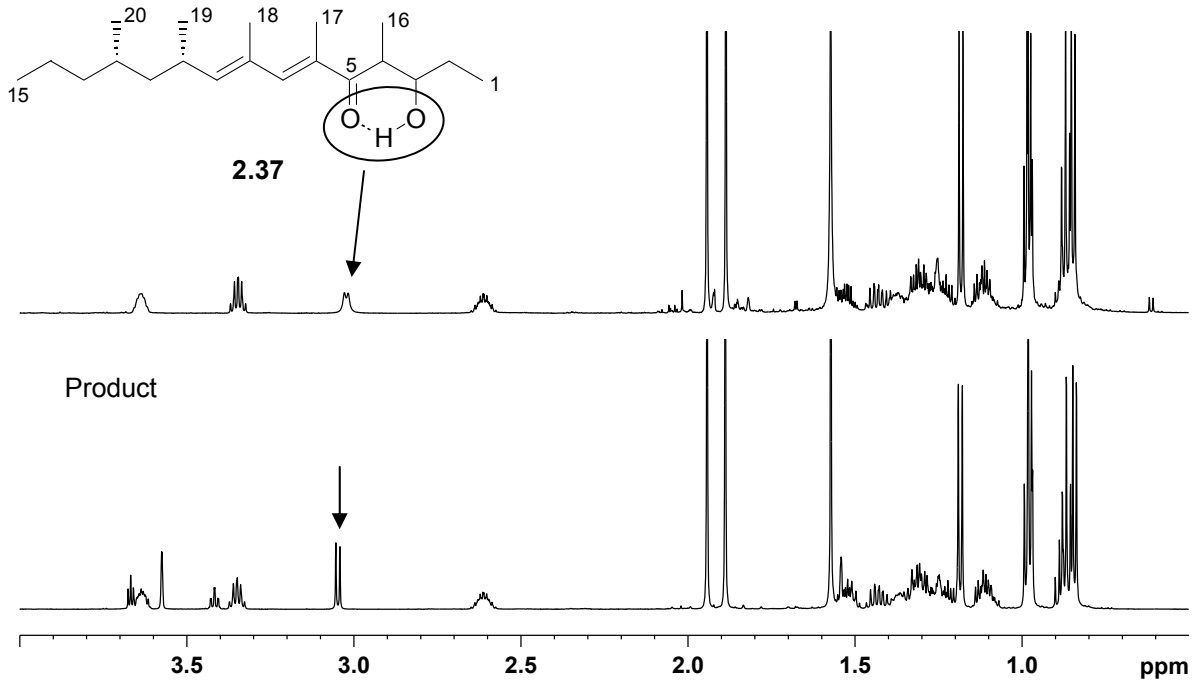

Figure 2.21: Upfield section (0.50-4.00 ppm) of the ^{1}H NMR spectra of **2.37** (top) and the product of the attempted esterification of **2.37**. The arrows highlight the presence of the hydroxyl proton in both spectra.

2.4.2 Investigation into the cellular structure of the lateral pedal glands of *S. oculus*

Light microscope images of the cross-sectional view of the lateral pedal glands of *Siphonaria oculus* were obtained by Shirley Pinchuck at Rhodes University and are reproduced here with her permission. Figure 2.22 shows a section through a gland that has been stained with the general dye, Toluidine Blue. Toluidine Blue is a metachromatic dye which means it will change in colour (red-purple) when exposed to certain chromotropic tissue elements, and this dye is commonly used to stain mast cells, cartilage and certain acid mucins.[65] When the *S. oculus* sections were stained with this dye it was apparent that there were a number of different cell types within the

basic goblet cell structure of the pedal glands of *S. oculus* (Figure 2.22). It is possible that the different cell types may be responsible for producing different metabolites, which once released into the central lumen mix together, and may even undergo some minor transformations before being secreted as a form of chemical defence. This would ensure that the polypropionate rich mucus is only produced when needed, and the organism is less likely to be effected by its chemical properties as the toxic nature of the mucus may only arise once the different components are mixed in the lumen, and secreted.

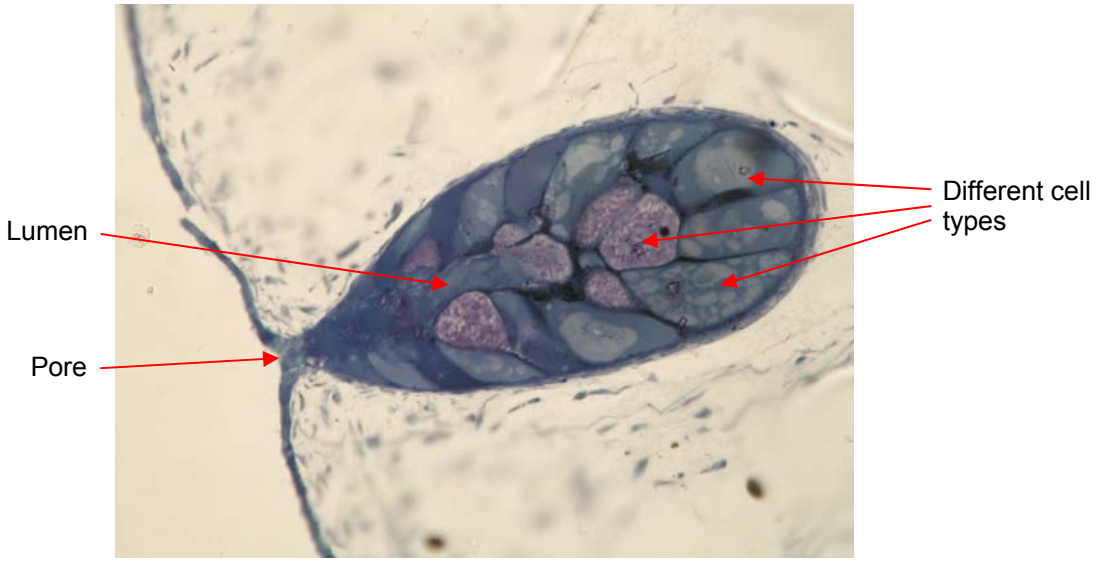

Figure 2.22: Light microscope image (x 40) of the cross-section through the pedal gland of *S. oculus,* stained with Toluidine Blue and showing the presence of different cell types (sectioning and staining by S. Pinchuck).

In an effort to establish the nature of the chemical constituents in the different cell types, two further biological stains were used, *viz* Alcian Blue and Aldehyde Fuchsin. Alcian Blue is a phthalocyanin dye that is primarily used for the differential staining of acidic polysaccharides. This dye will stain acidic metabolites and cell components blue, and neutral components magenta.[65] The image shown in Figure 2.23 (right) shows that glands of *S. oculus* stained with Alcian Blue and an area of blue stain is clearly seen in the centre of the gland, implying that the cells nearest to, or the contents of the lumen are acidic in nature. The second specialist stain used was Aldehyde Fuchsin, which is an aminotriarylmethane dye that is activated by carboxylated groups to produce a deep purple colour.[65] The cross-section of the glands stained with this dye (Figure 2.22, left) appear to have areas stained deep purple, again within the centre

of the gland, but this colouring appears to be contained within cells rather than spread through the lumen as is seen with the blue staining of Alcian Blue. These images would suggest that at least some of the cells contained in the glands of *S. oculus* are rich in carboxylated compounds, and when agitated the organism may release these into the lumen of the gland where they become more acidic in nature. It is difficult however, to determine the exact morphology of the cells that contain the carboxylated metabolites, as a detailed examination of the cell structure would require much greater magnification and the stains used to identify these cells are not appropriate for Transmission Electron Microscopy (TEM).

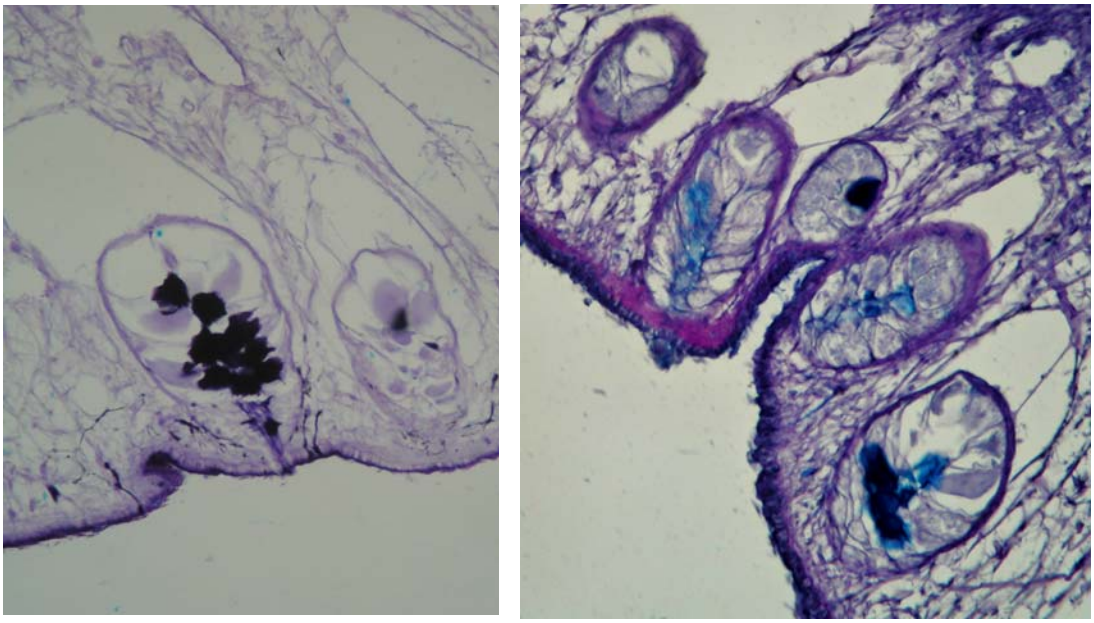

Figure 2.23: Light microscope image (x 20) of the cross section through glands of S. oculus, stained with Alcian Blue (right) and Aldehyde Fuchsin (left) (sectioning and staining by S. Pinchuck).

2.4.3 Analysis of the mucus secretions from *S. oculus*

The standard protocol for extracting polypropionates from *Siphonaria* species is to place multiple specimens directly into the same acetone solution. This extraction method does not provide information as to whether the polypropionates are present in the mucus released when the *Siphonaria* are disturbed or are retained in the pedal glands and are slowly leached out of the glands into the acetone solution during extraction. Therefore, to investigate the chemical nature of the mucus secretions of *S.oculus,* direct collection of the mucus was deemed necessary. In October 2009, 36 *S.oculus* false limpets were aggravated with a capillary tube and the cloudy

mucus produced was taken up in the same capillary tube (Figure 2.24). The capillary tubes containing mucus were placed in cholorform to dissolve the metabolites, the solvent was subsequently removed to yield a crude mucus extract (10.4 mg) which was analysed using ^{1}H NMR ($CDCl_3$, 600 MHz).

Figure 2.24: Photographs of the agitation of the underside of a *S.oculus* false limpet (left) and the capillary collection of the defensive mucus produced after agitation (right).

The ^{1}H NMR spectrum obtained for the crude mucus extract was compared with the ^{1}H spectra obtained for each of the pure metabolites isolated from the bulk, acetone extraction of numerous *S. oculus* species (Figure 2.24). The upfield region (δ_H 0.50-2.20) of the ^{1}H NMR spectra obtained for the crude mucus extract was complex with the prominent methyl doublet signals in addition to numerous methylene multiplets corresponding to the polypropionate metabolites clearly evident. The downfield region (δ_H 2.30 to 7.20) of the ^{1}H NMR spectra obtained for the crude mucus extract is less complex enabling easier visual comparisons (Figure 2.25). From the relative signal intensities, it would appear from Figure 2.25 that the polypropionates are only minor constituents of the mucus exudate. Interestingly, the characteristic olefinic downfield doublets of the three compounds containing a furanone ring (**2.2**, **2.35** and **2.36**) appear to be missing in the mucus extract while those corresponding to the linear polypropionate (**2.37**) are clearly evident. This observation might suggest that the furanone ring containing compounds may be artefacts, arising from cyclisation of the tautomeric acyclic triketone precursor (**2.39**) during work up of the extract (Scheme 2.7).

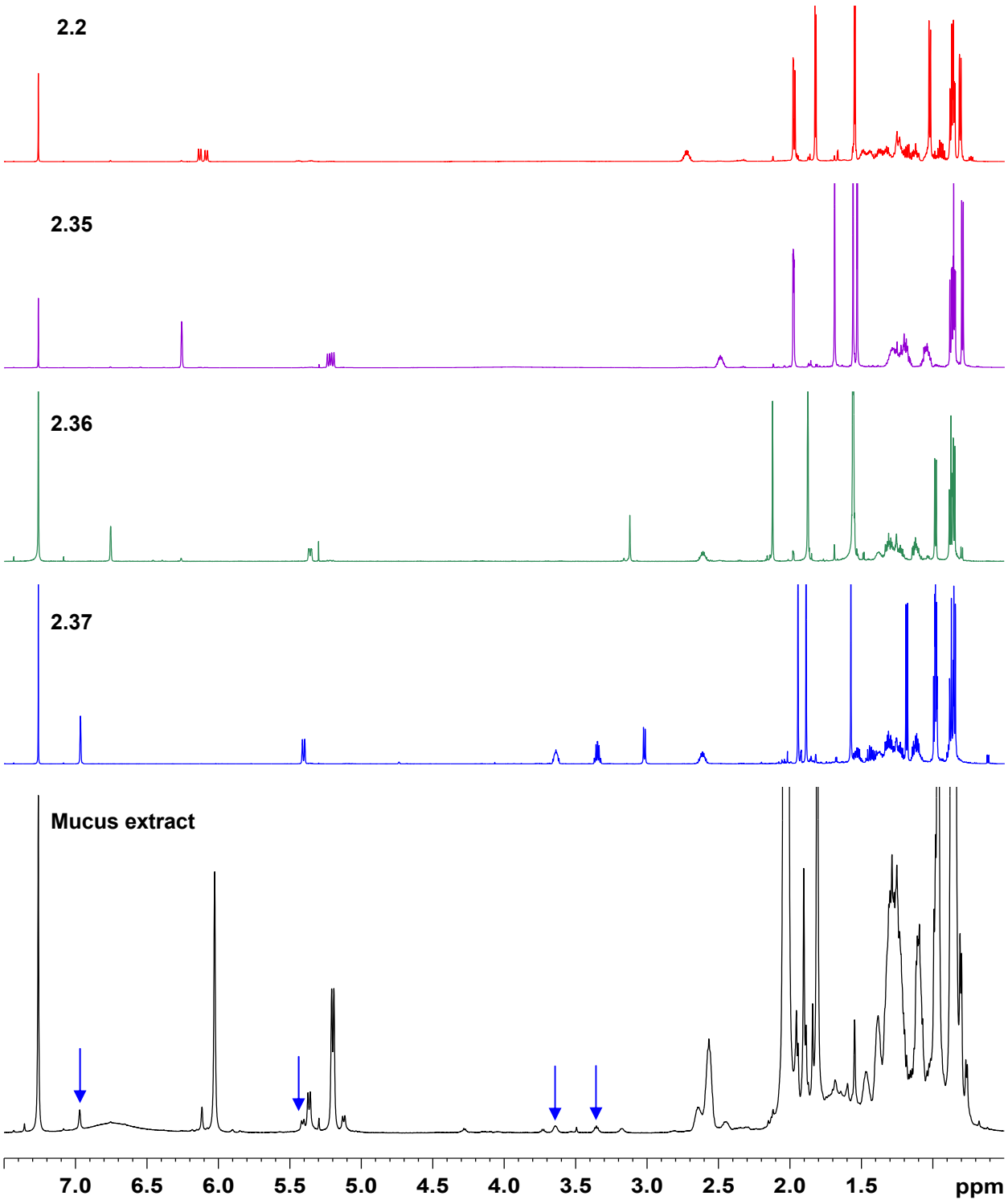

Figure 2.25: ^{1}H NMR ($CDCl_3$, 600 MHz) of the isolated metabolites **2.2**, **2.34**, **2.35**, **2.36** and the crude mucus extract (top to bottom respectively). Coloured arrows highlight common deshielded resonances.

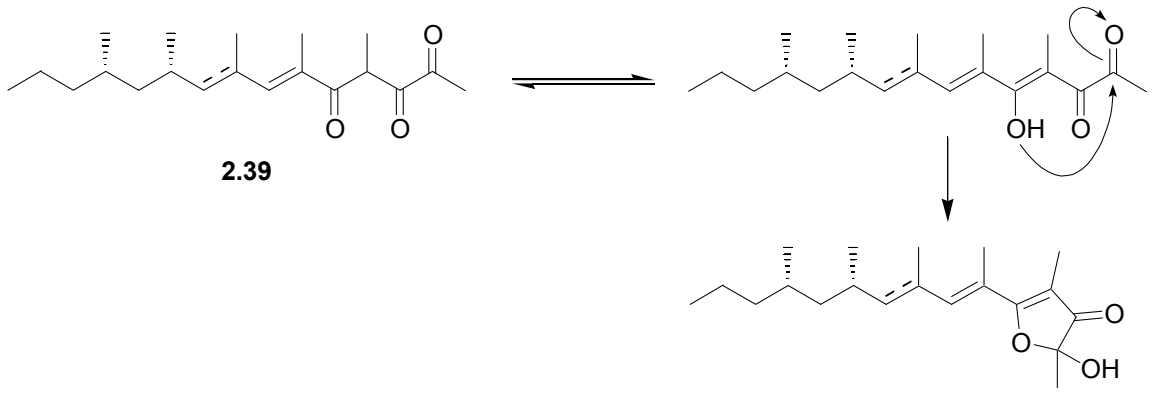

Scheme 2.7: Proposed formation of **2.2**, **2.35** and **2.36** from a theoretical precursor **2.39**.

2.5 Concluding remarks

Siphonarienfuranone (**2.2**) was the only common natural product in both the 1998 and the 2009 collections of *Siphonaria capensis* as well as the collection of *Siphonaria oculus*, suggesting inter-species overlap in polypropionate biosynthesis. Compound **2.29**, the geometric isomer of **2.2** was not isolated in either of the *Siphonaria* collections which suggests that **2.29** is possibly an artifact formed through isomerisation of **2.2** during extraction. The use of milder chromatography media is a possible reason why **2.29** was not isolated from extracts of either *S. capensis* and *S. oculus* in the most recent collections. The absence of capensifuranone, **2.12**, and capensinone, **2.30**, in the 2009 collection of *S. capensis* may be due to seasonal or even genetic variation in this species. However the possibility that **2.12** and **2.30** were artifacts of the original isolation cannot be excluded. Our 2009 collection also afforded the sterol **2.33**, which was not isolated from the 1998 collection of *S. capensis*. The ubiquitous occurrence of **2.33** and its precursor **2.34** in different marine phyla suggest that **2.33** may be a common minor primary metabolite.

Three new polypropionate metabolites, **2.35**, **2.36** and **2.37** were isolated from *S. oculus*, two of which (**2.35** and **2.36**) are geometric isomers of each other. An unsuccessful attempt was made to establish the absolute configuration of **2.37** using the modified Mosher's method and the limited amount of **2.37** in hand prevented any further attempts at resolving the absolute configuration of this compound. An investigation of the chemical make up of the defensive mucus produced by *S. oculus* revealed the presence of the acyclic polypropionate **2.37** metabolite, albeit in minute quantities in the crude mucus extracted directly from the mollusc. The absence of characteristic signals for the furanone containing compounds **2.2**, **2.35** and **2.36**, might suggest that these cyclise from a hypothetical acyclic precursor (**2.39**) during standard work up of bulk acetate extracts of *Siphonaria* species.

Chapter Three
Sesquiterpenes from the South African Nudibranch, *Leminda millecra*

3.1 Introduction

3.1.1 Opisthobranch nudibranchs

Nudibranchia is the largest order of Opisthobranchia, and there are believed to be four suborders, Doridina, Dendronotina, Arminina and Aeolidina, however this taxonomic assignment is currently under review.[65, 66] The name nudibranch comes from the Latin *nudus* (naked), and the Greek *brankhia* (gills) which relates to the respiratory systems which are often a set of external gills located dorsally, encircling the anus, although some nudibranchs use finger-like protrusions called cerata to respire.[66] Nudibranchs, also commonly known as sea slugs, make use of rhinophores found near the front of the animal to relay chemosensory information from the environment.[66] They are carnivores, feeding on other invertebrates such as sponges, soft corals, anemones, and hydroids, by rasping their prey with a radula (a series of small teeth made of chitin).[66] Some nudibranchs have a specific diet, only eating a single species, or even one part of it, whilst others are general grazers.[66]

Mature nudibranchs lack a protective shell, and so have developed other forms of protection. Some have adopted camouflage, or burrow under sand for protection, whilst others make use of chemical defenses.[66] Aeolid nudibranchs are able to store nematocysts obtained from their diet in their cerata and when attacked, they release these stinging cells as a defense.[66] Other nudibranchs secrete toxins that make them unpalatable to predators. These toxins are either sequestered from the nudibranchs diet, or through evolution, are synthesised *de novo*.[26] Most nudibranchs employing a chemical defense have adapted elaborate physiology and are brightly coloured (aposematic colouration), as a warning to predators.[66]

3.1.2 *Leminda millecra*

Leminda millecra are small to medium sized nudibranchs, which lack external gills and cerata but have well developed parapodia that form a distinctive, convoluted mantle, that is usually pinkish orange with a pale blue margin (Figure 3.1), but exact colouring varies and is dependant on the food contained in the digestive tract.[67, 68] The digestive gland of *L. millecra* is divided into relatively fine branching ducts which is consistent with a shift to a cnidarian based diet.[26] This species of nudibranch is endemic to South Africa and occurs at depths of -10 to -40 m, from both sides of the Cape peninsula up to Kwazulu Natal.[68] This nudibranch is the most common species in Algoa Bay, South Africa.

Figure 3.1: Two *Leminda millecra* specimens photographed in Algoa Bay. (Photograph provided by Shirley Parker-Nance, and used here with her permission.)

First described by Griffiths in 1985, *L. millecra* was placed within the smallest sub-order of nudibranchs, the Arminacea, as the only member of the Lemindidae family.[67, 68] The Arminidae, defined by the longitudinal striations on their notum, and the Janolidae, defined by the presence of highly developed cerata, are the two other families in the sub-order Arminacae.[67, 68] However, the Arminacea sub-order is often seen as a reservoir for species that do not fit within the other three sub-orders of nudibranchia, for example Janolid nudibranchs are possibly more closely related to Aeolid nudibranchs than the Arminacae.[67] Recently, Pola and Gosliner[68] re-evaluated the taxonomic relationships between opisthobranchs by examining the DNA sequences of two mitochondrial and one nuclear gene of 95 specimens from 22 families and 38 genera of nudibranchia. This study revealed the potential sister group relationship between *Leminda millecra* and the Charcotiidaen nudibranch, *Dirona albolineata*, although more research needs to be carried out to confidently place these two species into the correct sub-order.[68] These inconsistencies in the classification of *L. millecra* mean that one can not confidently make any assumptions about the feeding habits, or origin of the metabolites isolated from *L. millecra*, based on comparisons with other theoretically closely related species of nudibranch.

Pika and Faulkner[27] were the first to investigate the diet and metabolites contained in *L. millecra*.[27] Specimens of *L. millecra* were collected from Coffee Bay in the Transkei, and yielded four sesquiterpene metabolites, millecrone A (**3.1**), millecrone B (**3.2**), millecrol A (**3.3**), and millecrol B (**3.4**). In an attempt to establish the origin of these metabolites, Faulkner and Pika[27] dissected the digestive glands of two specimens of *L. millecra*, which revealed the presence of spicules from the soft corals *Alcyonium foliatum*, *Alcyonium valdiviae*, and *Capnella thyrsoidea*, giving the first evidence of an octocoral (cnidarian) diet, which correlates with later visual observations in Algoa Bay of individuals feeding on ocotcorals e.g. gorgonians (sea fans) (Figure 3.2).[27] It was proposed that *L. millecra* sequesters these compounds from the soft corals it feeds on as *Alcyonium* and *Capnella* species are well-known sources of sesquiterpenes.[27]

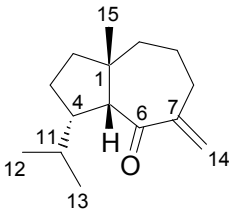

3.1

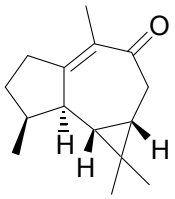

3.2

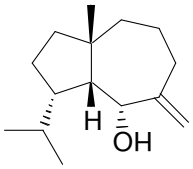

3.3

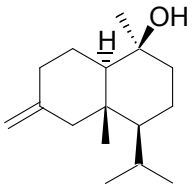

3.4

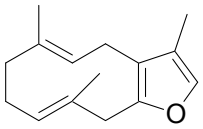

3.5

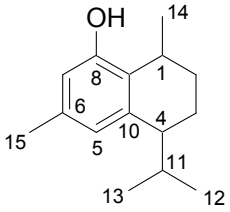

3.6

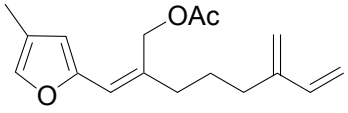

3.7

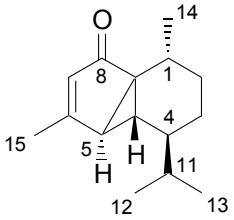

3.8

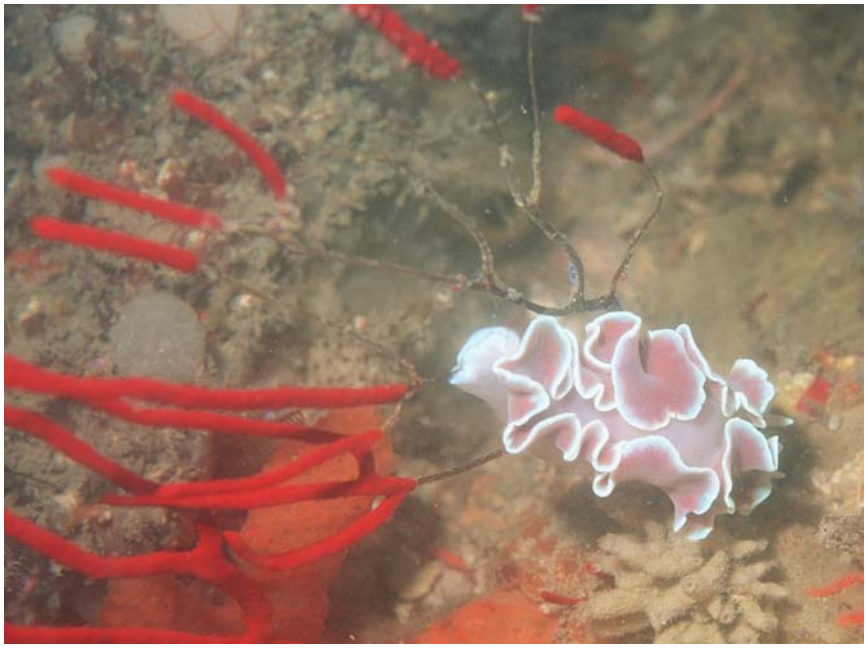

Figure 3.2: *Leminda millecra* photographed feeding on a species of gorgonian (sea fan).

A later study of *L. millecra* secondary metabolites by McPhail *et al.*[28] yielded the sesquiterpenes, millecrone A (**3.1**) and B (**3.2**), isofuranodiene (**3.5**), 8-hydroxycalamenene (**3.6**), algoafuran (**3.7**), cubebenone (**3.8**) as well as a series of seven triprenyl toluquinones and toluhydroquinones (**3.9**-**3.15**) from *L. millecra* specimens collected in Algoa Bay *ca* 400 km south west of Coffee Bay.[28] McPhail *et al.*[28] carried out a GC-MS analysis of 21 octocoral species believed to be possible *L. millecra* prey, in order to determine the origin of the metabolites isolated from *L. millecra*.[28] This investigation revealed that the soft coral *Alcyonium fauri* was the source of **3.1** whilst the gorgonian *Leptogorgia palma* was the source of **3.2** and **3.8**.[28] The presence of the octocoral spicules in their digestive tracts, and the evidence that *L. millecra* sequesters metabolites from different species of octocoral, suggests that they are not discriminate feeders, and that their diet includes a variety of octocoral species, from which they sequester secondary metabolites possibly for chemical defence.[28]

One of the motivations for us to return to *L. millecra* was to source more of the cytoxic triprenyl toluquinones and toluhydroquinones (**3.9**-**3.15**) originally isolated by McPhail *et al.*[28] who were able to establish the activity of these compounds against oesophageal cancer cells (WHCO1 cell line) using the 3-(4,5-dimethylthiazol-2-yl)-2,5-diphenyltetrazolium bromide (MTT) assay.[69] The cytotoxicity observed (Table 3.1) revealed that **3.11** and **3.12** had the lowest IC_{50} values of 9.5 μM and 12.9 μM respectively.[69] Compound **3.11** was also screened against the cervical carcinoma

cell lines ME180 and SiHa, the non-malignant breast epithelial cancer line MCF-12 as well as another oesophageal cancer cell line, WHCO6; where it was found to be moderately active against the majority of these cell lines, and very cytotoxic towards WHCO6 oesophageal cancer line, with an IC_{50} value of 5.8 μM.[69] Whibley *et al.*[69] proposed that the triprenyl toluquinones and toluhydroquinones act by producing reactive oxygen species (ROS) which induce a cell cycle arrest, leading ultimately to apoptosis of the cancer cell.[69]

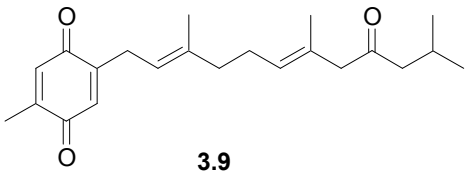

3.9

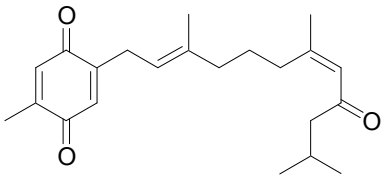

3.10

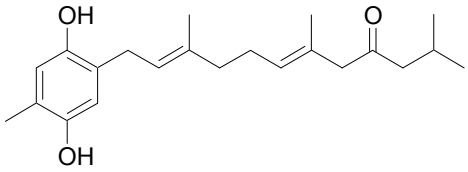

3.11

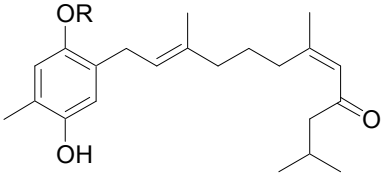

3.12 R = H
3.13 R = Ac

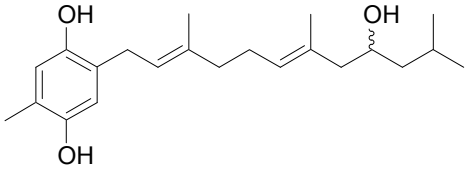

3.14

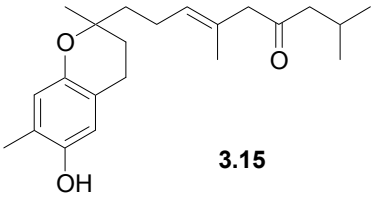

3.15

Table 3.1: IC_{50} values of compounds **3.9**-**3.15** tested against oesophageal cancer cells (WHCO1 cell line).[69]

Compound	IC_{50} (μmol/L)	95% Confidence interval
3.9	37.9	37.7-38.0
3.10	83.3	82.1-84.5
3.11	9.5	9.4-9.5
3.12	12.9	12.5-13.3
3.13	42.7	42.6-42.7
3.14	32.7	32.5-33.0

3.2 Re-isolation of known sesquiterpenes from *Leminda millecra*

In February 2010 a collection of *Leminda millecra* (40 nudibranchs) was made by hand using SCUBA (-15 to -20 m) off Phillips Reef (Algoa Bay). Specimens were steeped in acetone overnight, sonicated and the solvent removed before being steeped, overnight, in fresh acetone. The two acetone extracts were combined and organic metabolites adsorbed onto HP-20 resin through cyclic-loading, following the same procedure discussed in Section 2.2. The HP-20 resin beads were sequentially stripped with aqueous acetone mixtures of decreasing polarity (20%, 40%, 60%, 80% acetone/water, and 100% acetone) to afford five crude fractions (Scheme 3.1). The ^{1}H and ^{2}C NMR data obtained for compounds **3.1**, **3.2**, and **3.5**-**3.15** isolated from the 1999, Algoa Bay collection of *L. millecra*,[28] were available to us and were used to establish which of the crude HP-20 fractions contained the compounds of interest. The 80% acetone/water fraction was chosen for further purification and subjected to open chromatography on a DIOL column using a dichloromethane/hexane gradient system (Scheme 3.1).

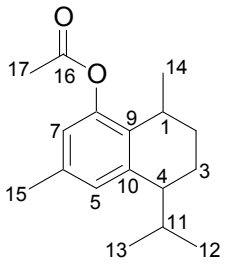

3.16

Fraction 3 afforded pure millecrone A (**3.1**, 4.3 mg/nudibranch), whilst, fraction 8 yielded 8-hydroxycalamenene (**3.6**, 0.3 mg/nudibranch) and cubebenone (**3.8**, 1.1 mg/nudibranch) after normal phase HPLC (10% dichloromethane/hexane) on a DIOL column. Compound **3.6** (0.6 mg/nudibranch) was also isolated from fraction 9 after HPLC (20% dichloromethane/hexane). Fraction six was subjected to normal phase HPLC (10% dichloromethane/hexane) on a DIOL column and yielded the new metabolite 8-acetoxycalamenene (**3.16**, 0.1 mg/nudibranch).

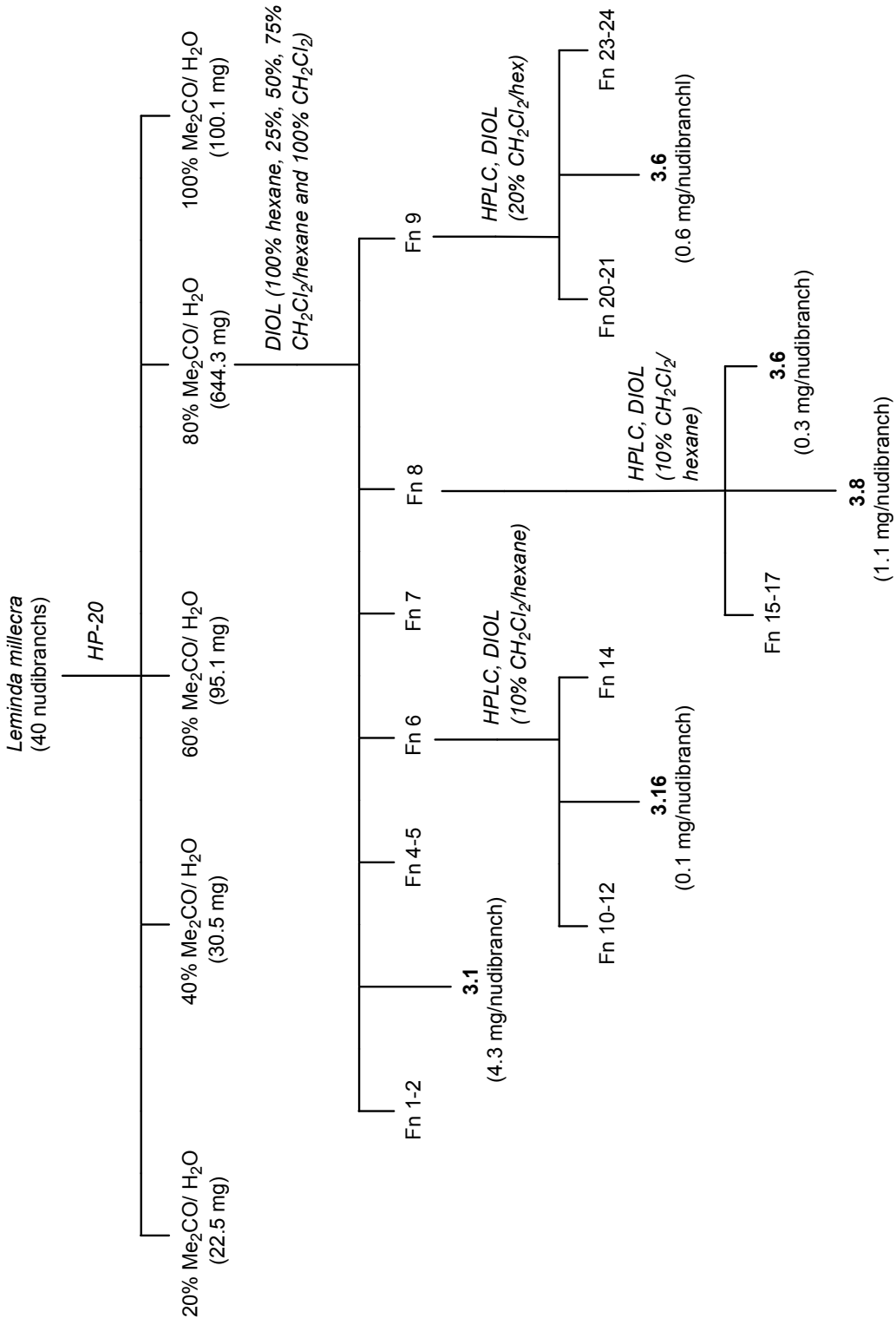

Scheme 3.1: Chromatography procedure used to isolate metabolites from *Leminda millecra*.

Only three (**3.1**, **3.6**, and **3.8**) of the eight sesquiterpenes originally isolated from the *L. millecra* collected in 1998[28] were re-isolated from the 2010 collection. The ^{1}H (Figure 3.3) and ^{13}C (Figure 3.4) NMR spectra of **3.1**, **3.6** and **3.8** were consistent with those acquired for these compounds by McPhail *et al.*[28] Assignment of the ^{1}H and ^{13}C chemical shifts for those compounds were made by direct analogy with McPhail *et al*.'s[28] previously assigned data (Table 3.2). The high resolution mass data and optical rotations (Table 3.3) of the re-isolated compounds are similarly consistent with the data obtained by McPhail *et al*.[28] The initial ^{1}H and ^{13}C NMR chemical shift assignments of compounds **3.1**, **3.6** and **3.8** were subsequently confirmed where necessary by a series of 2D NMR experiments (gCOSY and gHMBC).

Table 3.2: ^{13}C (150 MHz, $CDCl_3$) NMR data obtained for compounds **3.1**, **3.6** and **3.8** alongside those obtained by McPhail *et al*.[28]

	3.1		**3.6**		**3.8**	
		Lit.[28]		Lit.[28]		Lit.[28]
Position	δ_C ppm	δ_C ppm	δ_C ppm	δ_C ppm	δ_C ppm	δ_C ppm
1	46.1	46.0	26.6	26.6	26.4	26.3
2	41.9	41.9	27.2	27.2	30.5	30.5
3	27.9	27.9	19.1	19.1	26.3	26.3
4	45.7	45.7	43.1	43.1	45.3	45.2
5	62.4	62.4	122.9	123.0	35.5	35.5
6	202.1	201.8	135.1	135.0	178.0	177.9
7	146.0	146.0	113.5	113.3	123.5	123.4
8	29.6	29.6	153.2	153.0	209.1	209.0
9	23.8	23.8	126.1	126.0	42.8	42.8
10	35.3	35.3	141.3	141.2	54.3	54.2
11	34.1	34.0	33.2	33.2	32.8	32.8
12	21.6	21.6	19.6	19.6	19.7	19.6
13	20.7	20.7	22.1	22.1	19.6	19.6
14	121.6	121.4	21.2	21.2	19.8	19.7
15	25.2	25.2	21.1	21.1	18.8	18.8

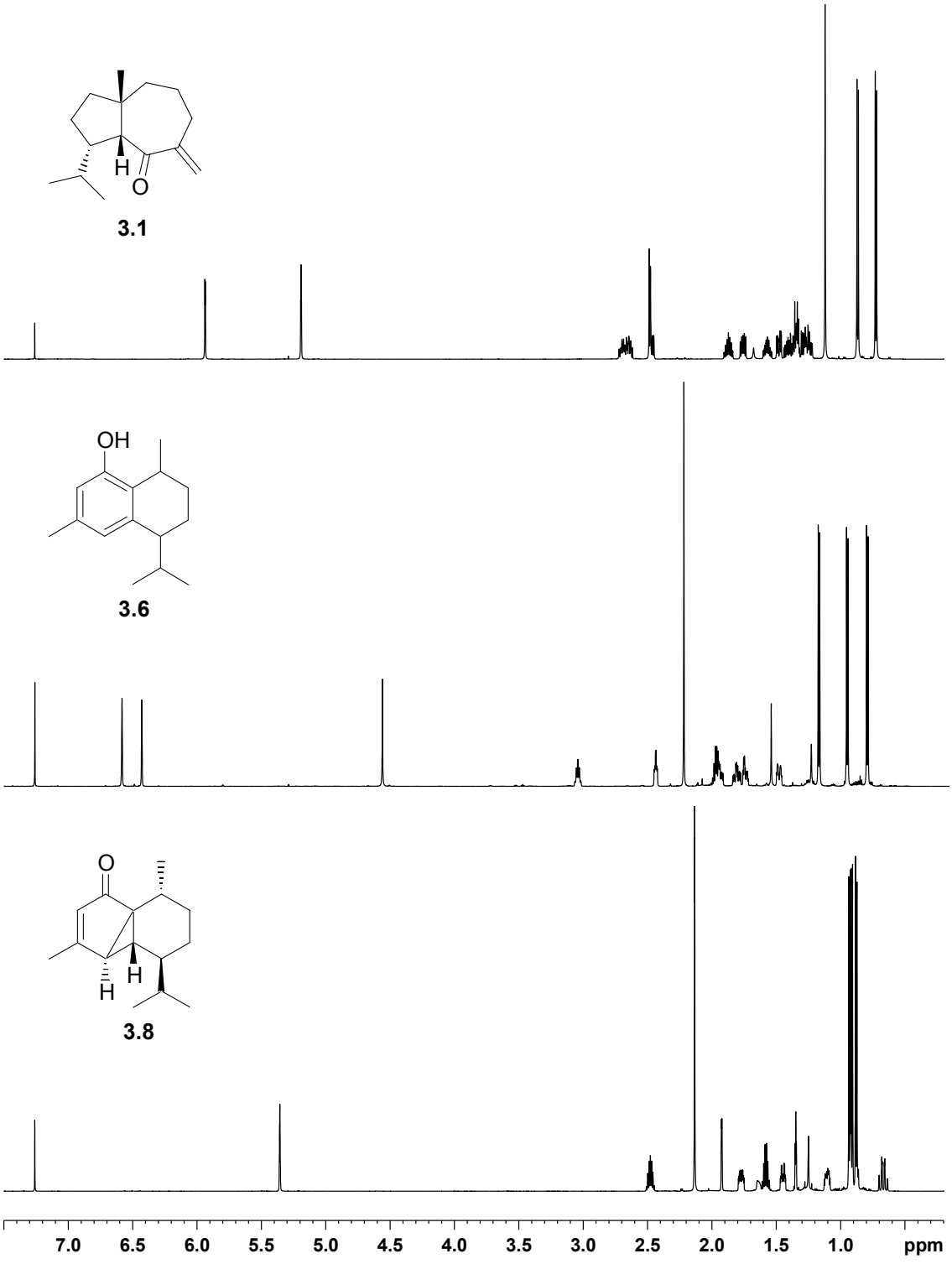

Figure 3.3: ^{1}H ($CDCl_3$, 600 MHz) NMR spectra of the known metabolites, **3.1**, **3.6** and **3.8**, isolated from *L. millecra*.

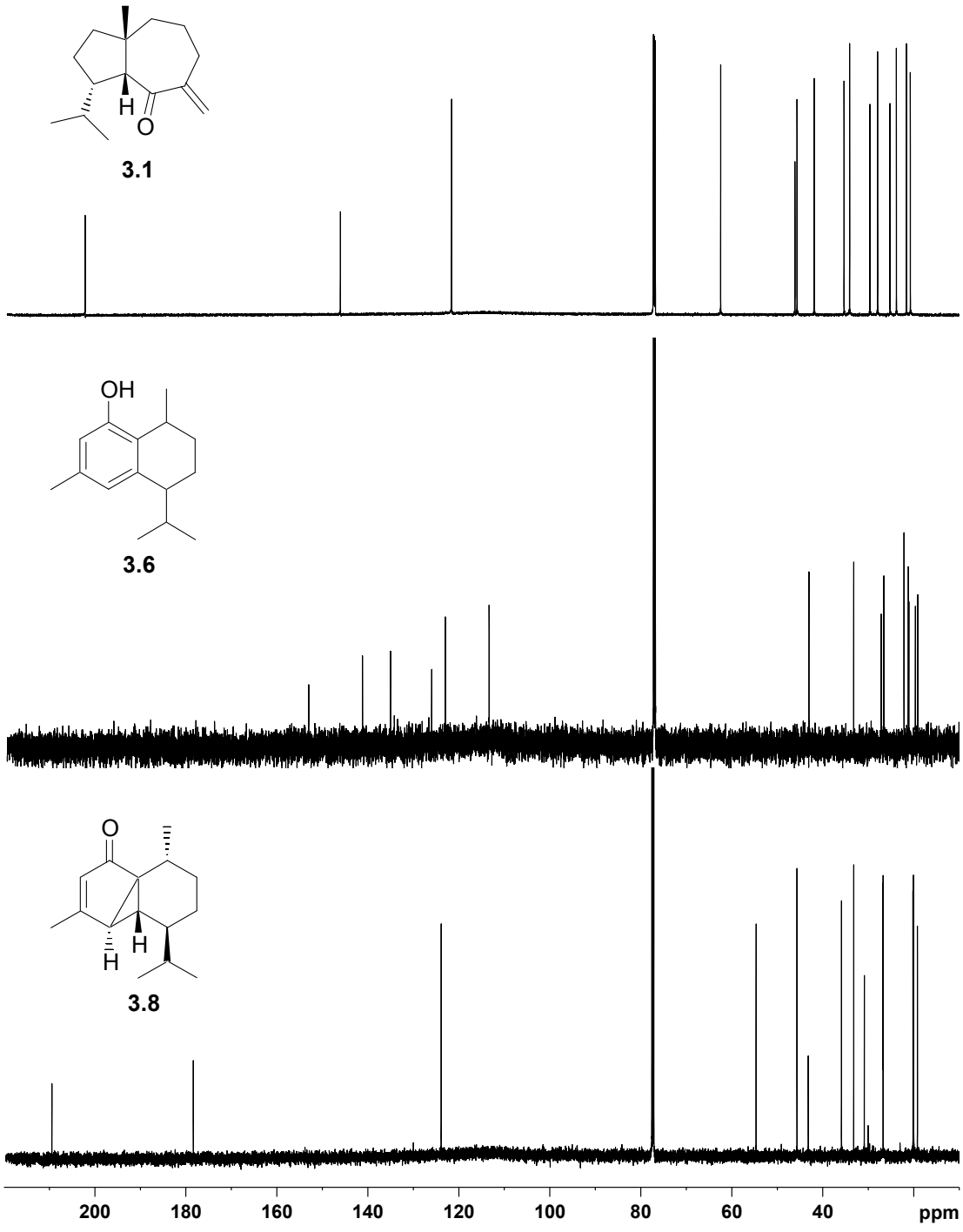

Figure 3.4: ^{13}C ($CDCl_3$, 150 MHz) NMR spectra of the known metabolites, **3.1**, **3.6** and **3.8**, isolated from *L. millecra*.

Table 3.3: Optical rotation data obtained for compounds **3.1**, **3.6** and **3.8** compared with those obtained by McPhail *et al.*[28]

Compound	Optical Rotation $[\alpha]_D$	Literature Data [28] $[\alpha]_D$
3.1	+31	+41
3.6	+34	+36
3.8	+136	+126

Interestingly, none of the prenylated toluquinones and hydroquinones isolated by McPhail *et al.*[28] were isolated from the 2010 collection. However, millecrone A (**3.1**) has been consistently found in *L. millecra* extracts from both Coffee Bay[27] and Algoa Bay[28] suggesting that the source of this compound, *Alcyonium fauri*, is a primary dietary species for *L. millecra*.

3.3 Isolation and structure elucidation of a new sesquiterpene from *L. millecra*

The new secondary metabolite 8-acetoxycalamenene (**3.16**, 0.1 mg/nudibranch, $[\alpha]_D$ +20), was isolated after normal phase HPLC (10% dichloromethane/hexane) of fraction 6. The ^1H and ^{13}C NMR spectra of **3.16** (Figure 3.5) were similar to those obtained for **3.6** (Figures 3.3 and 3.4), thus a related structure was anticipated. The molecular formula of **3.16** ($C_{17}H_{24}O_2$) was deduced from ^{13}C and ^1H NMR and confirmed by HREIMS, which implied six degrees of unsaturation, and differs from the molecular formula determined for **3.6** by C_2H_2O, suggesting the addition of an acetate group. The six aromatic resonances in the ^{13}C NMR spectrum (δ_C 120.3, 128.0, 131.4, 135.0, 141.3, and 148.6 ppm) and the two deshielded proton signals in the ^1H NMR spectrum (δ_H 6.69 and 6.87 ppm) of **3.16** suggested the presence of a benzene ring system, consistent with that observed for **3.6**, and accounting for four of the six double bound equivalents. Correlations observed in a two-dimensional COSY NMR experiment (Figure 3.6 and Table 3.4) from the methyl protons (δ_H 1.13, d, J = 6.8 Hz) through to the two methyl protons (δ_H 0.81, d, J = 6.8 Hz and 0.99 d, J = 6.8 Hz) indicated the presence of a contiguous carbon chain. Key gHMBC correlations (Table 3.4) *e.g.* between the aromatic H-5 (δ_H 6.87 ppm) and C-4 (δ_C 42.8 ppm) established the bicyclic nature of **3.16**, consistent with that observed in **3.6**. The presence of an absorbance at 1621 cm^{-1} in the IR spectrum of **3.16** suggested a carbonyl moiety, which was confirmed by the presence of an acetate carbonyl resonance (δ_C 169.7) in the ^{13}C NMR spectrum. The presence of two similar, deshielded methyl proton resonances in the ^1H NMR spectrum (δ_H 2.29 and 2.30 ppm) and their corresponding ^{13}C NMR resonances (δ_C 21.0 and 21.1

ppm respectively) were assigned to a *meta*-substituted methyl group on a benzene ring system and an acetate methyl moiety. The ^{2}J, ^{3}J and ^{5}J gHMBC correlations from these two methyl proton resonances were used to establish their position relative to the surrounding carbon signals, and confirmed the acetate functionality contained in **3.16** (Figure 3.6). As a final confirmation of the structure of **3.16**, a portion of **3.6** was acetylated by stirring this compound with pyridine and acetic anhydride (18 h) in the normal manner. The ^{1}H and ^{13}C NMR (Figure 3.7) data and HREIMS mass data obtained for the synthetic **3.16** were identical to those obtained for **3.16** isolated from *L. millecra*.

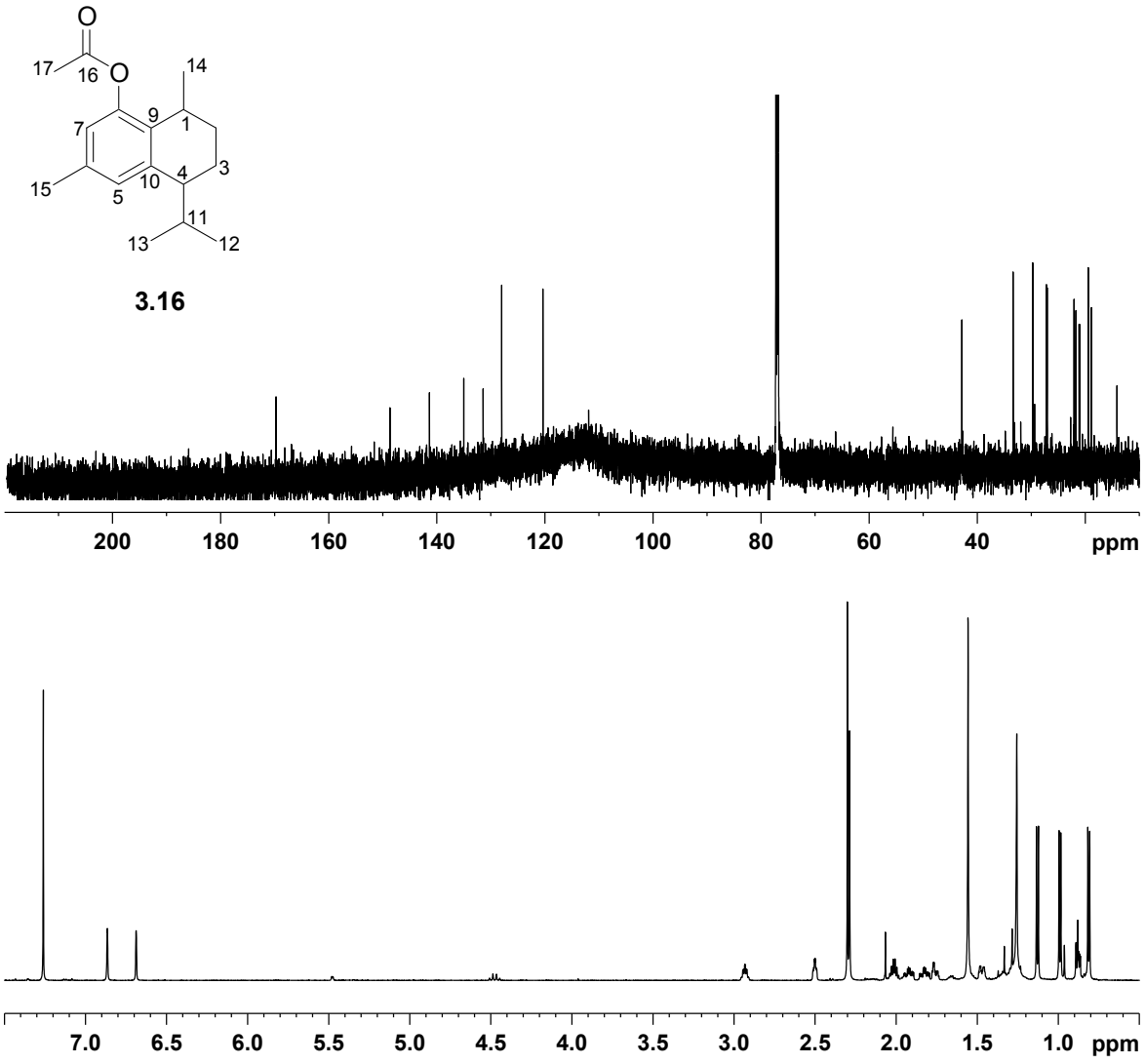

Figure 3.5: ^{1}H ($CDCl_3$, 600 MHz) and ^{13}C ($CDCl_3$, 150 MHz) NMR spectra obtained for **3.16**.

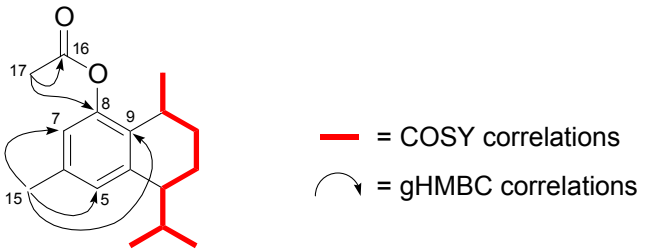

3.16

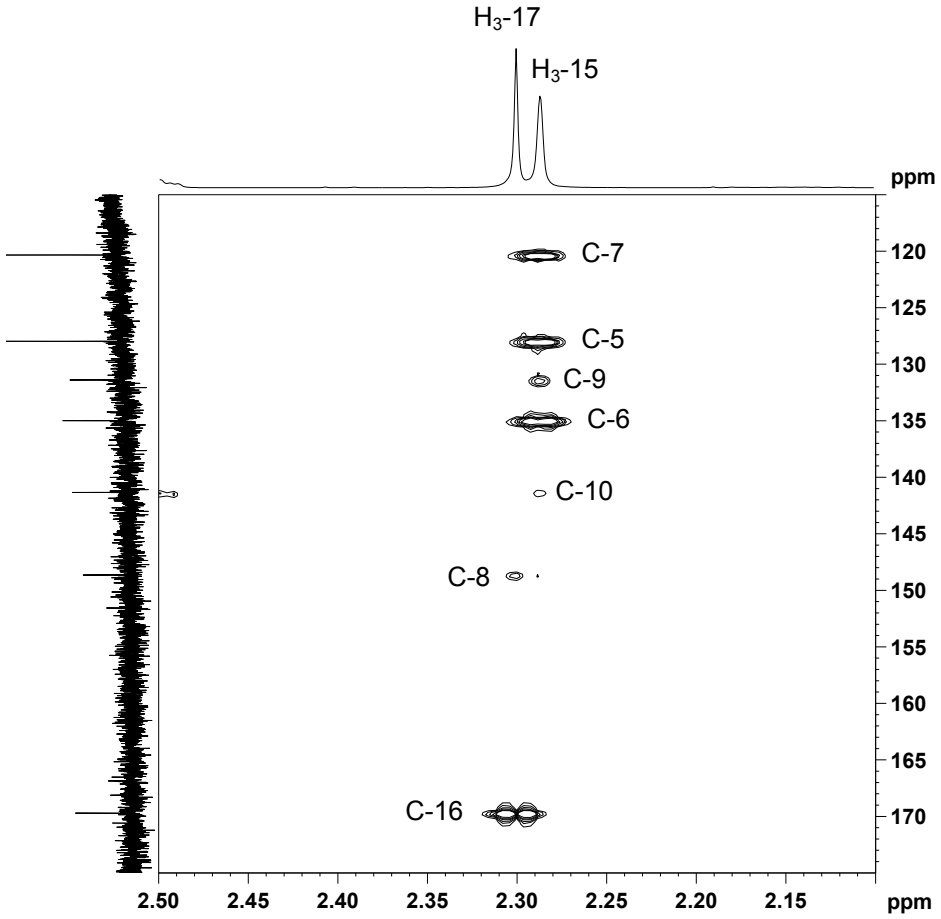

Figure 3.6: A region (F1 = δ 2.1-2.5 ppm; F2 = δ 115-175 ppm) of the gHMBC spectrum ($CDCl_3$, 600 MHz) of **3.16**. The accompanying structure illustrates the key gHMBC and COSY correlations used to elucidate the structure of **3.16**.

Table 3.4: ^{1}H ($CDCl_3$, 600 MHz), ^{13}C ($CDCl_3$, 150 MHz) and 2D NMR data obtained for **3.16**.

Position	δ_C ppm	δ_H ppm (int., mult., *J*/Hz)	gHMBC	COSY
1	27.2	2.93 (1H, qn.d, 6.7, 1.8)	C-3, C-8, C-9, C-10, C-14	H-2a, H-2b, H_3-14
2a	27.0	1.48 (1H, ddt, 13.2, 4.1, 3.0)	C-1, C-3, C-4, C-9, C-14	H-1, H-2b, H-3a, H-3b
2b		1.92 (1H, tdd, 13.2, 6.0, 3.6)	C-1, C-3, C-4, C-9, C-14	H-1, H-2a, H-3a, H-3b
3a	18.8	1.76 (1H, dq, 13.9, 3.4)	C-1, C-2. C-4, C-10, C-11	H-2a, H-2b, H-3b, H-4
3b		1.83 (1H, tdd, 13.3, 6.0, 3.4)	C-1, C-2. C-4, C-10, C-11	H-2a, H-2b, H-3a, H-4
4	42.8	2.50 (1H, td, 5.7, 2.5)	C-2, C-5, C-9, C-10, C-11, C-12, C-13	H-3a, H-3b, H-11
5	128.0	6.87 (1H, s)	C-4, C-7, C-8, C-9, C-15	H-7, H_3-15
6	135.0	-	-	-
7	120.3	6.69(1H, s)	C-5, C-8, C-9, C-17	H-5, H_3-15
8	148.6	-	-	-
9	131.4	-	-	-
10	141.3	-	-	-
11	33.3	2.01 (1H, octet, 6.6)	C-3, C-4, C-10, C-12, C-13	H-4, H_3-12, H_3-13
12	19.4	0.81 (3H, d, 6.8)	C-4, C-11, C-13	H-11
13	22.1	0.99 (3H, d, 6.8)	C-4, C-11, C-12	H-11
14	21.7	1.13 (3H, d, 6.8)	C-1, C-2, C-9	H-1
15	21.0	2.29 (3H, s)	C-5, C-6, C-7, C-9, C-10	H-5, H-7
16	169.7	-	-	-
17	21.1	2.30 (3H, s)	C-8, C-16	-

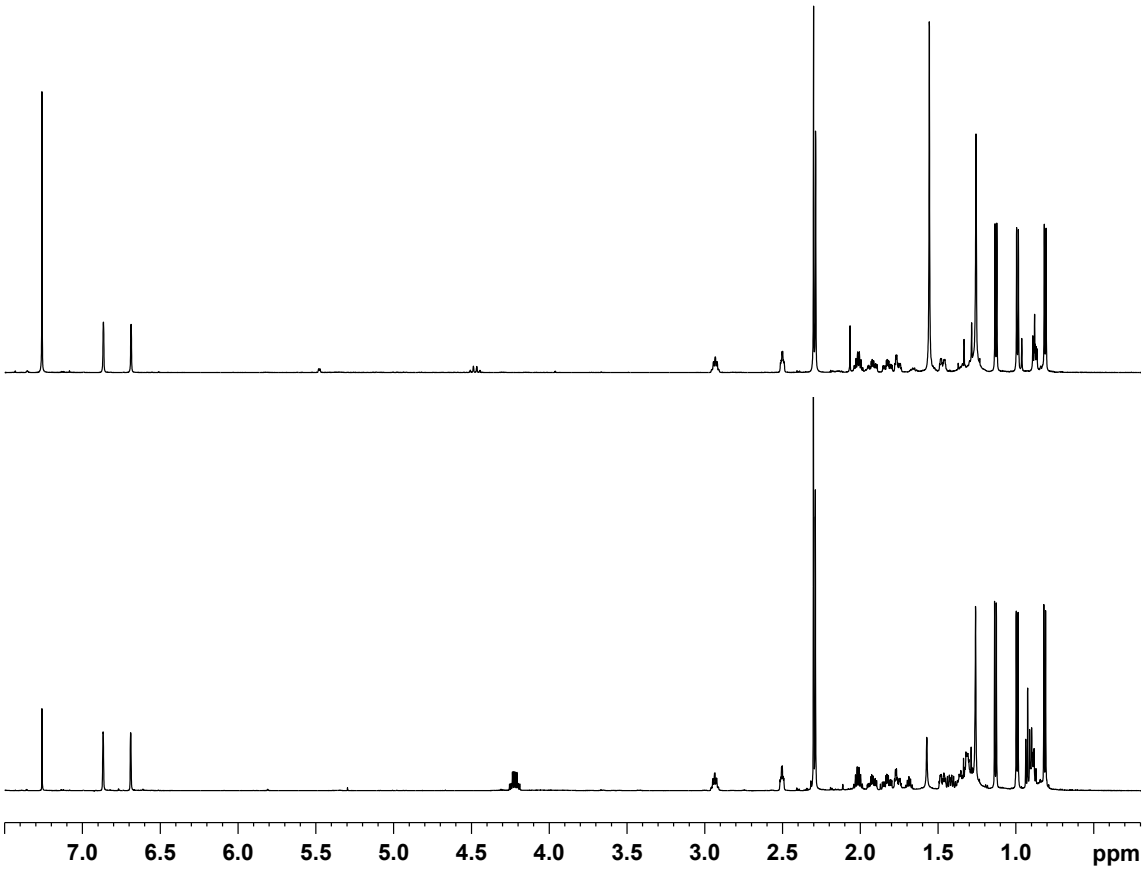

Figure 3.7: ^{1}H ($CDCl_3$, 600 MHz) NMR spectra obtained for **3.16** isolated from *L. millecra* (top) and **3.16** synthesised from acetylation of **3.6** (bottom). Note EtOAc impurities in both spectra.

Extensive overlap in the methylene envelop region of the ^{1}H NMR spectra of both **3.6** and **3.16** prevented an assignment of the relative configuration at C-1 and C-4 in these two compounds. Our attempt to assign the absolute configuration in **3.1**, **3.6** and **3.8** is described in the following Section.

3.4 An attempt to establish the absolute configuration of millecrone A (3.1), 8-hydroxycalamenene (3.6) and cubebenone (3.8)

The relative configuration of compounds **3.1**, **3.6** and **3.8** were previously determined,[27, 28] however, the absolute configuration of these compounds was not established. This section describes our attempts to determine the absolute configuration of **3.1**, **3.6** and **3.8** through X-ray crystallography using esterification with (1*S*)-camphanic chloride as a possible chiral 'handle'. It is generally only possible to obtain the relative stereochemistry of chiral compounds using X-ray structural analysis, however, if the compound is derivatised with a reagent containing a

stereogenic centre of known absolute configuration, the absolute configuration of the chiral centre(s) in the compound can consequently be determined.[69] (1*S*)-camphanic chloride has commonly been chosen as a chiral 'handle' because of its tendency to produce crystalline diastereomeric esters from alcohols that can subsequently be separated by chromatography or fractional crystallisation often yielding crystals suitable for X-ray analysis.[70-72] This particular method has successfully been applied in our laboratory to determine the absolute configuration of metabolites isolated from *Trimusculus costatus*,[58] which encouraged us to attempt this method on the secondary metabolites isolated from *L. millecra*.

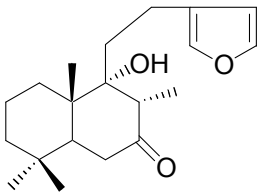

3.17

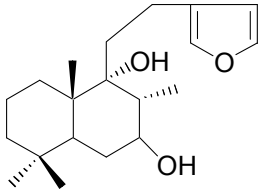

3.18

The preparation of a camphanate ester obviously first requires the metabolite of interest to possess an alcohol functionality, and thus, compounds **3.1** and **3.8** required initial reduction of their ketone moieties before esterification. As mentioned previously in Chapter 2 the quantity of marine secondary metabolites available is usually limited, and so trial investigations, are often deemed necessary to practise functional group transformations before applying them to scarce natural products. Hispanolone (**3.17**), a natural product readily available in our laboratory was used to determine the best method for ketone reduction. Reaction of hispanolone with both lithium aluminium hydride and sodium borohydride successfully reduced **3.17** to afford a mixture of 7α and 7β epimeric hispanolol (**3.18**). The crude product of the lithium aluminum hydride reaction was deemed cleaner from inspection of the ^{1}H NMR spectrum of the product mixture and this method was employed to reduce **3.1**, and **3.8**. The 1,3 arrangement of the phenol and methyl substituents in **3.6** is reminiscent of a similar arrangement of these functionalities in *meta*-cresol (**3.19**) and so was chosen as a trial compound for the esterification reaction. The camphanate ester of *meta*-cresol (**2.20**) was successfully prepared, and the methodology for the esterification step was accordingly established.

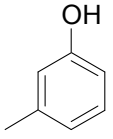

3.19

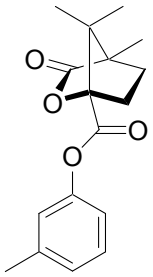

3.20

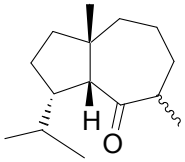

3.21

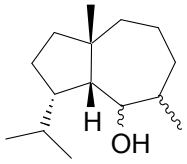

3.22

Compound **3.1** was reduced with lithium aluminum hydride, however on analysis of the ^{13}C NMR data of the product (**3.21**) a resonance at δ_C 216.1/216.6 was present, unexpectedly suggesting that the carbonyl moiety had been retained. The disappearance of the olefinic carbon resonances (δ_C 121.6 and 146.0 ppm) from the ^{13}C NMR spectrum of **3.1** confirmed that this carbonyl was no longer α, β unsaturated, thus requiring conjugate addition of the hydride leading to the reduction of the exocyclic alkene, instead of the ketone (Scheme 3.2).[73] The duplication of resonances in the ^{13}C NMR spectrum (Figure 3.8) suggested that the product was a mixture of epimers at C-7, however, all attempts to separate these epimers using HPLC were unsuccessful.

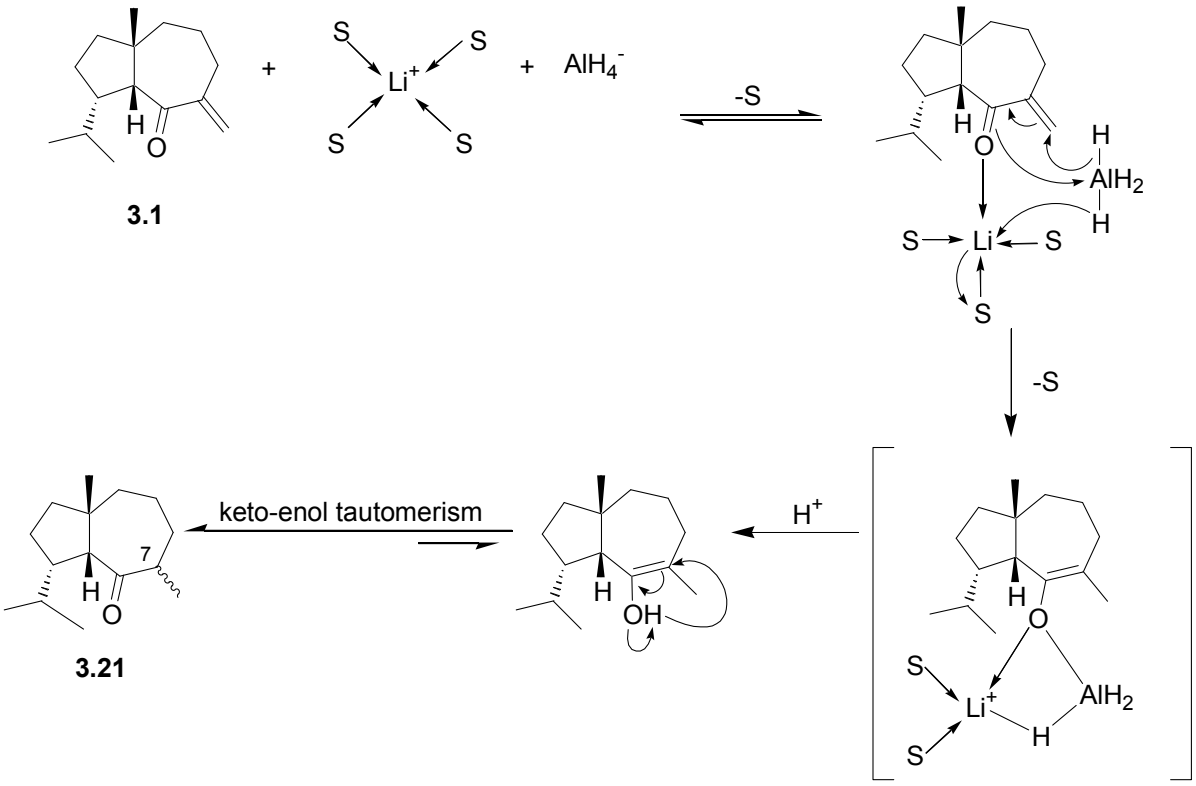

Scheme 3.2: Proposed mechanism for the conjugate addition of hydride in the reduction of **3.1** to yield **3.21**. (S = solvent (*i.e.* THF).[73]

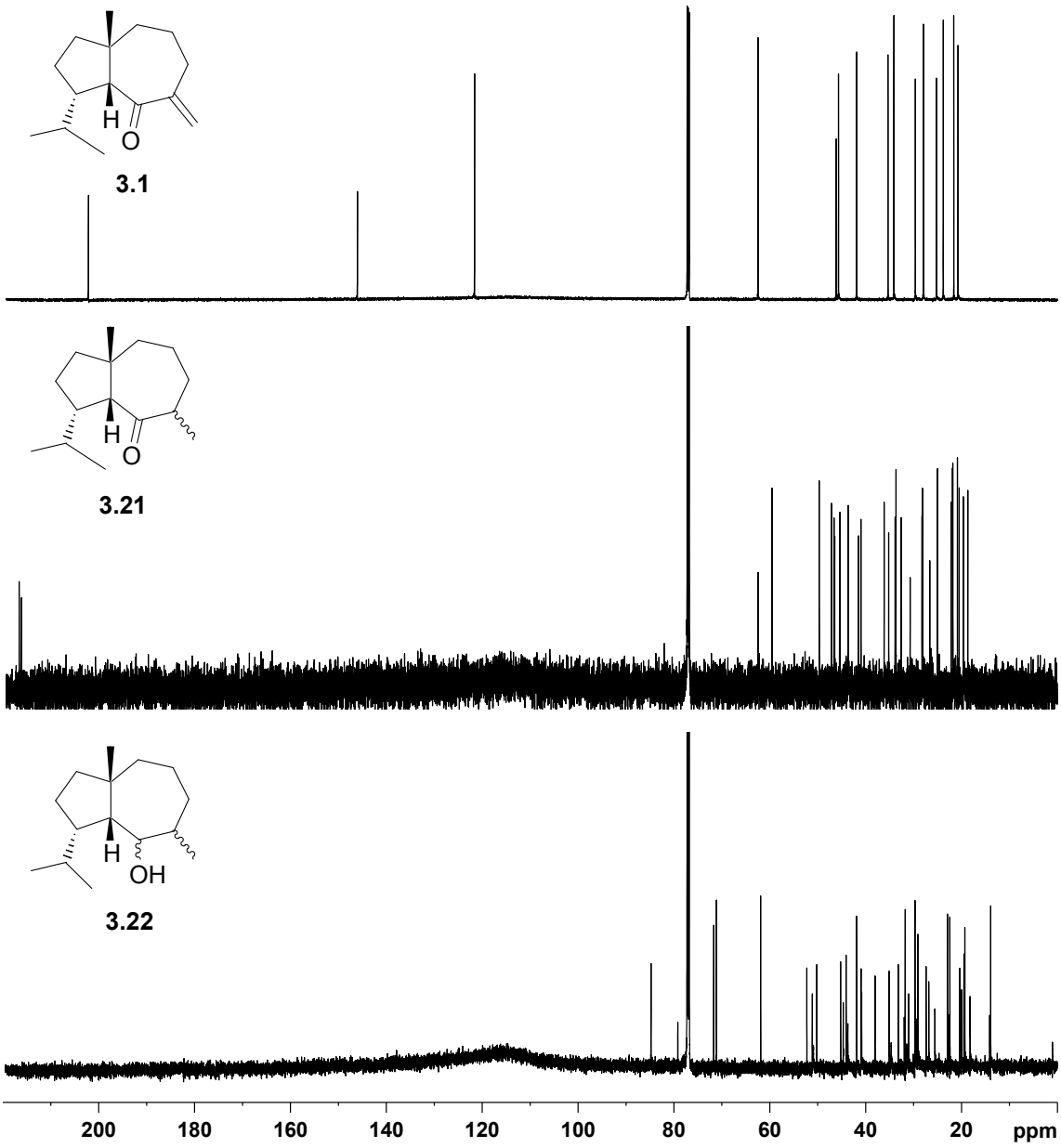

Figure 3.8: ^{12}C NMR ($CDCl_3$, 150 MHz) spectra of **3.1** (top), **3.21** (middle) and **3.22** (bottom).

Molecular modeling studies were used to investigate the reasons why **3.1** underwent conjugate addition of hydride reducing the alkene rather than direct reduction of the ketone. The arrangement of the bulky isopropyl group at C-4 appears to create steric hindrance for the hydride if it were to directly attack the ketone moiety (Figure 3.9). The exocyclic alkene is therefore clearly more accessible to hydride attack. It was proposed that the use of a milder reducing agent *e.g.* sodium borohydride might eliminate conjugate hydride addition. Reduction of **3.1** with sodium borohydride was however unsuccessful and yielded only unreacted **3.1**.

To determine if the carbonyl functionality would be reduced, if no other position of reduction was present, **3.21** was subjected to further reduction with lithium aluminum hydride, to afford **3.22**. Analysis of the ^{13}C NMR spectrum (Figure 3.8) obtained for **3.22** revealed the absence of carbonyl resonances (δ_C 216.1/216.6), and the appearance of new oxymethine signals (δ_C 71.1, 71.7, 79.2 and 84.78) suggesting the successful reduction of the ketone moiety to yield a mixture of four diastereomers. Given the paucity of material at hand after two reductions, separation of these distereomers was not pursued, nor was the further esterification of **3.22** in an attempt to establish the absolute stereochemistry of **3.1**.

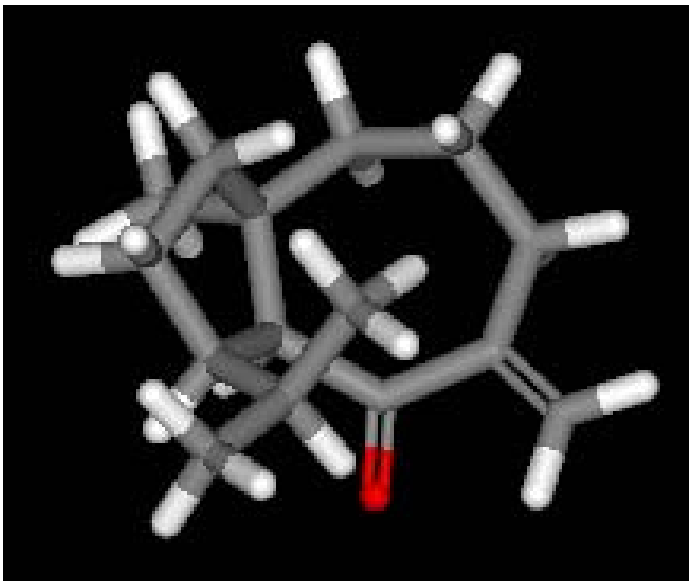

Figure 3.9: Stick representation of the computer-modelled global energy minimum conformation of millecrone A (**3.1**).

Unsuccessful in our attempts to reduce and esterify **3.1** we turned out attention to **3.6**. Compound **3.6** was reacted with (1*S*)-camphanic chloride and esterification was successful, yielding the pure camphanate ester (**3.23**, 62.3%) after normal phase HPLC (20% dichloromethane/hexane) as a colourless oil. The ^{3}J gHMBC correlation between the phenyl H-7 (δ_H 6.69) and C-1' (δ_C 166.3) was used to confirm the ester linkage between the camphanate functionality and the oxygen at C-8 (Figure 3.10). Unfortunately, all attempts at crystallisation of **3.23** from a variety of solvents (*e.g.* hexane, methanol, ethanol and water) and mixtures of these solvents failed to yield any crystals, and therefore X-ray analysis of the camphanate ester **3.23** was not possible. Other methods of establishing the absolute configuration of **3.6** were not investigated.

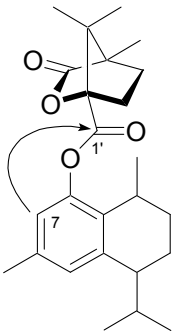

3.23

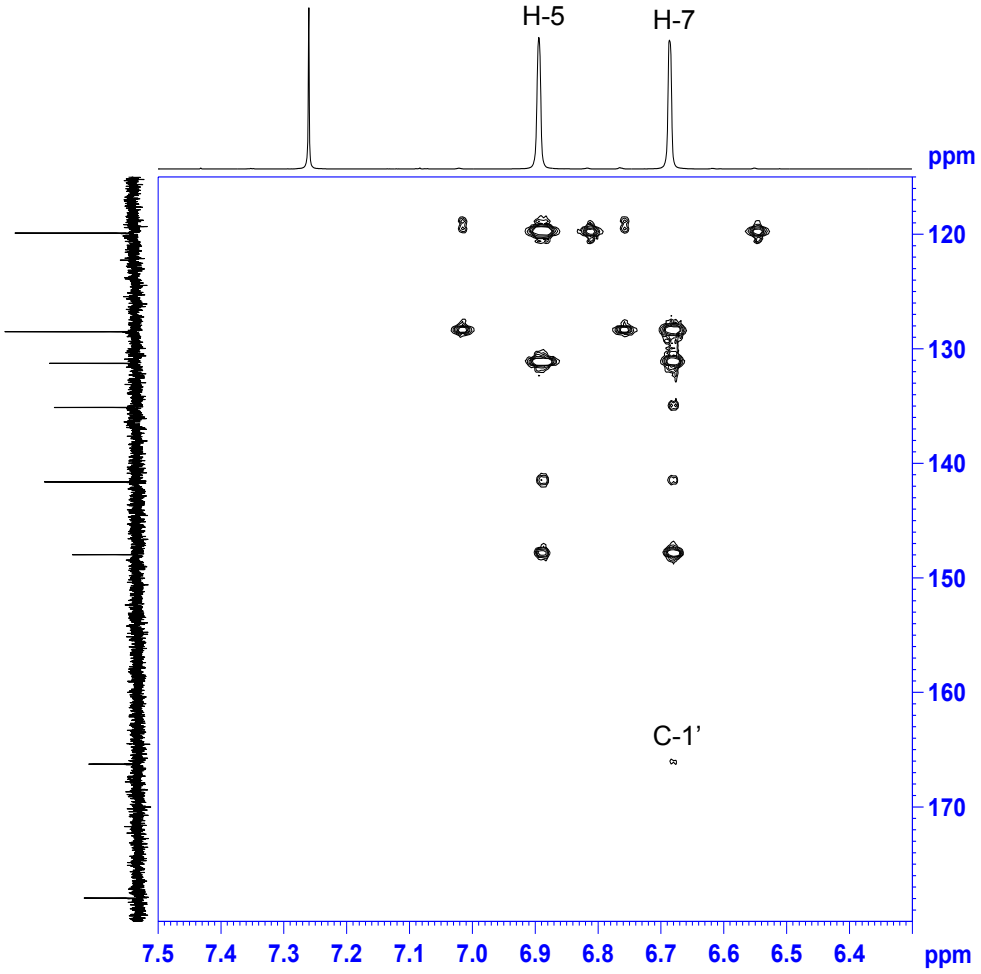

Figure 3.10: Downfield region (F1 = δ 6.3-7.5 ppm; F2 = δ 115-180 ppm) of the gHMBC spectrum ($CDCl_3$, 600 MHz) of **3.23**. The accompanying structure illustrates the key gHMBC correlation used to confirm the formation of the ester **3.23**.

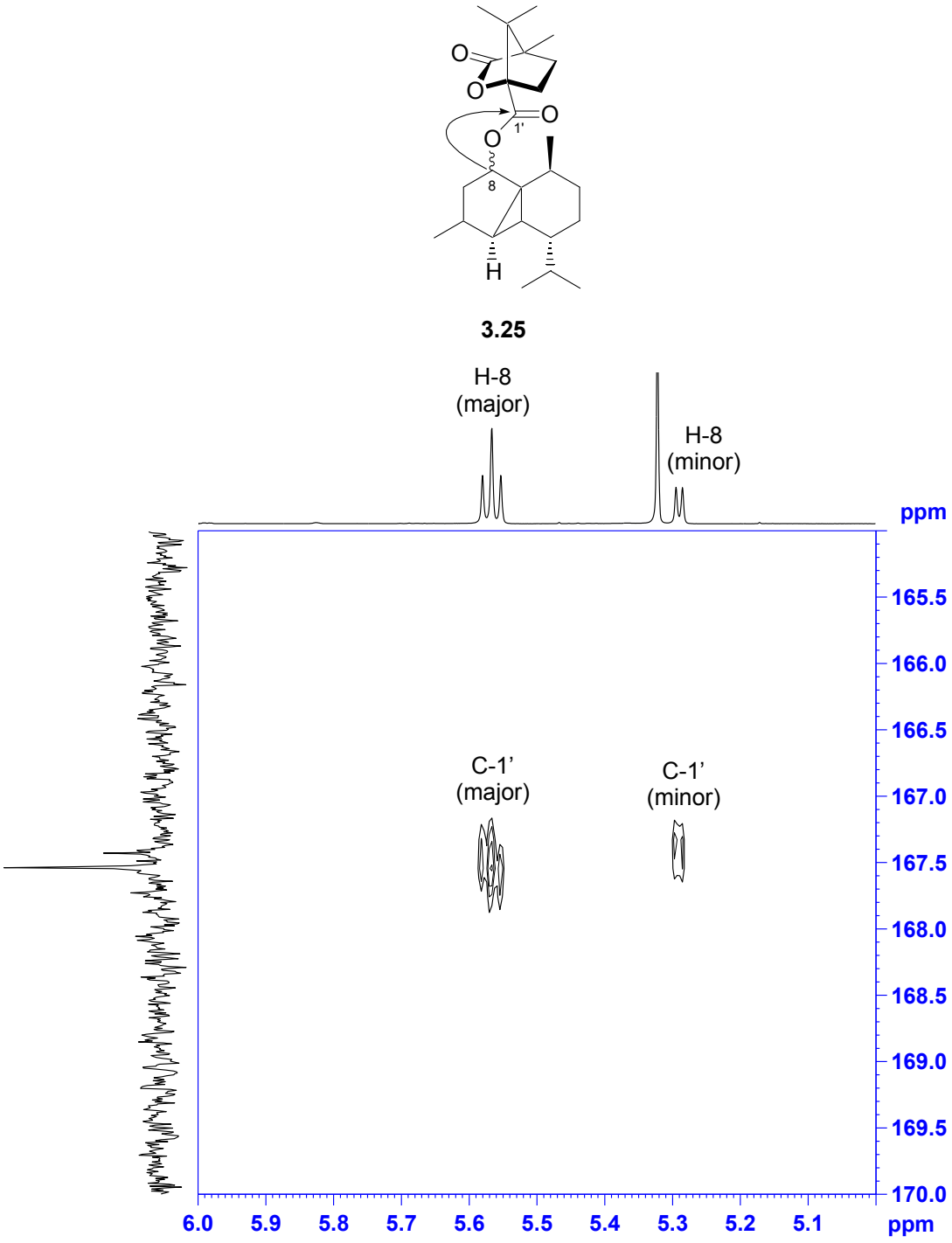

3.25

Figure 3.11: Downfield region (F1 = δ 5.0-6.0 ppm; F2 = δ 165-170 ppm) of the gHMBC spectrum ($CDCl_3$, 600 MHz) of **3.25**. The accompanying structure illustrates the key gHMBC correlation used to confirm the formation of the minor and major ester **3.25**.

The ketone moiety of **3.8** was initially reduced using lithium aluminum hydride to yield the alcohol **3.24**. This reaction also reduced the olefin in **3.8** and although a mixture of four diastereomers was obtained the chirality at C-1, C-4, C-5, C-8 and C-10 remained intact and esterification with (1*S*)-camphanic chloride was carried out. This diastereomeric mixture of **3.24** was reacted with (1*S*)-camphanic chloride to form the diastereomeric mixture of esters, **3.25**. The three bond gHMBC correlation between oxymethine proton H-8 (δ_H 5.27/5.54) and C-1' (δ_C 167.5/167.4) was used to confirm the ester linkage (Figure 3.11). Separation of these epimers using normal phase HPLC was unsuccessful as were any further attempts at isolating an individual diastereomer through fractional crystallisation of the camphanate ester mixture. Therefore X-ray crystal analysis of **3.25** was not possible, and the absolute configuration of **3.8** could not be determined.

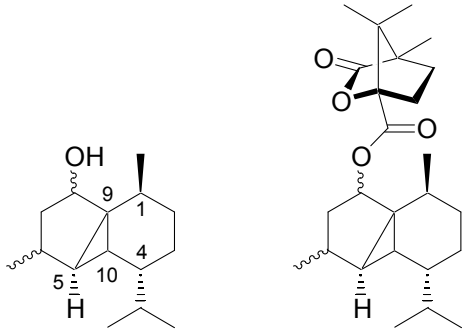

3.24 **3.25**

3.5 Concluding remarks

Only three, (**3.1**, **3.6** and **3.8**) of the eight sesquiterpenes, originally isolated by McPhail *et al*.[28] from extracts of the 1998 collection of *L. millecra* in Algoa Bay, were isolated and identified in extracts of the 2010 collection of *L. millecra* from the same reef in Algoa Bay. The absence of the cytotoxic prenylated toluquinones and toluhydroquinones (**3.9**-**3.15**) supports the hypothesis that these compounds may be of fungal origin and that *L. millecra* may have originally sequestered these compounds from a fungal contaminated soft coral.[74] A further new minor sesquiterpene metabolite, **3.16**, was isolated from the 2010 collection of *L. millecra*. Our re-investigation of the sequestered secondary metabolites of *L. millecra* clearly shows variability in the compounds sequestered by this species with millecrone A (**3.1**) being the sole common metabolite in the three investigations of *L. millecra* to date.[27, 28]

An attempt was made to establish the absolute configuration of **3.1**, **3.6** and **3.8** through initial LAH reduction of the ketone moiety in **3.1** and **3.8** and esterification of the resultant

diastereomeric alcohol mixtures and the phenol in **3.6** with (1*S*)-camphanic chloride. Crystallisation of the (*S*)-camphanate esters of **3.6** and **3.8** for X-ray analysis were unsuccessful, while the unexpected conjugate addition of a hydride in **3.1** resulted in complex diastereomeric mixtures which could not be separated by HPLC.

Chapter Four

Experimental

4.1 General Experimental Procedures

4.1.1 Analytical

NMR spectra were acquired using standard pulse sequences on Bruker Avance 400 MHz and 600 MHz Avance II spectrometers. Chemical shifts are reported in ppm and referenced to residual solvent resonances ($CDCl_3$ δ_H 7.26, δ_C 77.0, CD_3OD δ_H 3.34 δ_C 49.9). Coupling constants are reported directly from the NMR spectra and corresponding coupling constants have not been matched. Optical rotations were measured on a Perkin-Elmer 141 polarimeter at the sodium-D line (589 nm). Following standard protocol, the concentration of solutions used to determine optical rotations is expressed in g/100 mL. Infra-red spectra were recorded on a Perkin-Elmer Spectrum 2000 FT-IR spectrometer and Digilab FTS 3100 Excalibur HE Series with compounds as films (neat) on NaCl discs. Mass spectrometry was performed on a Waters API Q-TOF Ultima instrument using electron-spray ionisation in the positive ion mode (ESI+) at the University of Stellenbosch Central Analytical Facility.

4.1.2 Chromatography

General laboratory solvents were distilled from glass before use. Analytical normal phase thin layer chromatography was performed on DC-Plastikfolien Kieselgel 60 F_{254} plates. Plates were viewed under UV light (254 nm) and developed by spraying with 10% H_2SO_4 in MeOH followed by heating. HP-20 beads used were manufactured by Diaion and supplied by Supelco. Open column chromatography was performed using Discovery® DSC-DIOL supplied by Supelco, and flash chromatography was performed using Kieselgel 60 (230-400 mesh) silica gel. Normal phase DIOL semipreparative HPLC separations were performed on a Machery-Nagel VP 250/10 Nucleosil 100-7 OH column using an Agilent 1100 Series quad pump and a Agilent 1100 diode array detector. Reverse phase semi-preparative HPLC separations were performed on a Phenomenex Onyx Monolithic Semi-PREP C-18 column using an Agilent 1100 Series quant pump and a Agilent 1100 diode array detector.

4.1.3 Synthesis

All reactions requiring anhydrous conditions were conducted in either flame-dried or oven-dried apparatus under an atmosphere of dry argon/nitrogen or using an anhydrous calcium chloride drying tube. Dry solvents were prepared by standard procedures as described by Perin and

Armarego[75] and stored over appropriate drying agent under an atmosphere of dry nitrogen. Immediately prior to their use in dry reactions, THF was distilled from Na/benzophenone ketyl, while CH_2Cl_2 was distilled from calcium hydride. Organic extracts were dried over anhydrous $MgSO_4$ or $NaSO_4$. All reactions were magnetically stirred.

4.1.4 Computer modelling

Theoretical models were constructed and subjected to structural optimisation using DFT methods, followed by full frequency analyses to confirm that the final structures were true stationary points. All DFT calculations (energy optimisations and frequency analyses) were performed using the Gaussian 03[76] suite of algorithms with the 6-31G(d) vector basis set and the B3LYP[77, 78] energy gradient correcting functional. Models were constructed and visualised using DS Visualizer.[78]

4.2 Chapter Two Experimental

4.2.1 Extraction and Isolation of *Siphonaria capensis* metabolites

A collection of 2114 specimens (910.8 g) of the pulmonate false limpet *Siphonaria capensis* was made by hand in May 2009 at low tide along the coastline of the Kariega River Mouth. The collection was steeped in Me_2CO (1.5 L) overnight and the extract subjected to cyclic loading onto HP-20 beads until an eluent concentration of 12.5% Me_2CO/H_2O was achieved. Crude fractions of siphonariid metabolites were obtained by eluting the HP-20 beads with Me_2CO/H_2O mixtures in a decreasing polarity gradient (20%, 40%, 60%, 80% Me_2CO/H_2O and 100% Me_2CO). On inspection of the ^1H NMR spectra of these crude fractions, the 80% Me_2CO/H_2O (1.33 g) fraction was chosen for further purification. As shown in Scheme 2.7, the 80% Me_2CO/H_2O fraction was subjected to open chromatography (20% EtOAc/hexane) on a DIOL column and the 11 fractions collected were combined using their TLC profiles. Further purification of fraction number two using normal phase HPLC (12% EtOAc/hexane) on a DIOL column afforded the known *S. capensis* metabolite siphonarienfuranone (**2.2**, 0.03 mg/animal). Fraction number four was subjected to normal phase HPLC (20% EtOAc/hexane) on the same DIOL column to afford the new *S. capensis* metabolite cholest-7-en-3,5,7-triol (**2.33**, 0.01 mg/animal).

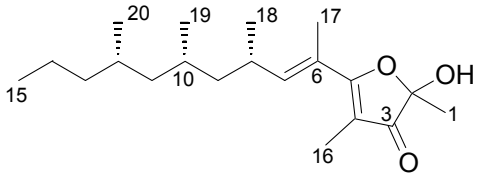

2.2

Siphonarienfuranone (2.2)[42, 49]: colourless oil; $[\alpha]_D^{20}$ +95 (*c* 0.76, $CHCl_3$), lit.[42, 49] +102, +54; IR (film) ν_{max} 3411, 2952, 2928, 1700, 1625, 1458, 1379, 1221 cm^{-1}; ^1H and ^{13}C NMR data see Table 2.1; EIMS *m/z* (rel. int.) 323 [$(M+H)^+$] (100), 321 (4), 281 (14). 277 (8); HREIMS *m/z* 323.2572 (calcd for $C_{20}H_{35}O_3$ [$(M+H)^+$], 323.2586).

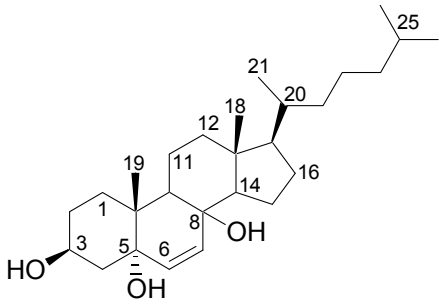

2.33

Cholest-7-en-3,5,7-triol (2.33)[58]: white amorphous solid; $[\alpha]_D^{20}$ +7 (*c* 0.37, $CHCl_3$), lit.(vanWyk PhD thesis) +4; IR (film) ν_{max} 3534, 3398, 3241, 2953, 2871, 1633, 1616, 1466 cm^{-1}; ^1H and ^{13}C NMR data see Table 2.2; EIMS *m/z* (rel. int.) 418 (M^+) (28), 417 (88), 415 (25), 399 (28), 383 (100), 365 (62), 363 (58).

4.2.2 Extraction and Isolation of *Siphonaria oculus* metabolites

In August 2009, a collection of 704 specimens (303.3 g) of the false limpet *Siphonaria oculus* was made near Terrivonne Wharf 3 km up the Kariega River. The false limpets were steeped in Me_2CO and the extract was cyclic loaded onto HP-20 beads until a concentration of 12.5% Me_2CO/H_2O was achieved. The HP-20 resin was eluted with aqueous Me_2CO mixtures (20%, 40%, 60%, 80% Me_2CO/H_2O, and 100% Me_2CO) to afford 5 crude fractions. The 80% aqueous Me_2CO fraction was purified further with normal phase HPLC (20% EtOAc/hexane) on a DIOL column affording 7 fractions and the subsequent chromatographic procedures carried out on these fractions is represented in Scheme 2.8, leading to the isolation of known siphonariid

metabolite siphonarienfuranone (**2.2**, 0.04 mg/animal) alongside three new polypropionate metabolites **2.35** (0.07 mg/animal), **2.36** (0.01 mg/animal) and **2.37** (0.03 mg/animal).

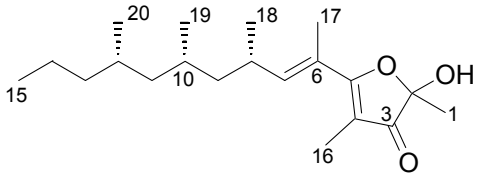

2.2

Siphonarienfuranone (2.2)[42, 49]: colourless oil; $[\alpha]_D^{20}$ +105 (*c* 0.53, $CHCl_3$), lit. [42, 49] +102, +54; IR (film) ν_{max} 3418, 2957, 1681, 1633, 1451, 1377, 1214 cm^{-1}; ^1H NMR ($CDCl_3$, 600 MHz) and ^{13}C NMR ($CDCl_3$, 150 MHz) data are consistent with those reported previously.

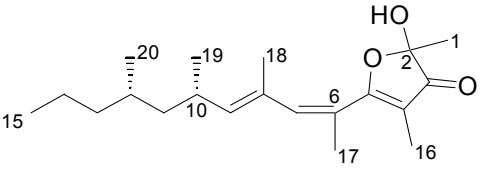

2.35

Polypropionate 2.35: colourless oil; $[\alpha]_D^{20}$ -38 (*c* 0.97, $CHCl_3$); IR (film) ν_{max} 3339, 3019, 2959, 2927, 2871, 1686, 1590, 1216 cm^{-1}; ^1H and ^{13}C NMR data see Table 2.3; EIMS *m/z* (rel. int.) 320 [M^+] (16), 277 (10), 207 (100), 189 (26), 165 (40), 137 (94); HREIMS *m/z* 320.2350 (calcd for $C_{20}H_{32}O_3$ [M^+], 320.2351).

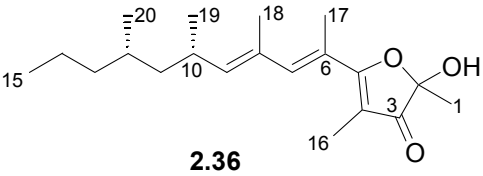

2.36

Polypropionate 2.36: colourless oil; $[\alpha]_D^{19}$ -160 (*c* 0.08, $CHCl_3$); IR (film) ν_{max} 3429, 2957, 2845, 1634, 1459, 1381, 1018 cm^{-1}; ^1H and ^{13}C NMR data see Table 2.4; EIMS *m/z* (rel. int.) 320 [M^+] (10), 277 (7), 207 (100), 189 (14), 163 (32), 137 (88); HREIMS *m/z* 320.2350 (calcd for $C_{20}H_{32}O_3$ [M^+], 320.2351)

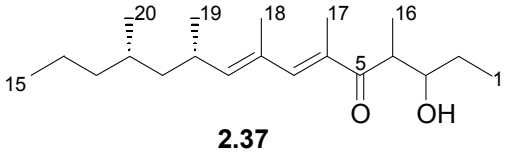

2.37

3-Hydroxy-4,6,8,10,12-pentamethyl-pentadeca-6,8-dien-5-one (2.37): yellow oil; $[\alpha]_D^{19}$ +61 (*c* 0.35, $CHCl_3$); IR (film) ν_{max} 3422, 2957, 2927, 1639, 1451, 1381, 1206 cm^{-1}; ^1H and ^{13}C NMR data see Table 2.5; HREIMS *m/z* 308.2860 (calcd for $C_{20}H_{36}O_2$ [M^+], 308.2715).

4.2.2.1 Mosher's esterification of hexanol

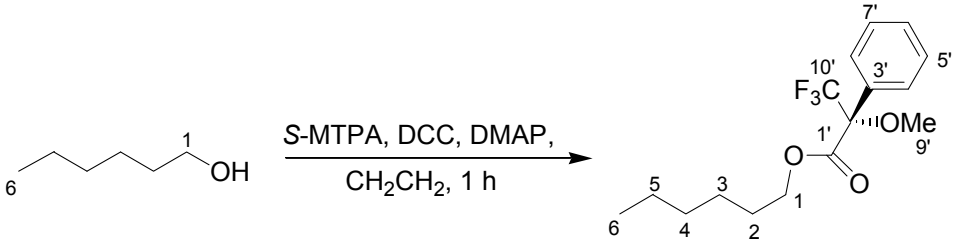

2.38

S-α-Methoxy-α-trifluoromethylphenylacetic acid (93.5 mg), DCC (206 mg) and DMAP (36.5 mg) were added to a solution of hexanol (10 mg, 0.10 mmol) in anhydrous CH_2Cl_2 (5 mL). The solution was shaken periodically at room temperature for 1 h before being diluted with H_2O (2 mL) and EtOAc (6 mL) and filtered. The resulting solution was washed consecutively with 1M HCl (2 mL), H_2O (2 mL), sat, $NaHCO_3$ (2 mL) and once more with H_2O (2 mL). The EtOAc fraction was dried over anhydrous $MgSO_4$, the solvent removed under reduced pressure and the resultant oil purified by semi-preparative HPLC (87.5% hexane/EtOAc) to afford a mixture of the two *S*-MTPA diastereomers **2.38** (10.5 mg, 0.033 mmol, 33%) as a colourless oil.

Mosher's ester (2.38): colourless oil; IR (film) ν_{max} 3028, 2957, 2871, 1751, 1638, 1451, 1259, 1170 cm^{-1}; ^1H NMR ($CDCl_3$, 600 MHz) δ 7.56 (2H, m, H_2-4', 8'), 7.40 (1H, m, H-6'), 7.39 (2H, m, H_2-5', 7'), 4.54 (1H, dt, *J* = 11.7, 5.1 Hz, H-1b), 4.40 (1H, dt, *J* = 11.7, 4.5 Hz, H-1a), 3.67 (2H, t, *J* = 4.7 Hz, H_2-2), 3.57 (3H, s, H_3-9), 3.42 (2H, t, *J* = 6.4 Hz, H_2-3), 1.51 (2H, m, H_2-4), 1.33 (2H, sext, *J* = 7.4 Hz, H_2-5), 0.89 (3H, t, *J* = 7.5 Hz, H_3-6)**;** ^{13}C NMR ($CDCl_3$, 150 MHz) δ 166.5 (q_c, C-1'), 132.3 (q_c, C-3'), 129.6 (CH, C-7'), 128.3 (2 x CH, C-5', C-7'), 127.4 (2 x CH, C-4', C-8'), 123.3 (q_c, q, $^1J_{CF}$ = 287.7 Hz, C-10'), 84.7 (q_c, q, $^2J_{CF}$ = 27.5 Hz, C-2'), 71.1 (CH_2, C-3, 68.0 (CH_2, C-2), 65.2 (CH_2, C-1), 55.4 (CH_3, C-9'), 31.7 (CH_2, C-4), 19.2 (CH_2, C-5), 13.8 (CH_3, C-6).

*4.2.2.2 Attempted Mosher's esterification of **2.37**.*

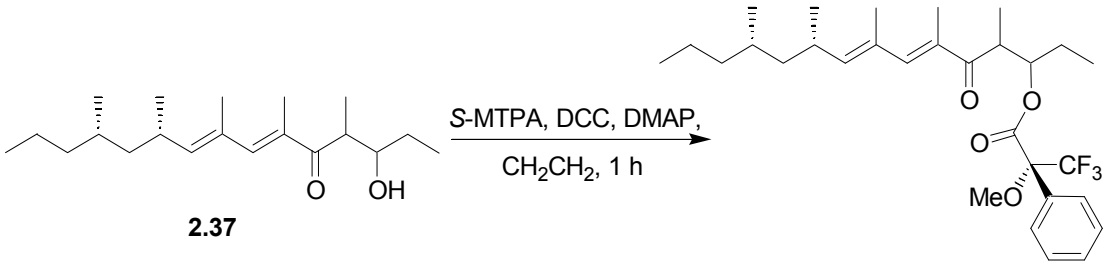

2.37

The polypropionate **2.37** was reacted with Mosher's reagent following the method described above in Section 4.2.2.1. The ^{1}H and ^{13}C NMR spectra of the crude reaction mixture revealed the presence of unreacted starting material, **2.37**, only.

4.2.2.3 Collection of mucus from Siphonaria oculus

In October 2009, the mucins of 36 *S.oculus* specimens were collected into capillary tubes. The capillary tubes were rinsed with $CHCl_3$ to dissolve the mucus. The solution of mucus was concentrated to afford a crude extract (10.4 mg) which was analysed using ^{1}H NMR ($CDCl_3$, 600 MHz).

4.3 Chapter Three Experimental

4.3.1 Extraction and Isolation of *Leminda millecra* metabolites

In February 2010 a SCUBA (-15 to -20 m) collection of 40 specimens of the nudibranch *Leminda millecra* was made from Phillips Reef, Algoa Bay. Specimens were steeped in Me_2CO (500 mL) overnight to allow for extraction of metabolites. The Me_2CO was filtered from the *Leminda millecra* specimens and subjected to cyclic loading onto HP-20 beads (200 mL) until an eluent concentration of 12.5% Me_2CO/H_2O was achieved. Crude fractions were eluted off the HP-20 resin with Me_2CO/H_2O mixtures in a decreasing polarity gradient (20%, 40%, 60%, 80% Me_2CO/H_2O, and 100% Me_2CO). The 80% Me_2CO/H_2O (644.3 mg) fraction was subjected to open chromatography on a DIOL column using a CH_2Cl_2/ hexane gradient system (100% hexane, 25%, 50%, 75% CH_2Cl_2/hexane and 100% CH_2Cl_2). Fractions collected were combined using

their TLC profiles to afford nine fractions (Scheme 3.1). Fraction three afforded pure millecrone A (**3.1**, 4.3 mg/nudibranch). Normal phase HPLC (10% CH_2Cl_2/hexane) of fraction 6 afforded the new metabolite 8-acetoxycalamenene (**3.16**, 0.1 mg/animal), whilst fraction 8 yielded 8-hydroxycalamenene (**3.6**, 0.3 mg/animal) and cubebenone (**3.8**, 1.1 mg/animal) after HPLC (10% CH_2Cl_2 /hexane). Purification of fraction 9 *via* HPLC (20% CH_2Cl_2/hexane), afforded more 8-hydroxycalamenene (**3.6**, 0.6 mg/animal).

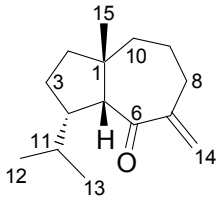

3.1

Millecrone A (3.1)[27, 28]: colourless oil; $[\alpha]_D^{20}$ +31 (*c* 0.68, $CHCl_3$), lit.[28] +41; IR (film) ν_{max} 2956, 2863, 1692, 1634, 1463, 1382, 1218, 1089 cm^{-1}; ^1H NMR ($CDCl_3$, 600 MHz) δ 5.94 (1H, d, *J* = 2.2 Hz, H-14a), 5.19 (1H, t, *J* = 1.9 Hz, H-14b), 2.69 (1H, m, H-8a), 2.67 (1H, m, H-4), 2.48 (1H, d, *J* = 6.5 Hz, H-5), 2.46 (1H, m, H-8b), 1.87 (1H, m, H-9a), 1.75 (1H, m, H-3a), 1.57 (1H, m, H-9b), 1.48 (1H, ddd, *J* = 14.7, 5.7, 1.8 Hz, H-10a), 1.42 (1H, m, H-3b), 1.36 (1H, m, H-11), 1.34 (1H, m, H-2b), 1.28 (1H, m, H-2a), 1.25 (1H, m, H-10b), 1.12 (3H, s, H_3-15), 0.87 (3H, d, *J* = 6.7 Hz, H_3-13), 0.73 (3H, d, *J* = 6.7 Hz, H_3-12); ^{13}C NMR data see Table 3.2: EIMS *m/z* (rel. int.) 220 [M^+] (12), 178 (18), 177 (100), 137 (46), 123 (15), 81 (23); HREIMS *m/z* 220.1841 (calcd for $C_{15}H_{24}O$ [M^+], 220.1827).

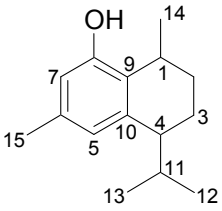

3.6

8-hydroxycalamenene (3.6)[28]: yellow oil; $[\alpha]_D^{20}$ +34 (*c* 0.5, $CHCl_3$), lit.[28] +36; IR (film) ν_{max} 3436, 2949, 2927, 1619, 1464, 1287, 1237 cm^{-1}; ^1H NMR ($CDCl_3$, 600 MHz) δ 6.59 (1H, s, H-5), 6.44 (1H, s, H-7), 3.07 (1H, qn.d, *J* = 6.6, 1.6 Hz, H-1), 2.46 (1H, td, *J* = 6.0, 2.6 Hz, H-4), 2.25 (3H, s, H_3-15), 1.99 (1H, octet, *J* = 6.7 Hz, H-11), 1.96 (1H, m, H-2b), 1.84 (1H, tdd, *J* = 13.6, 6.0, 3.5 Hz, H-3b), 1.77 (1H, dq, *J* = 13.7, 3.7 Hz, H-3a), 1.51 (1H, ddt, *J* = 13.3, 3.9, 2.9 Hz, H-2a), 1.21 (3H,

d, *J* = 6.7 Hz, H_3-14), 0.99 (3H, d, *J* = 6.7 Hz, H_3-13), 0.83 (3H, d, *J* = 6.7 Hz, H_3-12); ^{13}C NMR data see Table 3.2.

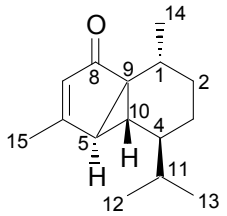

3.8

Cubebenone (3.8)[28]: yellow oil; $[\alpha]_D^{20}$ +136 (*c* 1.13, $CHCl_3$), lit.[28] +126; IR (film) ν_{max} 2956, 2922, 2866, 1790, 1695, 1607, 1439, 1323 cm^{-1}; ^{1}H NMR ($CDCl_3$, 600 MHz) δ 5.36 (1H, q, *J* = 1.2 Hz, H-7), 2.48 (1H, sept *J* = 6.0 Hz, H-1), 2.13 (3H, d, *J* = 1.2 Hz, H_3-15), 1.92 (1H, d, *J* = 2.3 Hz, H-5), 1.77 (1H, dtd, *J* = 13.4, 5.1, 2.2 Hz, H-2b), 1.58 (1H, octet, *J* = 6.7 Hz, H-11), 1.45 (1H, dtd, *J* = 12.8, 4.6, 2.3 Hz, H-3b), 1.35 (1H, t, *J* = 3.0 Hz, H-10), 1.10 (1H, tdd, *J* = 6.5, 6.0, 4.1 Hz, H-4), 0.93 (3H, d, *J* = 6.4 Hz, H_3-14), 0.91 (3H, d, *J* = 6.8 Hz, H_3-12), 0.89 (1H, m, H-3a), 0.88 (3H, d, *J* = 6.8 Hz, H_3-13), 0.67 (1H, qd, *J* = 13.2, 2.2 Hz, H-2a); ^{13}C NMR data see Table 3.2**;** HREIMS *m/z* 219.1745 (calcd for $C_{15}H_{23}O$ [$(M+H)^+$], 219.1749).

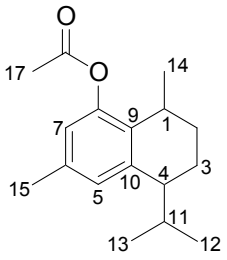

3.16

8-acetoxycalamenene (3.16): colourless oil; $[\alpha]_D^{20}$ +20 (*c* 0.12, $CHCl_3$); IR (film) ν_{max} 2924, 2856, 1767, 1621, 1460, 1360, 1206, 1032 cm^{-1}; ^{1}H and ^{13}C NMR data see Table 3.4**;** HREIMS *m/z* 260.1825 (calcd for $C_{17}H_{24}O_2$ [M^+], 260.1776).

*4.3.1.1 Acetylation of 8-hyxdroxycalamenene (**3.6**)*

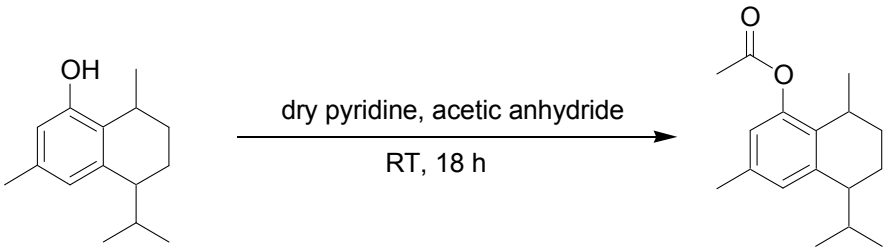

3.6 **3.16**

A solution of 8-hydroxycalamene (**3.6**, 7.3 mg, 0.033 mmol) in anhydrous pyridine (0.5 mL) and acetic anhydride (0.5 mL) was stirred at ambient temperature overnight (18 h). The reaction was quenched with MeOH (2.5 mL) and concentrated *in vacuo* to give a pale yellow oil (13 mg). The crude product was passed through a silica gel (10 mL) plug using 5:1 hexane/EtOAc to yield the 8-acetoxycalamene (**3.16**, 13 mg, 0.050 mmol). No further purification was required. Both ^{1}H and ^{13}C NMR data were consistent with previous NMR spectral data obtained for **3.16** (section 4.3.1)**;** HREIMS *m/z* 260.1781 (calcd for $C_{17}H_{24}O_2$ [M^+], 260.1776).

4.3.2 Attempts to establish the absolute configuration of 3.1, 3.6 and 3.8

4.3.2.1 Lithium aluminium hydride reduction of hispanolone

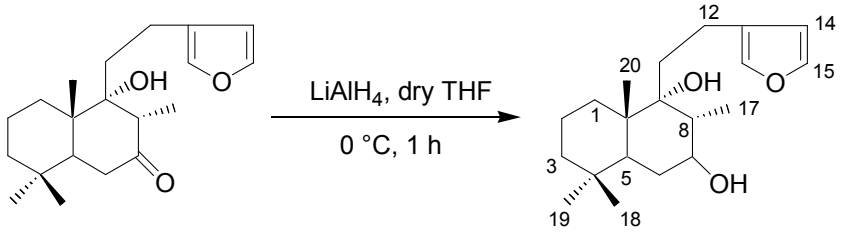

3.17 **3.18**

This procedure is representative. A solution of hispanolone (**3.17**, 52 mg, 0.163 mmol) in anhydrous THF (2.5 mL) was added to a solution of $LiAlH_4$ (12 mg, 0.318 mmol, 2 eq.) in dry THF (5 mL) at 0 ^{o}C. The reaction mixture was stirred at 0 °C for 1 h and then allowed to reach ambient temperature before being quenched with 5% $NaHCO_3$ (3 drops) followed by 1 M HCl (3 drops). The resulting mixture was concentrated to dryness, taken up with EtOAc and washed

with water (3 x 5 mL) and dried over anhydrous $MgSO_4$. The solvent was removed *in vacuo* to afford hispanolol (**3.18**, 51.2 mg, 0.160 mmol). No further purification was attempted.

7-hispanolol (3.18)[79]: yellow amorphous solid; IR (film) ν_{max} 3392, 2938, 1637, 1463, 1387, 1025, 759 cm^{-1}; ^1H NMR ($CDCl_3$, 600 MHz) δ 7.34 (1H, br s, H-15), 7.21 (1H, br s, H-16), 6.28 (1H, br s, H-14), 3.88 (1H, m, H-7), 2.55 (1H, m, H-12b), 2.46 (1H, m, H-12a), 1.88(1H, ddd, *J* = 14.6, 11.2, 5.6, H-11b), 1.84 (1H, m, H-5), 1.80 (1H, m, H-6a), 1.79 (1H, m, H-8), 1.62 (1H, m, H-11a), 1.61 (1H, m, H-6b), 1.58 (1H, m, H-2b), 1.51 (1H, m, H-2a), 1.51 (2H, m, H_2-1), 1.40 (1H, m, H-3b), 1.21 (1H, m, H-3a), 1.18 (3H, d, *J* = 7.0, H_3-17), 0.92 (3H, s, H_3-20), 0.91 (3H, s, H_3-18), 0.86 (3H, s, H_3-19); ^{13}C NMR ($CDCl_3$, 150 MHz) δ 142.7 (CH, C-15), 138.4 (CH, C-16), 125.8 (q_c, C-13), 110.9 (CH, C-14), 79.3 (q_c, C-9), 73.8 (CH, C-7), 43.4 (q_c, C-10), 41.69 (CH_2, C-3), 39.42 (CH, C-5), 38.9 (q_c, C-8), 34.4 (CH_2, C-11), 32.9 (q_c, C-4), 33.5 (CH_3, C-18), 31.4 (CH_2, C-1), 30.3 (CH_2, C-6), 21.8 (CH_3, C-19), 21.4 (CH_2, C-12), 18.6 (CH_2, C-2), 15.8 (CH_3, C-20), 13.3 (CH_3, C-17).

4.3.2.2 Sodium borohydride reduction of hispanolone

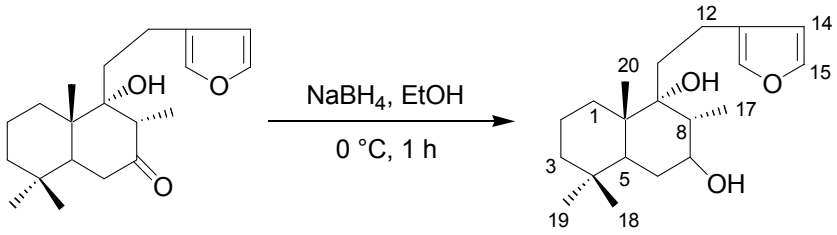

3.17 **3.18**

This method is representative. An excess of $NaBH_4$ (10 mg, 0.264 mmol, 1.6 eq) was added to a solution of hispanolone (**3.17**, 52 mg, 0.162 mmol) in EtOH (6 mL) at 0 °C. The reaction mixture was stirred at this temperature for 1 h and then brought to ambient temperature naturally before being quenched with sat. NH_4Cl (5 mL). The aqueous solution was extracted with Et_2O (3 x 5 mL) and the combined organic fractions were washed with H_2O (2 x 5 mL), sat. brine (2 x 5 mL), dried over $MgSO_4$ and concentrated *in vacuo* to afford a pale yellow amorphous solid (**3.18**, 47.8 mg, 0.149 mmol). No further purification was attempted. ^1H and ^{13}C NMR data were consistent with those obtained fro **3.18** from the LAH reduction of **3.17**.

4.3.2.3 Esterification of meta*-cresol*

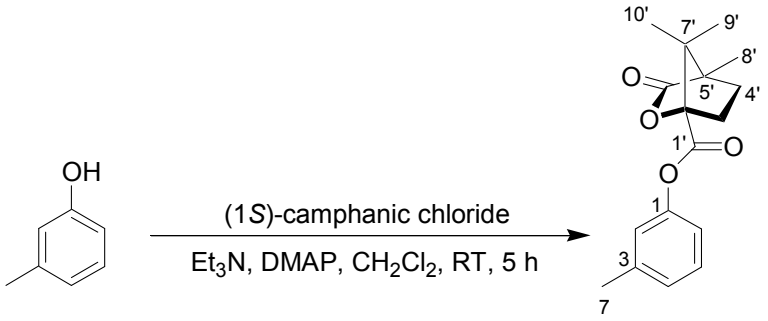

3.19 **3.20**

Meta-cresol (**3.19**, 10.1 mg, 0.092 mmol), Et_3N (105.9 μL, 0.555 mmol, 6.0 eq), DMAP (5.7 mg, 0.046 mmol, 0.5 eq) and (1*S*)-camphanic chloride (46.2 mg, 0.213 mmol, 2.3 eq) were dissolved in anhydrous CH_2Cl_2 (2.5 mL) and allowed to stir at ambient temperature for 5 h. The reaction mixture was concentrated to dryness, taken up with diethyl ether (5 mL) and washed with 1 M HCl (5 mL) followed by water (5 mL). The organic fraction was dried over $MgSO_4$ and concentrated *in vacuo* to yield an amorphous white solid (**3.20**, 37.9 mg, 0.132 mmol). No further purification was deemed necessary.

Camphanate ester 3.20: white amorphous solid; IR (film) ν_{max} 2970, 2929, 1786, 1767, 1615, 1449, 1263, 1103, 1052 cm^{-1}; ^1H NMR ($CDCl_3$, 600 MHz) δ 7.28 (1H, d, *J* = 7.5 Hz, H-5) , 7.08 (1H, d, *J* = 7.5 Hz, H-4), 6.93 (1H, s, H-2), 6.92 (1H, m, H-6), 2.56 (1H, ddd, *J* = 13.5, 10.2, 4.4 Hz, H-3'b), 2.37 (3H, s, H_3-7), 2.19 (1H, ddd, *J* = 13.5, 8.8, 4.5 Hz, H-3'a), 1.99 (m, H-4'b), 1.78 (m, H-4'a), 1.17 (s, H_3-8'), 1.15 (s, H_3-9'), 1.11 (s, H_3-10'); ^{13}C NMR ($CDCl_3$, 150 MHz) δ 177.9 (q_c, C-6'), 166.2 (q_c, C-1'), 149.9 (q_c, C-1), 139.9 (q_c, C-3), 129.3 (CH, C-5), 127.2 (CH, C-4), 121.8 (CH, C-2), 118.2 (CH, C-6), 90.9 (q_c, C-2'), 54.9 (q_c, C-7'), 54.6 (q_c, C-5'), 30.7 (CH_2, C-3'), 29.0 (CH_2, C-4'), 21.3 (CH_3, C-7), 16.8 (CH_3, C-9'), 16.6 (CH_3, C-10'), 9.7 (CH_3, C-8'); HREIMS 289.1435 (calcd for $C_{17}H_{21}O_4$ [$(M+H)^+$], 289.1440).

4.3.2.4 Reduction of millercrone A using lithium aluminium hydride

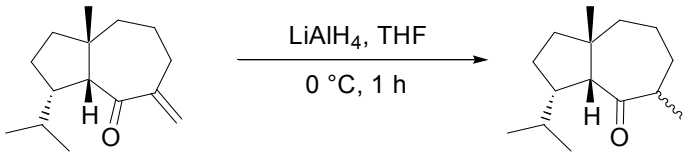

3.1 **3.21**

A solution of millecrone A (**3.1**, 40 mg, 0.182 mmol) was reacted with $LiAlH_4$ following the procedure described in Section 4.3.2.1 to give a colourless oil (55.7 mg). This crude oil was subjected to normal phase HPLC (98% hexane/EtOAc) to yield a mixture of epimers (**3.21**, 10.2 mg, 0.046 mmol, 25%). Further attempts to separate these epimers using HPLC were unsuccessful.

Compound 3.21: colourless oil; IR (film) ν_{max} 2949, 2868, 1642, 1466, 1376, 1212, 1101 cm^{-1}; ^1H NMR ($CDCl_3$, 600 MHz) δ 2.68; 2.53, 2.49, 2.46, 1.71, 1.68, 1.58, 1.381, 1.28, 1.20, 1.07, 0.78, 0.73; ^{13}C NMR ($CDCl_3$, 150 MHz) δ 216.6, 216.1, 62, 4, 59.5, 46.6, 45.4, 43.6, 41.5, 36.1, 33.8, 32.6, 28.1, 25.0, 21.8, 20.5, 18.7; EIMS *m/z* (rel. int.) 222 [M^+] (100), 208 (69), 177 (25), 165 (39), 123 (58), 95 (35), 81 (54).

*4.3.2.5 Further lithium aluminium hydride reduction of **3.21***

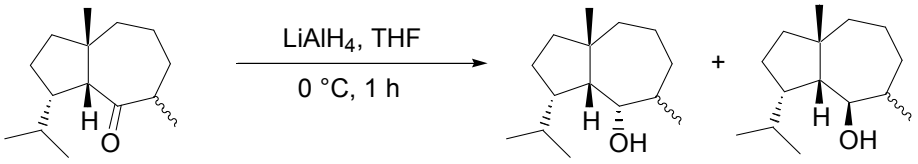

3.1 **3.22A** **3.22B**

A sample (5 mg) of the mixture of epimers was subjected to a second reduction following the procedure detailed in Section 4.3.2.1 to afford a colourless oil (4.8 mg). Analysis of the ^1H and ^{13}C NMR data obtained for the crude product indicated that the carbonyl functionality was successfully reduced, producing a mixture of 4 diastereomers (**3.22**, 4.8 mg, 0.021 mmol). No further purification was attempted.

Compound 3.22: colourless oil; IR (film) ν_{max} 3423, 2960, 2929, 1464, 1385, 1215, 1089 cm^{-1}; ^1H NMR ($CDCl_3$, 600 MHz) δ 3.73, 3.53, 3.48, 3.23, 2.00, 1.68, 1.62, 1.54, 1.48, 1.43, 1.41, 1.37, 1.25, 0.99, 0.96, 0.94, 0.89, 0.87; ^{13}C NMR ($CDCl_3$, 150 MHz) δ 84.8, 79.2, 71.7, 71.0, 61.9, 52.2, 51.1, 45.2, 44.1, 41.9, 40.8, 38.0, 33.2, 31.7, 29.7, 29.4, 29.1, 27.4, 26.8, 25.3, 22.9, 22.4, 20.0, 19.3, 13.6.

4.3.2.6 Attempted reduction of millecrone A using sodium borohydride

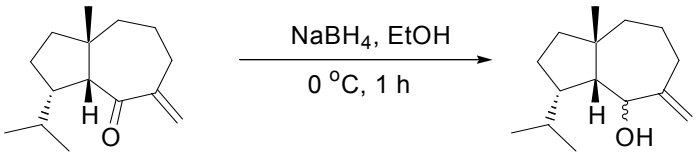

3.1

Millecrone A (10.1 mg, 0.046 mmoles) was subjected to the reaction conditions described in Section 4.3.2.2 in an attempt to reduce its carbonyl functionality. The ^{1}H and ^{13}C NMR spectra of the crude product (11.1 mg) revealed the presence of starting material only.

*4.3.2.7 Preparation of the camphanate ester **3.23** from **3.6***

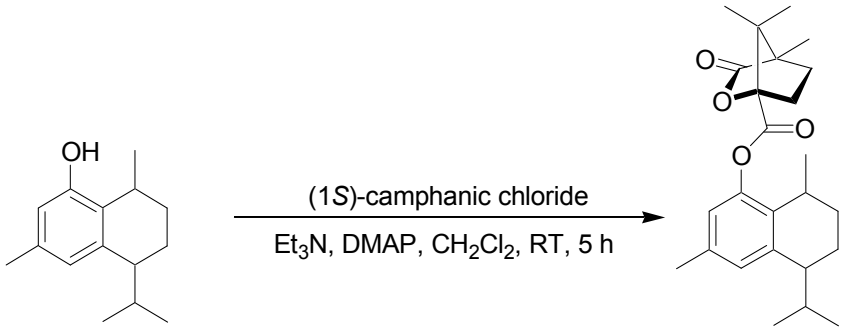

3.6 **3.23**

8-hydroxycalamenene (**3.6**, 18.6 mg, 0.085 mmol) was reacted with (1*S*)-camphanic chloride following the reaction procedure described in Section 4.3.2.3 to yield a yellow oil (39.3 mg). The crude product was purified using normal phase HPLC with a semi-preparative DIOL column (80% hexane/CH_2Cl_2) to afford the camphanate ester (**3.23**, 21.1 mg, 0.053 mmol, 62.3%). All attempts at crystallisation of **3.23** from a variety of solvents (*e.g.* hexane, MeOH, EtOH, H_2O) and mixtures of these solvents were unsuccessful.

8-hydroxycalamene camphanate ester (3.23): colourless oil; $[\alpha]_D^{19}$ +1 (*c* 1.27, $CHCl_3$); IR (film) ν_{max} 2960, 2927, 1793, 1772, 1620, 1466, 1309, 1257, 1059 cm^{-1}; ^{1}H NMR ($CDCl_3$, 600 MHz) δ 6.89 (1H, s, H-5), 6.69 (s, H-7), 2.96 (1H, qn.d, *J* = 7.0, 1.6 Hz, H-1), 2.58 (1H, ddd, *J* = 13.6, 10.9, 4.2 Hz, H-3'b), 2.51 (1H, td, *J* = 6.0, 2.5 Hz, H-4), 2.30 (3H, s, H_3-15), 2.21 (1H, ddd, *J* = 13.5, 9.4, 4.6 Hz, H-3'a), 2.00 (1H, m, H-11), 1.99 (1H, m, H-4'b), 1.93 (1H, tdd, *J* = 13.3, 6.1, 4.0

Hz, H-2b), 1.83 (1H, tdd, *J* = 13.6, 6.0, 3.3 Hz, H-3b), 1.79 (1H, m, H-3a), 1.77 (1H, m, H-4'a), 1.47 (1H, ddt, *J* = 13.3, 3.9, 2.9 Hz, H-2a), 1.19 (3H, s, H_3-9'), 1.17 (3H, s, H_3-8'), 1.13 (3H, s, H_3-10'), 1.13 (3H, d, *J* = 6.7 Hz, H_3-14), 0.99 (3H, d, *J* = 6.7 Hz, H_3-13), 0.83 (3H, d, *J* = 6.7 Hz, H_3-12); ^{13}C NMR ($CDCl_3$, 150 MHz) δ 177.9 (q_c, C-6'), 166.3 (q_c, C-1'), 147.9 (q_c, C-8), 141.7 (q_c, C-10), 135.1 (q_c, C-6), 131.3 (q_c, C-9), 128.5 (CH, C-5), 119.9 (CH, C-7), 91.1 (q_c, C-2'), 54.9 (q_c, C-7'), 54.4 (q_c, C-5'), 42.8 (CH, C-4), 33.4 (CH, C-11), 30.9 (CH_2, C-3'), 29.0 (CH_2, C-4'), 27.1 (CH, C-1), 26.7 (CH_2, C-2), 22.0 (CH_3, C-14), 22.0 (CH_3, C-13), 21.0 (CH_3, C-15), 19.5 (CH_3, C-12), 18.8 (CH_2, C-3), 16.9 (CH_3, C-9'), 16.7 (CH_3, C-10'), 9.7 (CH_3, C-8'); HREIMS *m/z* 399.2534 (calcd for $C_{25}H_{35}O_4$ [$(M+H)^+$], 399.2535).

4.3.2.8 Lithium aluminium hydride reduction of cubebenone

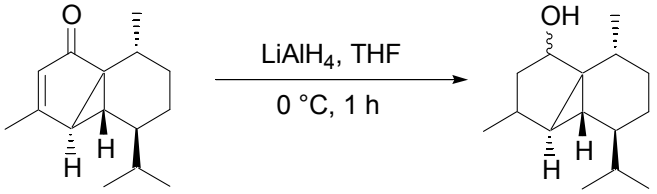

3.8 **3.25**

A solution of cubebenone (**3.8**, 69.0 mg, 0.316 mmol) was reduced with $LiAlH_4$ following the procedure described in Section 4.3.2.1 to give a colourless oil (**3.24**, 60.2 mg). The ^{1}H and ^{13}C NMR spectra of the crude product revealed that the carbonyl was successfully reduced along with the cyclic alkene. This crude product was used in the formation of the ester **3.24** before any other spectral data was obtained.

*4.3.2.9 Preparation of the camphanate ester of **3.24***

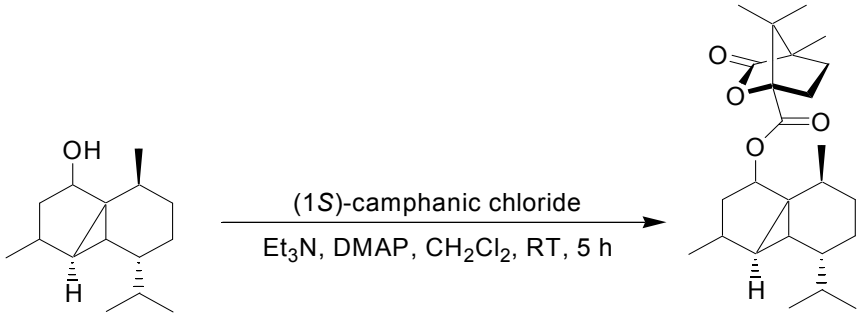

3.24 **3.25**

The crude product **3.24** (60.2 mg, 0.271 mmol) was reacted with (1*S*)-camphanic chloride following the reaction procedure described in Section 4.3.2.3 to yield a colourless oil (109.6 mg). The crude product was initially purified using normal phase HPLC with a semi-preparative DIOL column (80% hexane/CH_2Cl_2) followed by normal phase DIOL HPLC (87.5% hexane/EtOAc) and finally by analytical DIOL HPLC (90% hexane/EtOAc) to give the camphanate ester as a mixture of epimers (**3.25**, 24.5 mg, 0.061 mmol, 22.5%). All attempts to separate the epimers using normal phase HPLC were unsuccessful. Further attempts at crystallisation of the camphanate ester **3.25** from a variety of solvents (*e.g.* hexane, MeOH, EtOH, H_2O) and mixtures of these solvents were unsuccessful.

Camphanate ester 3.25: colourless oil; IR (film) ν_{max} 3020, 2959, 1785, 1739, 1457, 1275, 1216 cm^{-1}; EIMS *m/z* (rel. int) 403 [$(M+H)^+$] (68), 396 (10), 395 (37), 394 (23), 393 (100), 385 (9).

Major product

^{1}H NMR ($CDCl_3$, 600 MHz) δ 5.54 (1H, t, *J* = 8.3 Hz, H-8), 2.37 (1H, ddd *J* = 13.6, 10.6, 4.1 Hz, H-3'b), 2.23 (1H, m, H-6), 2.14 (1H, dt, *J* = 13.2, 7.8 Hz, H-7b), 2.01 (1H, m, H-3'a), 1.90 (1H, ddd, *J* = 13.6, 10.6, 4.1 Hz, H-4'b), 1.77 (1H, sept, *J* = 6.0 Hz, H-1), 1.69 (1H, m, H-4'a), 1.62 (1H, m, H-2b), 1.62 (1H, m, H-11), 1.39 (1H, dtd, *J* = 12.5, 4.3, 1.9 Hz, H-3b), 1.11 (3H, s, H_3-8'), 1.07 (3H, s, H_3-9'), 1.02 (1H, m, H-4), 1.00 (3H, d, *J* = 6.4 Hz, H_3-15), 0.99 (3H, d, *J* = 6.4 Hz. H_3-14), 0.97 (3H, s, H_3-10'), 0.97 (3H, m, Hz, H_3-13), 0.96 (1H, m, H-5), 0.94 (3H, d, *J* = 7.1 Hz, H_3-12), 0.92 (1H, m, H-10) , 0.85 (1H, m, H-7a), 0.78 (1H, m, H-3a), 0.54 (1H, m, H-2a); ^{13}C NMR ($CDCl_3$, 150 MHz) δ 178.1 (q_c, C-6'), 167.5 (q_c, C-1'), 91.3 (q_c, C-2'), 79.3 (CH, C-8), 54.7 (q_c, C-7'), 53.8 (q_c, C-5'), 43.8 (CH, C-4), 36.7 (q_c, C-9), 35.1 (CH_2, C-7), 33.8 (CH, C-11), 33.5 (CH, C-5), 32.9 (CH, C-6), 31.3 (CH_2, C-2), 30.6 (CH_2, C-3'), 29.0 (CH_2, C-4'), 28.1 (CH, C-1), 26.9 (CH_2, C-3), 20.0 (CH_3, C-12), 19.7 (CH_3, C-13), 18.9 (CH, C-10), 18.7 (CH_3, C-14), 17.9 (CH_3, C-15), 17.1 (CH_3, C-9'), 16.9 (CH_3, C-10'), 9.7 (CH_3, C-8').

Minor product

^{1}H NMR ($CDCl_3$, 600 MHz) δ 5.27 (1H, d, *J* = 5.7 Hz, H-8), 2.50 (1H, m, H-6), 2.44 (1H, ddd, *J* = 13.6, 10.6, 4.1 Hz, H-3'b), 2.39 (1H, m, H-4'b), 2.02 (1H, m, H-3'a), 1.89 (1H, m, H-1), 1.69 (1H, m, H-2b), 1.68 (1H, m, H-4'a), 1.56 (1H, m, H-11), 1.56 (1H, m, H-7b), 1.34 (1H, m, H-3b), 1.28 (1H, m, H-7a), 1.11 (3H, s, H_3-8'), 1.09 (1H, m, H-5), 1.07 (3H, m, H_3-9'), 1.06 (3H, m, H_3-14), 1.02 (3H, m, H_3-15), 1.00 (3H, m, H_3-10'), 0.95 (3H, m, H_3-13), 0.91 (3H, d, *J* = 6.8 Hz, H_3-12), 0.81 (1H, m, H-3a), 0.80 (1H, m, H-4), 0.52 (1H, m, H-2a), 0.43 (1H, m, H-10); ^{13}C NMR ($CDCl_3$, 150 MHz) δ 178.1 (q_c, C-6'), 167.4 (q_c, C-1'), 91.2 (q_c, C-2'), 85.2 (CH, C-8), 54.8 (q_c, C-7'), 54.1 (q_c, C-5'), 44.3 (CH, C-4), 38.7 (CH_2, C-7), 34.5 (q_c, C-9), 34.3 (CH, C-5), 33.6 (CH, C-11), 33.4 (CH, C-6), 32.6 (CH_2, C-2), 30.6 (CH_2, C-3'), 29.1 (CH_2, C-4'), 27.4 (CH, C-1), 26.2 (CH_2, C-3),

22.1 (CH_3, C-14), 22.0 (CH, C-10), 20.3 (CH_3, C-12), 19.9 (CH_3, C-13), 17.6 (CH_3, C-15), 17.0 (CH_3, C-9'), 16.8 (CH_3, C-10'), 9.6 (CH_3, C-8').

References

1. Anderson, R. J.; Williams, D. E. *Issues Environ. Sci. Technol.* **2000**, 13, 55-79.

2. Blunt, J. W.; Copp, B. R.; Munro, M. H. G.; Northcote, P. T.; Prinsep, M. R. *Nat. Prod. Rep.* **2010**, 27, 165-237.

3. Hamann, M. T.; Hill, R.; Roggo, S. *CHIMA* **2007**, 61, 313-321.

4. Srivastava, M.; Simakov, O.; Chapman, J.; Fahey, B.; Gauthier, M. E. A.; Mitros, T.; Richards, G. S.; Conaco, C.; Dacre, M.; Hellsten, U.; Larroux, C.; Putnam, N. H.; Stanke, M.; Adamska, M.; Darling, A.; Degnan, S. M.; Oakley, T. H.; Plachetzki, D. C.; Zhai, Y.; Adamski, M.; Calcino, A.; Cummins, S. F.; Goodstein, D. M.; Harris, C.; Jackson, D. J.; Leys, S. P.; Shu, S.; Woodcroft, B. J.; Vervoort, M.; Kosik, K. S.; Manning, G.; Degnan, B. M.; Rokhsar, D. S. *Nature* **2010**, 466, 720-727.

5. Grabowski, K.; Baringhaus, K.; Schneider, G. *Nat. Prod. Rep.* **2008**, 25, 892-904.

6. Bon, R. S.; Waldmann, H. *Accounts Chem. Res.* **2010**, 43, 1103-1114.

7. Li, J. W. H.; Vederas, C. *Science* **2009**, 325, 161-165.

8. Glaser, K. B.; Mayer, M. S. *Biochem. Pharmacol.* **2009**, 78, 440-448.

9. Proksch, P.; Edrada-Edel, R.; Edel, R. *Mar. Drugs* **2003**, 1, 5-17.

10. Sashidhara, K. V.; White, K. N.; Crews, P. *J. Nat. Prod.* **2009**, 27, 588-603.

11. European Science Foundation: *Marine Biotechnology* **2010**, 15, 44-50.

12. Sipkema, D.; Osinga, R.; Schatton, W.; Mendola, D.; Tramper, J.; Wijffels, R. H. *Biotechnol. Bioeng.* **2005**, 90, 201-222.

13. Corey, E. J.; Gin, D. Y.; Kania, R. S. *J. Am. Chem. Soc.* **1996**, 118, 9202-9203.

14. Endo, A.; Yanagisawa, A.; Abe, M.; Tohma, S.; Kan, T.; Fukuyama, T. *J. Am. Chem. Soc.* **2002**, 124, 6552-6554.

15. Chen, J.; Chen, X.; Bios-Choussy, M.; Zhu, J. *J. Am. Chem. Soc.* **2006**, 128, 87-89.

16. Menchaca, R.; Martinez, V.; Rodriguez, A.; Rodriguez, N.; Flores, M.; Gallego, P.; Manzanares, I.; Cuevas, C. *J. Org. Chem.* **2003**, 68, 8859-8866.

17. Munro, M. H. G.; Blunt, J. W.; Dumdei, E. J.; Hickford, S. J. H.; Lill, R. E.; Li, S.; Battershill, C. N.; Duckworth, A. R. *J. Biotechnol.* **1999**, 70, 15-25.

18. Aicher, T. D.; Buszek, K. R.; Fang, F. G.; Forsyth, C. J.; Jung, S. H.; Kishi, Y.; Matelich, M. C.; Scola, P. M.; Spero, D. M.; Yoon, S. K. *J. Am. Chem. Soc.* **1992**, 114, 3162-3164.

19. Gradishar, W. *J. Curr. Oncol. Rep.* **2011**, 13, 11-16.

20. Laport, M. S.; Santos, O. C. S.; Muricy, G. *Curr. Pharm. Biotechnol.* **2009**, 10, 86-105.

21. Gademann, K.; Kobylinska, J. *Chem. Rec.* **2009**, 9, 187-198.

22. Vogel, G. *Science* **2008**, 320, 1028-1030.

23. Hamann, M.; Otto, C. S.; Scheuer, P. J. *J. Org. Chem.* **1996**, 61, 6594-6600.

24. Collett, L. A. BScHons Thesis Rhodes University, **1995**.

25. Hooper, G. J.; Davies-Coleman, M. T. *Tetrahedron Lett.* **1995**, 36, 3265-3268.

26. Cimino, G.; Ghiselin, M. T. *Chemoecology* **1999**, 9, 187-207.

27. Pika, J.; Faulkner, D. J. *Tetrahedron* **1994**, 50, 3065-3070.

28. McPhail, K. L.; Davies-Coleman M. T.; Starmer, J. *J. Nat. Prod.* **2001**, 64, 1183-1190.

29. Darias, J.; Cueto, M.; Diaz-Marrero, A. R. *Prog. Mol. Subcell. Biol.* **2006**, 43, 105-131.

30. Hodgson, A. N. *Oceanogr. Mar. Biol.* **1999**, 37, 245-314.

31. Davies-Coleman, M. T. *Prog. Mol. Subcell. Biol.* **2006**, 43, 133-157.

32. Garson, M. J. *Prog. Mol. Subcell. Biol.* **2006**, 43, 160-174.

33. McQuaid, C. D.; Cretchley, R; Rayner, J. L. *J. Exp. Mar. Biol. Ecol.* **1999**, 237, 141-154.

34. Davies-Coleman, M. T.; Garson, M. J. *Nat. Prod. Rep.* **1998**, 15, 477-493.

35. Cutignano, A.; Cimino, G.; Villani, G.; Fontana, A. *Tetrahedron* **2009**, 65, 8161-8164.

36. El-Sayed, A.; Hothersall, J.; Cooper, S. M.; Stephens, E.; Simpson, T. J.; Thomas, C. M. *Chem. Bio.* **2003**, 10, 419-430.

37. Manker, D. C.; Garson, M. J.; Faulkner, D. J. *J. Chem. Soc., Chem. Commun* **1988**, 1061-1062.

38. Garson, M. J.; Jones, D. D.; Small, C. J.; Liang, J.; Clardy, J. *Tetrahedron Lett.* **1994**, 35, 6921-6924.

39. Williams, D. R.; Nold, A. L.; Mullins, R. J. *J. Org. Chem.* **2004**, 69, 5374-5382.

40. Beye, G. E.; Ward, D. E. *J. Am. Chem. Soc.* **2010**, 132, 7210-7215.

41. Rovirosa, J.; San-Martin, A. *Quim. Nova* **2006**, 29, 52-53.

42. Norte, M.; Cataldo, F.; González, A. G.; Rodriguez, M. L.; Ruiz-Perez, C. *Tetrahedron* **1990**, 46, 1669.

43. Rovirosa, J.; Quezada, E.; San-Martin, A. *Bol. Soc. Chil. Quim.***1991**, 36, 233-235.

44. Brecknell, D. J.; Collett, L. A.; Davies-Coleman, M. T.; Garson, M. J.; Jones, D. D. *Tetrahedron* **2000**, 56, 2497-2502.

45. Manker, D. C.; Faulkner, D. J.; Stout, T. J.; Clardy, J. *J. Org. Chem.* **1989**, 54, 5371.

46. Paterson, I.; Perkins, M. *Tetrahedron Lett.* **1992**, 33, 801-804.

47. Sharpless, K. B.; Amberg, W.; Bennani, Y. L.; Crispino, G. A.; Hartung, J.; Kwong, J. H.; Morikawa, K.; Wang, Z.; Xu, D.; Zhang, X. *J. Org. Chem.* **1992**, 57, 2768-2771.

48. Blanchfield, J. T.; Brecknell, D. J.; Brereton, I. M.; Garson, M. J.; Jones, D. D. *Aust. J. Chem.* **1994**, 47, 2255-2269.

49. Beukes, D. R.; Davies-Coleman, M. T. *Tetrahedron* **1999**, 55, 4051-4056.

50. Van Liedekerke, B. M.; Nelis, H. J.; Lambert, W. E.; de Leenheer, A. P. *Anal. Chem*. **1989**, 61, 728.

51. Keyzers, R. A. PhD Thesis Victoria University **2003**.

52. van Wyk, A. W. W. PhD Thesis Rhodes University **2007**.

53. West, C.; Lesellier, E. *Chromatogr.* **2006**, 1110, 200-213.

54. Branch, G. M.; Griffiths, C. L.; Branch, M. L.; Beckley, L. E. *Two Oceans. A Guide to the Marine Life of South Africa*; 10th ed.; David Philip Publishers: Cape Town, **2010**.

55. Kawai, S.; Takada, Y.; Tsuchida, S.; Kado, R.; Kimura, J. *Fisheries Sci.* **2007**, 73, 902-906.

56. Abourriche, A.; Charrouf, M.; Chaib, N.; Bennamara, A.; Bontemps, N.; Francisco, C. *Il Farmaco* **2000**, 55, 492-494.

57. Findlay, J. A.; Patil, A. D. *Steroids* **1984**, 44, 261-265.

58. van Wyk, A. W.; Gray, C. A.; Whibley, C. E.; Osoniyi, O.; Hendricks, D. T.; Caira, M. R.; Davies-Coleman, M. T. *J. Nat. Prod.* **2008**, 71, 420-425.

59. Braun, S.; Kalinowski, H. O.; Berger, S. *gs-HMBC; 150 and More Basic NMR Experiments*; Wiley-VCH: New York, **1998** pp 489-492.

60. Antunes, E. M.; Beukes, D. R.; Kelly, M.; Samaai, T.; Barrows, L. R.; Marshall, K. M.; Sincich, C.; Davies-Coleman, M. T. *J. Nat. Prod.* **2004**, 67, 1268-1276.

61. Dale, J. A.; Mosher, H. S. *J. Am. Chem. Soc.* **1973**, 95, 512-519.

62. Jackson, P. T.; Kim, T. Y.; Carr, P. W. *Anal. Chem.* **1997**, 69, 5011-5017.

63. Ohtani, I.; Kusumi, T.; Kashman, Y.; Kakisawa, H. *J. Am. Chem. Soc.* **1991**, 113, 4092-4096.

64. Lillie, R. D. *Biological Stains;* 9th ed.; Waverly Press: Baltimore, 1977

65. Pola, M.; Gosliner, T. M. *Mol. Phylogenet. Evol.* **2010**, 56, 931-941.

66. King, D.; Fraser, V. *More Reef Fishes and Nudibranchs;* Struik Publishers: Cape Town, **2002**.

67. Zsilavecz, G. *Nudibranchs of the Cape Peninsula and False Bay;* Southern Underwater Research Group Press: Cape Town, **2007**.

68. Gosliner, T. *In Nudibranchs of Southern Africa. A Guide to Opisthobranch Molluscs of Southern Africa;* Sea Challengers & Jeff Hamann Publication: California **1987**.

69. Whibley, C. E.; McPhail, K. L.; Keyzers, R. A.; Maritz, M. F.; Leaner, V. D.; Birrer, M. J.; Davies-Coleman, M. T.; Hendricks, D. T. *Mol. Cancer. Ther.* **2007**, 6, 2535-2643.

70. Blumenthal, F.; Polborn, K.; Steffan, B. *Tetrahedron* **2002**, 58, 8433-8437.

71. Yamashita, M.; Shimizu, T.; Kawasaki, I.; Ohta, S. *Tetrahedron: Asymmetry* **2004**, 15, 2315-2317.

72. Esterhuysen, C.; Bredenkamp, M. W.; Lloyd, G. O. *Acta Cryst*. **2005**, 61, 32-34.

73. March, J. *Addition to Carbon-Carbon Multiple Bolnds; Advanced Organic Chemistry;* 4th ed.; John Wiley & Sons: New York, **1992**; pp 916-197.

74. Sunassee, S. N. PhD Thesis Rhodes Universtiy, **2010**.

75. Perin, D. D.; Armarego, W. L. F. *Purification of Laboratory Chemicals;* 3rd ed.; Permagon Press: Oxford, **1988**

76. Frish, M. J.; Trucks, G. W.; Schlegel, H. B.; Scuseria, M. A.; Robb, J. R.; Cheeseman, J. A.; Montgomery, J.; Vreven, T.; Kudin, J. C.; Burant, J. C.; Millam, J. M.; Iyengar, S. S.; Tomasi, J.; Barone, V.; Mennucci, B.; Cossi, M.; Scalmani, G.; Rega, N.; Petersson, G. A.; Nakatsuji, H.; Hada, M.; Ehara, M.; Toyota, K.; Fukuda, R.; Hasegawa, J.; Ishida, M.; Nakajima, T.; Honda, Y.; Kitao, O.; Nakai, H.; Klene, M.; Li, X.; Knox, J. E.; Hratchian, H. P.; Cross, J. B.; Bakken, V.; Adamo, C.; Jaramillo, J.; Gomperts, R.; Stratmann, R. E.; Yazyev, O.; Austin, A. J.; Cammi, R.; Pomelli, C.; Ochterski, J. W.; Ayala, P. Y.; Morokuma, K.; Voth, G. A.; Salvador, P.; Dannenberg, J. J.; Zakrzewski, V. G.; Dapprich, S.; Daniels, A. D.; Strain, M. C.; Farkas, O.; Malick, K.; Rabuck, A. D.; Raghavachari, K.; Foresman, J. B.; Ortiz, J. V.; Cui, Q.; Baboul, A. G.; Clifford, S.; Cioslowski, J.; Stefanov, B. B.; Liu, G.; Liashensko, A.; Piskorz, P.; Komaromi, I.; Martin, R. L.; Fox, D. J.; Keith, T.; Al-Laham, M. A.; Peng, C. Y.; Nanayakkara, A.; Challacombe, M.; Gill, P. M. W.; Johnson, B.; Chen, W.; Wong, M. W.; Gonzalez, C.; Pople, J. A. *Gaussian 03* [Computer Program]. Gaussian, Inc.: Wallingford CT, **2004**.

77. Becke, A. D. *Phys. Rev. A* **1988**, 38, 3098--3100.

78. *Discovery Studio Visualizer, Release 2.0* [Compounter Program]. Accelrys Software Inc.: San Diego, **2007**.

79. Hussein, A. A.; Meyer, M. J. J.; Rodriguez, B. *Magn. Reson. Chem.* **2003**, 41, 147-151.